Some Analysis on Electroless Nickel Composite Coating for Surgical Instruments: A Case Study of Business-University–Business Model for Technology Transfer to Rural Industrial Clusters in West Bengal

Thesis submitted by

Nibedita Saha

Doctor of Philosophy (Engineering)

Department of Mechanical Engineering

Faculty Council of Engineering &Technology

Jadavpur University

Kolkata, India

2024

JADAVPUR UNIVERSITY
KOLKATA-700032, INDIA

INDEX NO. 50/18/E
REGISTRATION NUMBER: 1021811040

1. Title of Thesis:

Some Analysis on Electroless Nickel Composite Coating for Surgical Instruments: A Case Study of Business-University–Business Model for Technology Transfer to Rural Industrial Clusters in West Bengal.

2. Name, Designation & Institution of the Supervisor(s):

Prof. (Dr.) Gautam Majumdar
Former Professor and Ex HOD
Mechanical Engineering Department,
Jadavpur University, Kolkata-700032

Dr. Jisnu Basu
Chairman, Workshop
Saha Institute of Nuclear Physics
Kolkata (W.B) – 700064

3. List of Publications (Referred Journals)

1. Saha N., Basu J., Sen P. & Majumdar G. (2023). Corrosion behaviour of electroless NiP coating in artificial blood plasma, Advances in Materials and Processing Technologies. https://doi.org/10.1080/2374068x.2023.2190667
2. Saha N., Basu J., Mondal S., Satapati B., Majumdar G. (2024), Effect of Electroless NiP/PTFE Composite Coating on Mechanical Properties of AISI 420 SS and Its Corrosion Behaviour in Human Blood, Journal of Bio- and Tribo-Corrosion 10:20, https://doi.org/10.1007/s40735-024-00825-5
3. N. Saha N., J. Basu J., P. Sen P., Majumdar G. (2019), Electrochemical behaviour of martensitic stainless steel with blood, Materials Today: Proceedings, https://doi.org/10.1016/j.matpr.2019.12.364

4. List of Presentations in National/International Conferences

1. N. Saha, J. Basu, P. Sen, G . Majumdar, Electrochemical behavior of martensitic stainless steel with blood, ICMPC 2020,
2. Nibedita Saha, Jhumpa De, Jisnu Basu, Gautam Majumdar, "Parametric optimization of electroless Ni-P-PTFE composite coating using RSM and GA“, Iinternational Conference on Chemical Engineering Innovation & Sustainability (ICEIS 2023)

5. **List of Patents: NIL**

6. **List of Book Chapters: NIL**

JADAVPUR UNIVERSITY
FACULTY OF ENGINEERING &TECHNOLOGY

PROFORMA – 1

"Statement of Originality"

I, Nibedita Saha registered on 28.06.2018, do hereby declare that this thesis entitled " Some Analysis on Electroless Nickel Composite Coating for Surgical Instruments: A Case Study of Business-University–Business Model for Technology Transfer to Rural Industrial Clusters in West Bengal" contains literature survey and original research work done by the undersigned candidate as part of Doctoral studies.

All information in this thesis have been obtained and presented in accordance with existing academic rules and ethical conduct. I declare that, as required by these rules and conduct, I have fully cited and referred all materials and results that are not original to this work.

I also declare that I have checked this thesis as per the "Policy on Anti Plagiarism, Jadavpur University, 2019", and the level of similarity as checked by iThenticate software is ____7____%.

Nibedita Saha
Signature of Candidate:

Date : 04/08/2025

Certified by Supervisor(s):

(Signature with date, seal)

1. Ex. Professor
Mechanical Engineering Dept.
Jadavpur Universi
Kolkata – 700 032

2. अध्यक्ष / Chairman
कार्यशाला समिति/ Workshop Committee
साहा इंस्टिट्यूट ऑफ न्यूक्लियर फिजिक्स
SAHA INSTITUTE OF NUCLEAR PHYSICS
1/ए एफ, विधाननगर, कोलकाता - 700 064
1/AF, Bidhan Nagar, Kolkata 700 064

JADAVPUR UNIVERSITY
FACULTY OF ENGINEERING &TECHNOLOGY

PROFORMA - 2

CERTIFICATE FROM THE SUPERVISOR/S

This is to certify that the thesis entitled "Some Analysis on Electroless Nickel Composite Coating for Surgical Instruments: A Case Study of Business-University–Business Model for Technology Transfer to Rural Industrial Clusters in West Bengal" submitted by Shri/Smt Nibedita Saha, who got his/her name registered on 28.06.2018 for the award of Ph. D. (Engg./Pharmacy) degree of Jadavpur University is absolutely based upon his/her own work under the supervision of Prof Gautam Majumdar and Dr. Jisnu Basu and that neither his/her thesis nor any part of the thesis has been submitted for any degree/diploma or any other academic award anywhere before.

Ex. Professor
Mechanical Engineering Dept.
Jadavpur University
Kolkata - 700 032

1._____

Signature of the Supervisor
and date with Office Seal

अध्यक्ष / Chairman
कार्यशाला समिति/ Workshop Committee
साहा इंस्टिट्यूट ऑफ न्युक्लियर फिजिक्स
SAHA INSTITUTE OF NUCLEAR PHYSICS
1/ए एफ , विधाननगर, कोलकाता - 700 064
1/AF, Bidhan Nagar, Kolkata 700 064

2._____

Signature of the Supervisor
and date with Office Seal
(if more than one supervisor)

ACKNOWLEDGEMENT

The present work has been carried out under the supervision of Dr Gautam Majumdar, former professor, Mechanical Engineering department, Jadavpur University and Dr Jisnu Basu, Chairman, Workshop, Saha institute of Nuclear Physics. I would like to express my sincere gratitude to my supervisors for their valuable guidance and constant support throughout my work. I would like to thank my advisors for their continuous support and motivation which made the submission of this dissertation possible.

The experimental work has been carried out at Surface Engineering Laboratory, Department of Mechanical Engineering, Jadavpur University. The characterizations have been conducted in academic institutions like Saha Institute of Nuclear Physics, Jadavpur University, Indian Institute of Engineering and Science Technology, Shibpur, Indian Institute of Technology Kharagpur, Indian Association for the Cultivation of Science, Jadavpur , Tezpur University, Tezpur. I would like to express my deepest gratitude to all the teaching and non-teaching staffs of the concerned institutions for their co-operation and help.

I am thankful to my lab mates, Dr. Jhumpa De, Dr. Nisantika Biswas, Vikash Kumar, Shovon Bhowmick and Rupam Mondal for helping me during the experiments and also sharing their knowledge regarding electroless coating.

I wish to record my gratitude to my husband Mr. Anindya Sarkar for his co-operation and help throughout this journey. I am forever indebted to my parents Mr. Nakul chandra Saha and Mrs. Suktara Saha for their encouragement, motivation and sacrifice for every achievement of my life. Thanks are due to all others who helped me directly or indirectly for the completion of this work.

Dedicated to my
beloved Father and Mother

INDEX

List of Figures

List of Tables

ABSTRACT

This work is an application of Business-University-Business Model (BUB). The BUB Model is an alternative methodology for technology transfer and assimilation to industrial clusters. In BUB Model, the university develops a new technology in order to provide a sustainable solution to the problem faced by an industrial cluster. Our work was based on Baruipur Surgical Instruments Cluster situated at Bauipur, West Bengal, India. This cluster is in existence since a long time and has been producing various types of surgical instruments. But, post globalization, this cluster is losing its place in the local as well as international market. Due to lack of technological upgradation, the instruments produced here do not meet the international standards. After visiting the cluster for quite a few times and analyzing the problems, we found that the main problem in the instruments are that they are very prone to corrosion. It has been observed that the instruments start to corrode just after 4-5 autoclaves.

Our main aim was to increase the corrosion resistivity of the instruments. In order to do so, coating the instrument with some protective layer could be an alternative solution. As electroless coating has many advantages and also economically feasible, this method was chosen for our work. Firstly, Ni-P electroless coating was performed and positive results were achieved after heat treatment of the coating. After that, Ni-P-PTFE composite coating was performed over the instruments and highly convincing results were seen after the composite coating.

Electrochemical impedance spectroscopy and potentiodynamic polarization test were performed to measure the corrosion properties. All the corrosion test were performed with blood plasma as the corrosive media. To confirm the presence of the coatings on the substrate, SEM, EDAX, TEM were performed. Also, to check the mechanical characteristics of the coatings, microhardness and nanohardness tests were performed. Furthermore, in order to increase hardness and mass deposition of the coatings, some statistical tools were used for modelling and optimization.

After performing all the tests, it was observed that the corrosion resistivity of the instruments increased to a great extent. So, it can be said that a new technology was successfully developed as a solution to the corrosion problem at Barupur cluster which is both sustainable and economically feasible.

Chapter 1

Indian industrial clusters: An Overview

Outline of the Chapter: *1.1 Introduction to Indian Industrial Cluster 1.2 Technology Transfer to industrial Clusters 1.3 Scope of BUB Model for technology Transfer and assimilation to Indian rural industrial clusters 1.4 Baruipur Surgical Industrial Cluster 1,5 Problems faced by the industry 1.6 Conventional manufacturing process followed at Baruipur 1.7 Problem Analysis 1.8 Different Methods of Surface Coating and Surface Modification 1.9 Aim of the Work 1.10 Objective of the present work 1.11 Outline of the Thesis*

1.1 Introduction to Indian Industrial Cluster

The Indian economy can be broadly divided into two parts- urban and rural. A very important role is played by rural part of India in the country's economy as 70 percent of the population resides in the rural India. It has been found that small and medium enterprises (SME) sectors provide employment to about 24 million people in over 13 million units and approximately contributes to 35 percent of manufacturing exports and 40 percent of industrial production of the country (Das and Das, 2011). These rural industrial clusters have naturally grown without any aid from the state. Though, they do not always produce world class quality products, but they fulfil the needs of millions of Indians at a price which middle class Indians can afford. These clusters have been saving the country from economic breakdown. These clusters have continued to satisfy the basic needs of food, clothing and shelter to millions of Indians for many years from now. Though, these clusters are making profit generation after generation by producing goods which satisfies the Indian market, whose major part of the customers are poor. But, post globalization, a change is clearly visible on the customer's front. Nowadays, the customers prefer to buy a good quality product with little bit more money than buying a cheaper item with degraded quality. With the advent of globalization, many foreign multinationals have been quite successful to make its place in Indian market. The Indians have accepted and adopted these foreign goods in their day-to-day life.

This possesses a big threat to the sustainability of the country's rural industrial clusters as the quality of goods produced by them is far behind the quality of the foreign goods. The main cause behind this is the lack of technology upgradation in these clusters. There are more than 2500 industrial clusters among which, about 2000 of them are rural/artisanal cluster. As per the report prepared by United Nations Industrial development organization (UNIDO), 457 industrial clusters are situated in eastern India. Eastern region has the biggest share in total number of 2500 clusters scattered all over India. Among 457 clusters, 115 are clusters of artistic and decorative products (Basu J, *et al*., 2010). Some of these naturally grown rural clusters are more than hundred years old. These clusters have come up naturally to supply the daily necessities of millions of Indians. Though the quality of the products produced by these clusters cannot match the world standards, but they were enough to satisfy the needs of the local people. But after globalization, the situation has changed. Now a village blacksmith has to compete with international market. Due to lack of technological advancement, the products produced by these clusters fail to compete with the international giants. In view of this, there is a increasing interest among the policy makers and the researchers for fast technology upgradation of Indian industrial clusters.

1.2 Technology transfer to Industrial Clusters

Commercialization and technology transfer are the most important steps in the modernization of any production unit. The reason behind this laid-back attitude was that, they had a market of billions of Indians, who were not aware of world class quality products. The regulating authorities only prepared projects for the name's sake and spent public money in the name of R&D. However, recently, there is an increasing interest among researchers and government regarding the effective transfer of technology to these naturally grown industrial clusters in this globalized world. The contribution of the small and medium entrepreneurs (SME) of a developing country towards the country's GDP is significant, but they have limited scope of adoption of technological innovations required for increasing productivity and quality of their products. A knowledgeable observer of Indian industrial clusters has rightly said that, in India, small firms account for the process of industrialization and development of the country. These SMEs have silently shaped the present economic scenario of the country,

providing about 80 percent of employment in manufacturing sector. 35 percent of the export volume is contributed by this section. Recently, a number of these naturally grown industrial clusters have attracted the interests of policy makers and researchers. In the late 90s, Government recommended the proposal of United Nations Industrial development organization (UNIDO) for cluster development. Cluster development programs (CDP) was designed according to UNIDO methodology for capacity and vision building. The CDP program proposed the establishments of Common Facility Centre (CFC) and support centres for training and up-gradation of Infrastructure Development (ID) projects as per requirements in clusters. Since 1996, this Italian model of cluster development has been implemented in about only 40 clusters of our country. It has also been observed that for bigger clusters, having more than 100 units, the outreach of such programs is not more than 20% which is a very small number. It appeared that the said methodology may not be suitable for a vast country like India. Secondly support centres mainly provided training on sophisticated management and marketing tools. Though this type of training needs less effort for preparation and field study of the service providers, but are very less beneficial for the cluster development. Michael E. Porter, a renowned expert in cluster dynamics, said that only the clusters of middle-income countries may start the initiatives to improve quality and sophistication of management. (Mitra A., *et al*., 2014). It is obvious that world class products cannot be produced by just giving training to the members of these clusters on sophisticated management techniques without availability raw material in the clusters and without improving the infrastructure and technology upgradation. It would not be a wise decision to drain precious public funds only in the name of training First and foremost step should be to ensure the production of marketable products. These industrial clusters have been satisfying the demands of the domestic market for years. Each and every rural industrial cluster have their own mode of production which, they have developed over the years and made them sustainable. A detailed study of the pre-existing technology, organizational behaviour and mode of production is required for understanding them. UNIDO observed that most of the clusters and specifically, the handicraft sector is very small having less than hundred workers, and so much technically specific that no one in the world can match quality of their product and skill. It is obvious that a ready-made solution for technology up gradation would not serve the purpose and also, the bookish knowledge of management would not enhance the performance of the cluster members. In our country, Business University relations are

also very weak. The technology transfer training provided by the service centres are just like classroom courses which merely increase their knowledge. They hardly use this knowledge in their production units. Author has observed that there are number of technology related problems in each and every rural cluster. The cluster members are ready to spend their time and money in order to get a cost-effective solution. But they want a feasible and affordable customized solution which will be one cheque away from installation. Our study is based on the rural industrial clusters of eastern India. It has been pointed out, though these SSEs have positive side of unique craftsmanship but some practical problems exist in operational level. UNIDO methodology proposed that the first step for cluster development program (CDP) is proper selection of a cluster. Selection criteria deal with the future prospects of the cluster and also the number of beneficiaries. However, in reality, like any other developing country, politics and regional influence plays a more important role than scientific optimization of strategic planning. In spite of these ambiguities, the overall experience of UNIDO on cluster development program movement in India is undoubtedly a success story. Interventions in the clusters of Jaipur, Pune, Tirupara and Ludhiana are now considered globally, as benchmarking points. In spite of all these achievements, there are five points which are identified as major constraints in the development of Indian SSE clusters. Their technological antiquity, information deficiency, relatively poor quality of products, inadequate management systems. And poor market linkages. Generally, the training programs are arranged mostly in the service institutes and often at the cluster sites. Many resource centres and technology support organizations are fully or partially involved with these technology transfers. These training programs are designed and delivered by knowledgeable faculties. After theoretical class and practical demonstration, study materials are also provided to the cluster members for easy assimilation of transferred technology. These service centres and resource centres have taken the initiative to develop business to business (B 2 B) or cluster to cluster relationship in order to provide the same level technology transfer. For achieving global competitiveness, merely the B2B relation within the country may not serve the purpose. An effective Business University Business (BUB) relationship can facilitate the clusters to compete with global giants in this globalized era. Except some handful of examples, this type of BUB relationship has not yet been developed in India.

1.3 Scope of BUB Model for technology Transfer and assimilation to Indian rural industrial clusters.

Development of rural industrial clusters is an important milestone for resurgence of the country. In earlier sections, it has been repeatedly mentioned the intrinsic competitiveness of rural industrial clusters. The main reason is that they are lacking in upgradation of appropriate technology in production units. Availability of proper raw material and transfer of affordable technology must be ensured to these clusters. At present scenario, technology upgradation has become very much essential for most of the rural clusters. Considering the volume of the job of technology transfer and availability of proper raw material, government can reach to a very small portion can through any national project. An alternative solution would be a district wise service centres whose primary objective would be to find the strength of a cluster. The intrinsic competitiveness and technological innovations of cluster members has to be studied. The technological modification must be designed with minimum diversion from the existing system. A new model has been proposed called Business University Bossiness (BUB) relationship for building a healthy environment of technology transfer. As per this model, the cluster members and entrepreneurs of small-scale industries would inform their technology related problems to District Industries Centre or other service institutions. For getting the service, they have to pay token amount of money for registration card. The monthly requirement of technology related problems will be given to the serving Universities. Here, the involvement of the university is to provide the technological support for spontaneous transfer of technology from the serving to the receiving cluster. In graduation and post-graduation courses, universities often do not get sufficient number of practical problems for student projects. During the project, there would be both way information transfer between universities and the clusters/SMEs. After six months, the cluster member would give a follow-up about the progress of the technological development. A comparative analysis with similar BUB effort in India and other developing countries has also been included in this study.

Aida Caldera and Olivier Debande investigated the performance of universities in transferring of technology using a special dataset for university-level in Spain (Aida Caldera and Debande, 2010). It was observed that the universities which had fixed procedures and policies of technology transfer, performed better. Universities with big and well-equipped technology transfer offices (TTOs) result in more numbers of

contract research. Also, those, universities which have science park perform better than those without. Therefore, the authors suggested that the universities technology transfer performance would be better if collection of knowledge is near to universities.

The problems related to international technology transfer and their effect in the development of the technology transfer policies in China was studied by Leong and Tugrul. In the literature, they opined that various factors coming from different levels and sources should be considered for setting the technology transfer policies (Leong and Tugrul, 2011). Government must try to support the native innovation capability, and build on the international technology transfer

The transfer of technology for sustainable growth and development was studied by Corsi (Corsi, A. et al., 2019). They also pointed out the social impacts related with it. The authors used a different software program for their analysis. The most important social impacts were identified to be Improvement of Health, Poverty Alleviation and Quality of Life. The approaches addressed are Strategies for development cleanliness, technologies and resources, actions and regulations. Their work was focussed mainly on developing countries. The results found by their work aligned with those provided by the Sustainable Development Goals.

Globally, China is the leading manufacturer of solar photovoltaic cells. More than 95% of its production is exported, accounting for over one-third of global production. Tour performed a study to understand the driving force behind this success along with their limitations, and also the role of technology transfer and innovation behind this achievement. The authors discovered that Chinese manufacturers picked up the necessary technologies and expertise from two main sources i.e the hiring of talented individuals from the Chinese exodus who established the first photovoltaic companies, as well as the acquisition of manufacturing equipment on the global market (Tour, A.,2011; Chan L.,& Daim T.U., 2011)

Formal association of universities with industries for technology transfer is a new occurrence. Presently, the role of a business–university-business collaboration (BUB) is to bridge the gap between industry and academia. An investigation by Wen-Hsiang Lai analyses the willingness of three organizations viz. university (technology transferor), industry (technology transferee) and the intermediate technology transfer

institute to engage in technology transfer association. It was found from the study that the transferor's willingness to participate in Technology Transfer in an BUB collaboration is related to two important factors that is, its 'enticement' and 'competence'. From the point of view of industry, the results show that the motivation for establishing technological resources of transferee has major influence on technology transfer program and from the viewpoint of the intermediate university, the results show that university's key resources and the transfer process have a positive impact on technology transfer in an business-university collaboration (Wen-Hsiang Lai, 2011).

Based on the literature review of various cases of technology transfer in India and in other developing countries, the present work is an application of the BUB model. The present work focuses on technology transfer and assimilation of one such rural industrial Cluster situated in the interiors of the state of West Bengal known as Surgical Instrument Cluster, Baruipur, Author has visited the cluster and have tried to understand the problems associated with the cluster. As said earlier, for effective technology transfer, it is important to understand the need of the cluster. Author has deeply studied the manufacturing procedure of the instruments and their drawbacks.

1.4 Baruipur Surgical Industrial Cluster

During the British colonial rule, Calcutta was the Capital of India. This city was the most vibrant location of Southeast Asia in 19th Century. In 1835, Medical College of Bengal (MCB) was founded. Later, at the beginning of last century, some small workshops developed near the city in order to repair surgical instruments and medical devices. People from the blacksmith community of Baruipur, a village about 25 km away from the town, were employed in these workshops. Gradually these workers, after becoming skilled in fitting, polishing etc. started their own business in and around Baruipur. Dr Bidhan Chandra Roy, the first chief minister of West Benga set one state governed Service centre at Baruipur in 1957 in order to flourish the surgical instrument manufacturing cluster with upgraded technology. Slowly, the cluster has spread throughout the district and became an income generator of 12000 villagers. Jalandhar of western India and Kochin of Southern India produce a huge quantity of surgical instruments. These two clusters are technologically advanced towards automation. But, Baruipur surgical Cluster have specialized craftsmanship and variety of instruments produced in this cluster is noteworthy. About 4000 instruments in general, dental,

ophthalmic, gynaecological, orthopaedic categories are regularly manufactured here (Basu J,. *et al*., 2010). But after globalization, there is a visible downfall of the cluster. A recent study shows that the volume of imported surgical instrument through the Kolkata port is much more than the total volume of instruments exported. It has been found that reputed Hospitals in and around Kolkata don't use indigenous instruments as they are not satisfied with the quality. Three important quality deficiencies of the indigenous products are:

A. Instruments are rust prone. After 8/9 autoclaves instruments get rusted.
B. Inaccuracy on machining. Due to this inaccuracy, there is no interchangeability of instrument components.
C. Due to unavailability of machine forging facility, defects like surface crack, dimensional inaccuracy become unavoidable for instruments produced in Baruipur cluster. It may be considered as most important reason for rejection by surgeons of reputed hospitals.

Social Impact:

At present the yearly turnover of the cluster is about Rupees 300 Crores (Basu J,. *et al*., 2010). The supply chain of the cluster is distributed throughout the district of South 24 Parganas. More than 700 micro enterprises are involved in forging of steel blanks for surgical instruments. About 1000 micro units are involved in fitting operations. 500 medium entrepreneurs are engaged in finishing operations. Some of the finishing units are very big and also export their products to Europe, North America and other countries. At least 15 units have a yearly turnover of more than 1 Crore.

1.5 Problems faced by Baruipur Industrial Cluster

Though this cluster has been functioning for many years, but with the advent of globalization, the existence of such clusters are at stake. The main reason behind this is the advancement in technology worldwide which, this clusters are unaware of.

Even though such manufacturing cluster is existing within the state, but still the big hospitals and medical practitioners of West Bengal are importing the surgical instruments from other countries with higher prices and the reason behind this is the poor quality of the products produced by this clusters. The products are far inferior to those imported from abroad. The technology used by these clusters are quite old and

has not undergone any upgradation ever since. Few major problems in the products produced by these clusters have been identified by visiting the cluster and listed down

Technological problems in products

- Raw materials
- Rust Propagation in the instruments
- Forging problems
- Machining problems

A special grade of Martensitic stainless steel is required to produce surgical instruments. Titanium, due to its high strength to weight ratio, is becoming a popular metal for ophthalmic instruments. None of these raw materials are produced in eastern India. For surgical instruments, the material used is martensitic stainless steel of grades **AISI 410** and **AISI 420.** Type 420 comprises of 12% chromium (Cr), up to 1.2% carbon (C) and Iron (Fe). They can be hardened through heat treatment procedures such as quenching, or by quenching followed by tempering. The composition of the alloy and cooling at high rate leads to the formation of martensite. Tempered martensitic steel shows improved hardness and toughness properties and, so, they are used mainly for medical tools (scalpels, razors and internal clamps). Both the annealed and hardened (heat treated) martensitic steels are magnetic in nature. Heat-treated steels have good resistance to corrosion in air, water, and certain mild chemicals. It has strong resistance to naphtha, diluted acetic acid and nitric acid. Nevertheless, this grade performs poorly as a corrosion resistor when it is annealed. AISI 420 shows corrosion resistive properties in fresh water, crude oil, gasoline, some dilute organic acids and other comparable corrosive media. AISI 410 and AISI 420 can be used in the hardened condition and also in stress relieved condition in order to maximize its corrosion resistivity (Candelarias A.F and Pinedo C. E., 2002).

Corrosion problem related with martensitic stainless steel could be either due to process inadequacy or substances confronted in clinical practice. Process inadequacy includes wrong heat treatment process (usually evident from the distribution of carbides in the microstructure), iron dispute from grinding/finishing operations, over-heating during grinding operations or selection of a wrong grade

In order to understand the problems faced by the cluster deeply, it is important to know about the manufacturing procedure followed by the cluster.

1.6 Conventional manufacturing process followed at Baruipur industrial cluster

As we visited the cluster quite a few numbers of times, the following points were noted. The entire manufacturing process of Artery Forceps are studied in details which consists of Hot forging, Annealing, Machining, Hardening and Polishing.

1.6.1 Hot forging:

The cluster does not follow any proper process for forging. The temperature before forging is not maintained. The raw materials are heated in open furnace and brought to a red-hot condition and then manually, forging is done. Sometimes, hydraulic forging machine is also used if required. The following pictures (Figure 1.1 a,b) show the forging operation done at Baruipur and the forged products.

If required, they are again heated and forged and the process continues until the final shape is obtained (Figure 1.2). During this forging operation, the metal is heated above its recrystallization temperature, beaten, cools again reheated, that affects the mechanical properties of the raw material to a great extent.

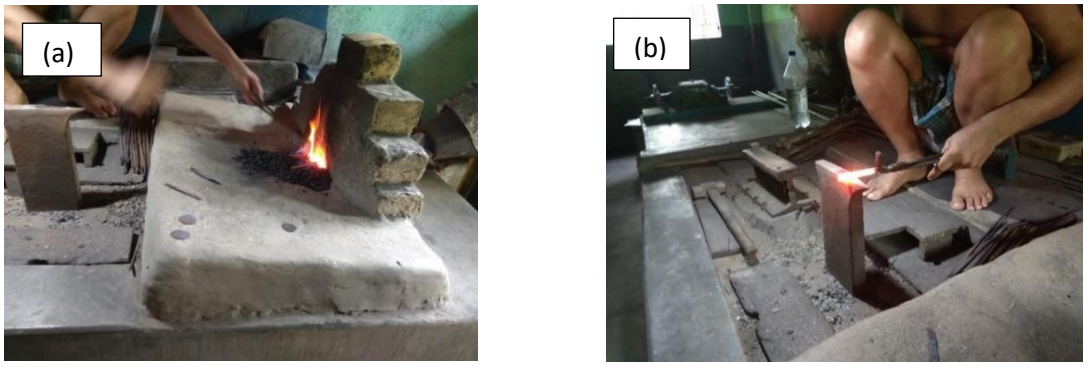

Figure 1.1 : Hot forging at Baruipur surgical cluster

Figure 1.2: Final product after forging

1.6.2 Annealing

After forging, the forged parts are sent to the Annealing shop. As the forged steels become hard, they are very difficult to machine and so, annealing has to be done to make the parts comparatively softer and machinable. The cluster uses either cowpat annealing furnace or coal fired open hearth furnace, or coke fired furnace for annealing. There is no means of temperature measurement or temperature maintenance. The cowpat furnace is ignited and the forged part is placed inside the furnace. The part is kept inside the furnace for almost 12-13 hours where it gets heated and normalized, both inside the furnace. The following picture (Figure 1.3) shows the annealing procedure and the annealed parts at Baruipur.

Figure 1.3: Annealing process at Baruipur in cow-pat furnace

But, as the surgical instruments are made of martensitic stainless-steel grades of AISI 410 or AISI 420, usage of coal fired furnace may lead to carbon contamination and hence may result to decrease chromium percentage. Thus, the instrument may lose in stainless property.

1.6.3 Fitting and Machining

The next step after annealing is machining that is cutting the teeth (in case of artery forceps). But, before, machining, the two parts are fitted together as shown in the figure (Figure 1.4).

Figure 1.4: After fitting the two parts

Figure 1.5: Machining after fitting operation

After that, machining is done by fixing the parts on the vice as shown in Figure 1.5. The requirement for the jigs and fixtures varies according to the instrument to be machined.

1.6.4 Hardening

After the completion of machining, the products need to be hardened. Again, here also, no controlled environment is there to maintain the temperature at the required level.

The pieces are heated as shown in Figure 1.6 and then oil quenched. The oil used for quenching is normally vegetable oil.

Figure 1.6: Oil Quenching process

1.6.5 Polishing

There are various stages and methods of polishing depending upon the type of instrument. The following pictures (Figure 1.7 a,b) show the polishing method of an artery forceps. However, before polishing, passivation is a must. But only few people follow this. The passivation is done by dipping the hardened parts in an acid solution (preferably water+nitric acid+sulphuric acid), for 25-30 minutes. After passivation, scales and other debris are removed from the surface of the instruments

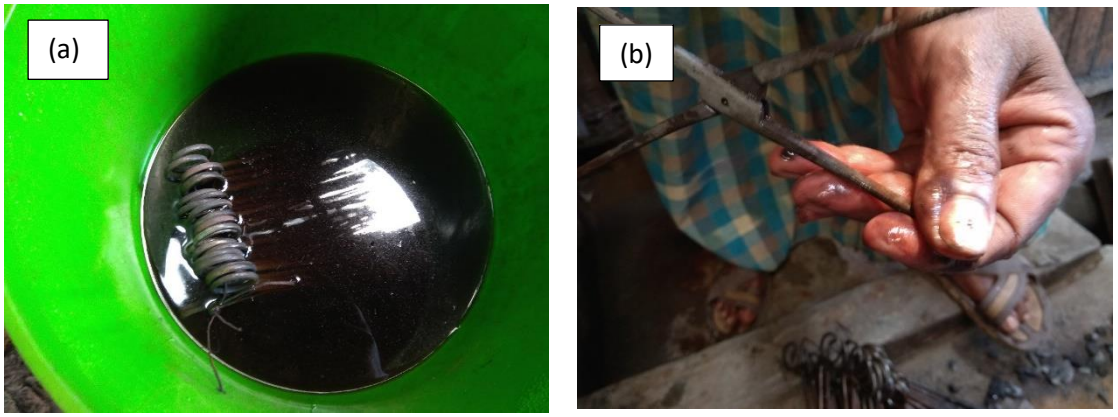

Figure 1.7: Passivation process for final cleaning.

The following pictures show the finishing processes (Figure 1.8 a,b).

Figure 1.8: Finishing process

Figure 1.8 (c): Final product

Figure 1.8 (c) shows the final product produced at Baruipur. As can be seen in the picture, everything is done manually, right from forging to machining. Due to this reason, the production rate is very low as well as proper precision cannot be maintained in the instruments.

With the advancement in medical sciences, the demand for the surgical tools has exponentially increased. But, due to the lack of automation, the cluster is unable to meet those demands. And hence, import is the only option.

Again, at the same time, even though there is high demand, the price of the tools produced at Baruipur are very low. We know that demand is directly proportional to price. But here, due to lack of technology, the products produced at Baruipur are of very poor quality and most importantly, prone to corrosion. Due to this, the products cannot

compete in the global market as well as in the local market and hence, they are compelled to sell their products at a very minimal cost.

1.7 PROBLEM ANALYSIS

CORROSION

The major problem that Baruipur surgical instrument cluster is facing is the rapid rust propagation of the instruments produced here. Though, this problem has been addressed by the cluster development programme about a decade ago, but the solution given by them was not feasible for the cluster. The cluster development agents had advised for the use of electric furnace. As the surgical instruments are made from martensitic stainless steel of AISI 410 or AISI 420 grade, usage of coal fired furnace may lead to carbon contamination and hence may lead to the formation of chromium carbide. Thus, the instrument may lose in stainless property. Therefore, the cluster development agents had advised to go for electric furnace. But, the cost of a single electric furnace equals to turnover of few months of these clusters. And moreover, the cluster members are not educated enough to realize the scientific reality. So, they were not convinced with the idea suggested by the cluster development agents. Therefore, Baruipur surgical cluster has still not been able to overcome this problem.

The first step of this work was to find the root cause of rust propagation and find an appropriate solution to it. The author's solution, which involved analysing the issue, was to apply a protective layer to the instrument surfaces, partly preventing corrosion. Therefore, a study on various possible surface treatment techniques has been done.

1.8 Different Methods of Surface Coating and Surface Modification:

There are various process which involves coating a material with a protective layer, which may not be metallic, but, to meet the requirement for a purpose. They are discussed as follows:

- **Thermal Spraying:**

To apply thermal spraying, a metal, ceramic powder, or a combination of both must be heated to a semi-molten state and sprayed at high velocity and pressure onto the substrate. The heating process can be categorized into Flame, Plasma Arc , Electric Arc, and Detonation Gun Techniques.

The primary steps associated with thermal spraying process are:

1. Preparation of the substrate
2. Masking and fixturing
3. Spray coating
4. Finishing and inspection
5. Stripping off when required

Substrate preparation generally involves descaling and removal of oil or grease and surface roughening. In order to ensure good bonding of the coating with the substrate, roughening is required.

- **Laser Alloying:**

Laser power can be used to amalgam a mixture of metal or ceramic powders on a surface. The process is simultaneous with the laser spotting followed by the nozzle spraying. In this way, the coating blends together to form an alloy and amalgamates with the outer regions of the substrate material.

- **Weld or Roll Cladding:**

For achieving thick layers (from 1mm up to few cm), weld or roll cladding is used. Weld cladding is mostly used where abrasive wear of the component is a problem. Coating tank trails, mineral handling equipment, and digger teeth are all part of the weld cladding application process. However, roll cladding is associated with mildly erosive or corrosive wear issues, which are typically seen in the food processing, paper, chemical, and wood pulp sectors.

- **Electroplating:**

The metal ions that are discharged from the cathode and deposit on the anode are the basis of this process. In the process of electrolysis, metal ions get reduced at the cathode that acts as an electron source, and the anode acts as the electron absorber. External current source serves as the supplier of electrons. One important point that is to be noted is that, for cathodic deposition of metals from an aqueous solution, the metal is present as anionic complex form rather than simple hydrated form. Then, as the metal ion goes through the inner Helmholtz layer, the potential gradient is high enough to

strip off the H_2O molecules from the metal ion so that, a simple anhydrate ion is left for the actual discharge process that occurs at the cathodic surface. The metal ion is at first absorbed at the cathode and then travels along the surface to a point where it is incorporated into the metal lattice.

- **Galvanizing:**

Galvanizing is the process of coating zinc on iron or any low carbon steel by immersing the substrate in a molten bath of zinc. Galvanizing is referred to originate from the concept of the galvanic (electro chemical) shielding to protect from corrosion offered by zinc coating over iron or steel. The galvanizing process can be carried out by four different processes namely Sherardizing, Electrolytic Plating, Spraying and Hot Dipping process. However, among these four processes, Hot Dipping is the most economical process and often used for mass production. In galvanization process, the zinc coating provides the corrosion resistivity to the substrate. This process is mostly used for outdoor applications such as structural pipes, roof sheets and walls of buildings, wash tubs, ash cans, various types of containers, fencing materials, transformer parts etc.

- **Anodizing:**

Sulfuric acid solution is utilized as the electrolyte in the anodizing process, while the aluminum component that has to be treated serves as the anode. In this process, the aluminum surface is converted to hard aluminum oxide. As aluminum is widely used in various engineering applications, particularly in automotive and aerospace areas, due to its light weight , anodizing has very wide applications as well,

- **Powder Coating:**

Painting is done using powder coating, which eliminates the need for liquid bases. The material to be coated is in the form of dry powder. They are applied by electrostatic means if the components to be coated are electrically conductive. And if the component is not conductive, the components dipped into the powder or immersed in a fluidized bed of powder. Powder coating is environmentally more friendly than paints as they do

not contain any solvents. Without a primer, powder coatings have strong adhesion, excellent corrosion resistance, and high impact resistance.

- **Physical Vapor Deposition:**

The coating flux is created by a physical process in the Physical Vapor Deposition (PVD) process. This is a low-pressure coating method in which an appropriate material source is used to either electrically sputter or evaporate thermally to create the coating atmosphere.

In the deposition chamber, a reactive gas is used for the deposition of compound coatings from an elemental source or to maintain the stereochemistry of coatings from compound sources. In general, the thickness of coatings for wear resistance falls between 1 and 10 μm. Also, thinner layers are used in microelectronics and thicker layers are used for high temperature gas turbine components for corrosion protection.

Advantages

1. Low deposition temperature.
2. Dense, adherent coatings.
3. Excellent process control.

Disadvantages

1. High capital cost since it is a vacuum process.
2. All sizes of components cannot be treated.
3. Coating rate is quite slow.

- **Chemical Vapor Deposition:**

A procedure called Chemical Vapor Deposition (CVD) uses gaseous reagents to react in a vacuum tank., for a deposit to accumulate on the surface of the sample. Between C and C is the temperature range in which the deposition is done. Due to this high temperature associated with CVD, there are chances of thermal distortion and chemical reaction. So, the choice of substrate is limited. The primary application of these processes is the deposition of ceramics, including alumina (Al2O3), titanium carbide (TiC), and titanium nitride (TiN). The coating thickness is limited to about 10 μm for

these materials. The coating of sharp-edged components is restricted since there are chances of mismatch stresses which develop on cooling due to thermal expansion.

Advantages:

1. Coating hardness is high.
2. For thinner coatings, adhesion is quite good.
3. Coating is adequately uniform due to high throwing power.

Disadvantages:

1. Since it is a high temperature process, there are chances of distortion.
2. Chances of mismatch of stresses due to thermal expanses, so difficult to coat sharp edges.

- **Electroless Coating:**

Electroless coating process is also known as auto-catalytic plating process. The reaction occurs when the reducing agent (sodium hypophosphite) gets reduced to release hydrogen and this hydrogen gets oxidized thus producing a negative charge on the surface of the substrate. Electroless nickel coating is the most widely used electroless coating process. Electroless nickel plating occurs by creating a thin nickel phosphate layer on the substrate. The coating layer's thickness is expressed in μm. Substate preparation is a crucial stage prior to the coating process. The surface of the substrate has to be cleaned by the application of various acids in order to remove any oil or grease or any foreign particles. If proper surface cleaning is not done, it may result in poor coating. Activation of the surface of the substrate is necessary for proper coating. Activation is normally done before the coating is done with a weak acid etching After the coating process is finished, the coated components are rinsed with pure water in order to prevent unwanted stains. As electroless nickel coating is a non-toxic process, they can be used for medical applications. Various items that are electroless coated includes kitchen utensils, door knobs, , bathroom fixtures, electrical / mechanical tools and office equipment.

Advantages

1. External power source is not required.
2. Uniform coating can be achieved.
3. No restriction in plating volume and coating thickness.

4. Excellent corrosion resistivity.

9. Wear and abrasion resistive.

10. High hardness can be achieved.

11. Friction coefficient is low.

12. Good reflectivity and resistivity

13. Good magnetic properties.

Disadvantages

1. There is a chance of bath decomposition.

2. Lifespan of chemicals is limited.

1.9 Aim of the Work

The primary goal of this work is surface modification of the surgical instruments to resist corrosion and increase their life span. After extensive study of the different surface treatment techniques, electroless coating has been chosen as the surface treatment technique in the present work due to its excellent properties and economic feasibility. The surface is to be coated with two types of coating viz Nickel-Phosphorus (Ni-P) followed by Nickel-phosphorus-polytetrafluorethylene (Ni-P-PTFE) composite coating. Firstly, the effect of nickel alloy (Ni-P) coating is to be studied and then, nickel composite (Ni-P-PTFE) coating on stainless steel (AISI 420 grade) is to be studied. After performing the coatings, the corrosion properties are to be checked for both the coatings. Apart from electrochemical study, some physical and mechanical properties are also to be studied.

1.10 Objective of the present work

The objective of the present work are as follows:

1. To synthesize NiP alloy and Ni-PTFE-P composite electroless coating on stainless steel substrate (grade AISI 410), used for surgical instrument.
2. To perform mechanical, chemical and physical characterization of electroless NiP and Ni-PTFE-P coatings.

3. To compare the corrosion behavior of uncoated, NiP coated and Ni-PTFE-P coated substrate and compare, which one shows better corrosion properties.
4. To create statistical models for Ni-PTFE-P and electroless NiP on a range of process parameters and identify the key variables influencing the response. Also to find the optimum value of the process parameters which gives best results.
5. Lastly and more importantly, to check whether the developed technology is beneficial for the cluster or not. And if so, to transfer and assimilate the developed technology to the cluster members.

1.11 Outline of the Thesis

This thesis work has seven chapters. The brief description of each chapter is given below:

Chapter 1 discusses the aim and objective of the present study. In the first part of the chapter, a detailed discussion has been done on the present scenario of the rural industrial clusters in India. The problems faced by these clusters have been addressed and the steps taken by the Government to address these problems has been discussed. A detailed discussion on Technology transfer and assimilation has been done. And the scope of Business-university-business model for technology transfer has been discussed. Also, as the present work deals with the problems faced by the Baruipur surgical instrument cluster, this chapter gives a detailed picture regarding the cluster, the manufacturing practices followed by the cluster and the practical problems faced by the cluster.

Chapter 2 presents a detailed study on electroless coating technique. The works carried out by different researchers on electroless coating has been reviewed. Different preparation techniques, types of electroless bath, classification of electroless coatings, applications, advantages and disadvantages of electroless coating has been discussed.

Chapter 3 discusses the many statistical methods and instruments applied in this investigation. The importance of Design of experiment, more specifically Central composite design has been discussed in details. Various modelling and optimization techniques used in the present study has been discussed thoroughly.

Chapter 4 describes the experimental details of electroless NiP and Ni-PTFE-P composite coating. The chapter contains the description of the different chemicals used for the coating, instrumental-setup and different characterization techniques involved for evaluation of the coating properties.

Chapter 5 deals with the characterization of electroless NiP and Ni-PTFE-P composite coating. The physical, mechanical and electrochemical properties of both the coatings have been studied in this chapter.

Chapter 6 is related to the statistical evaluation of the gathered data from this study and the optimization of process parameters considering different responses. This chapter deals with the formulation of mathematical model and prediction of the response by varying the input variables.

Chapter 7 discusses about the results and conclusions obtained from the present study. It also discusses about the future scopes of this study and electroless coating.

Chapter 2

Literature review on Electroless coating

Outline of the chapter: *2.1 Introduction 2.2 Objectives of Electroless Nickel-Phosphorus Coating 2.3 Bath Composition 2.4 Applications of Electroless Nickel-Phosphorus Coatings 2.5 Types of Electroless coating 2.6 Properties of Electroless Coating 2.6.1 Physical Properties 2.6.2 Mechanical Properties 2.6.3 Corrosion Properties*

2.1 Introduction

Electroless coating has many good characteristics, such as corrosion and wear resistance, due to which, it has grown significantly in the surface coating industry throughout time. The first discovery of electroless plating was done by Charles Adolphe Wurtz in 1844. However, it did not get much importance during that time. It was again rediscovered by Brenner and Riddle in year 1946 (Sudagar. J., *et al*., 2013). Since then, this subject has been a matter of interest among the researchers. The co-deposition of various other substances along with the coating film has given rise to a new era of electroless coatings, offering a wide range of applications in surface science, engineering, and other domains. Electroless coating has got several advantages over other coating techniques such as electroplating, immersion plating, etc, due to which it has got a huge demand in the market. The most important advantages of electroless coatings are its good adhesion, uniformity, very good corrosion resistivity and wear resistance properties, it can be easily brazed and soldered and also it is biocompatible (Fayyad E.M., *et al.,* 2019). Electroless coating has a wide range of applications in various industries, such as automotive industry, Air craft industry, Chemical industry, Electronics industry, Medical and pharmaceutical industry, etc.

Electroless process is an autocatalytic method where both oxidation and reduction process take place, without any external power supply. Here, the presence of the reducing agent supplies the required electrons to carry out the reaction by oxidizing

itself in the solution. Additionally, metal deposition occurs when the cations of the metal to be deposited are reduced by electrons leaving the substrate. (Brenner & Riddell., 1946).

2.2 Objectives of Electroless Nickel-Phosphorus Coating:

The main objectives of using electroless nickel-phosphorus coating are to provide:

1. Protection against corrosion.
2. Wear (mainly abrasive wear) resistance.
3. Increase in hardness (micro hardness).
4. Increase in lubricity.
5. High temperature resistivity. The melting point of electroless deposited Nickel-phosphorus varies from 890^{o} C (for mid to high phosphorus content) to 1300^{o} C (for low phosphorus content).
6. Low coefficient of thermal expansion ranging from 12×10^{-6} /^{o}C to 14.5×10^{-6} /^{o}C.
7. Thermal conductivity values around 0.15 cal/cm/s/k.
8. Good solder ability and bond ability properties.
9. Uniform deposit regardless of the geometry of the substrate.
10. Non-magnetic properties of high phosphorus nickel alloy.

2.3 Bath composition

An electroless plating bath contains the following components- a metal ion source which is to be deposited, reducing agent which gets reduced, complexing agent, buffering agent, stabilizer, wetting agent and the factors which are to be controlled are temperature and pH level. In electroless plating, when substrate is submerged in an electroless bath, it undergoes certain chemical reactions that cause it to produce a potential. By carefully reducing metallic ions chemically on a catalytic surface, the coating is created. The deposit or coating itself acts as a catalyst for the reduction reaction, which will proceed till the surface is in contact with the bath solution. The purpose of various bath components is shown in Table: 2.1.

Table: 2.1 Components of Electroless Nickel bath and their functions

Component	Function	Chemicals
Nickel ions	metal source	Nickel chloride, Nickel sulphate
Hypophosphite ions	Reducing agents	Sodium hypophosphite, Sodium borohydride, Hydrazine
Complexants	• Acts as a pH buffer • Stabilizes the solution • prevent free Ni ion concentration \	Ammonia, Monocarboxylic acids, di carboxylic acids, hydroxycarboxylic acids,
Accelerators	• Activate hypophosphite ions • accelerate the deposition rate.	Anions of some mono & di carboxylic acids, fluorides, borates
Buffers	• controls the pH of the bath	Sodium salt of certain complexants
Stabilizers	• Prevents bath decomposition	Thiourea, Lead, tin, arsenic, molybdenum, cadmium or thallium ions, , etc
Wetting agent	• Increase wettability • Uniform coating	Surfactants

Temperature: Temperature is the one of the important parameters which affects the rate of deposition. Virtually all acidic hypophosphite baths operate between 85^0C to 95^0 C. It is true in all cases that deposition rate increases with increasing temperature. At high temperatures there is always a danger due to possible instability of the bath. Temperature has an important impact on the amount of phosphorus deposition and, consequently, its characteristics. According to some researchers, deposits from acidic baths under otherwise constant conditions become poorer in phosphorus with the increase in temperature. Therefore, the maintenance of accurate bath temperature in

electroless nickel baths is necessary. In this context it should be recognized that only where, extremely vigorous agitation is used, the bath temperature is uniform and this is especially true for the electrolyte adjacent to the bath heaters. Local over-heating is a danger at all costs and is to be avoided and adequate air agitation will usually guard against this. The accuracy of thermostats used to control bath temperature should be checked periodically, using mercury-in-glass thermometer.

Effect of pH: The lower the bath pH, the greater the phosphorus content of the deposit. Raising the pH has the following effects:

1. Increased deposition rate, in a manner more or less linearly dependent on pH at a given temperature.
2. Hypophosphite reaction gets modified to homogeneous mode from catalytic reaction. A result could be fast decomposition of solution with nickel deposition.
3. The solubility of the nickel-phosphate alloy can decrease. Unwanted components may get deposited which may lead bath decomposition and also may result in rough deposits.
4. The phosphorus content of the deposit may get lowered.

Lowering of the pH can lead to:

1. The deposition of the salts and hydroxides used in the bath can be prevented.
2. The reductive power of the hypophosphite is lowered.
3. Effective buffering action occurs in the bath.
4. For acidic bath when pH is less than 4, the deposition rate may get slower and attack of the deposit by the solution.

Table: 2.2 Relationship between pH and Phosphorus content of deposit (wt %)

pH	Phosphorus Content(wt %)
5.8	2.2
5.0	3.5
4.5	8.9
4.0	11.4
3.0	14.1

2.4 Applications of Electroless Nickel-Phosphorus Coatings:

This coating can not only be applied to conductors but can also be applied to non-conductors and can be used to coat complex shapes. Different substrates can be used for electroless Ni-P coating. To name a few, Plastics, Mild Steels, Stainless Steels, Aluminum and its alloys, copper, etc. The main aspects of importance for electroless Ni-P applications are:

1. Nonconductors can be coated with electroless Ni-P deposits for both decorative and functional aspects.
2. Mild Steel or Aluminum which gets easily oxidized can be protected and the properties of the surface can be enhanced
3. Can be used to produce hard and wear resistive surface for relatively soft substrates.
4. Electroless Ni-P deposit can be more advantageous than hard chromium coating. Specially for internal coatings and for items with complex shapes.

Table: 2.3 Selected Applications of Electroless Ni-P Coatings

Application	**Typical Thickness (μm)**	**Application**	**Typical Thickness (μm)**
1. Motor Industry Industry		**2. Electronics**	
Carburetors	12.5-28	Floppy Discs	7.5-25.9
Gear Wheels	10-38	Switch Gears	2.5-30
Drive Shafts	5-10	Electronic	
Heat Sinks	2.5-7.5	components	2.5-18
Decorative		Resistors	2.5-18
Components	5-18	Disc Drivers	5-7.5
Ceramic Condensers	5-18		
3. Aerospace Industries		**4. Chemical Industry**	
Compressor Parts	7.5-38	Filters	12.5-200

Couplings	15-38	Pressure Cylinders	75-200
Motor Bearings	7.5-38	Pipes & Pipework	25.4-75
Drive Trains	25-50	Pump & Blower Housings	38-100
Hydraulic Components	12.5-38		

5. Mining Industry

Drilling Component	7.5-50
Conveyor Loaders	12.5-50
Hydraulic Cylinders	30-100
Pressure Cylinders	18-75

6. Material Handling

Conveyors	25-75
Chains	7-18
Hydraulic Equipment	30-100

7. Production Equipment

Molds	5-250
Associated Equipment	38-100
Extrusion Dies	7.5-50
Gears & Bearings	12.5-38
Piping	18-125

8. Transport Industry

Shafts for Diesel Engines	7-38
Engine Valves	12-25
Valve Shafts	7-38
Drive Components	18-30

9. Oil & Gas Industry

Valves	30-100
Pipe Castings	25-75
Conveyor Components	25-75
Exhaust Pipes	30-75

10. Textile Industry

Extrusion Nozzles	18-130
Needles	18-130
Filament Guides	18-130

11.Armaments Industry

Explosion Chamber	7.5-18
Laser Mirrors	12.5-100
Marine Vessel Equipment	38-100
Tracked Vehicles	38-50
Rollers	20-75

12. Food Industry & Meat Processing

Cutting Knives	18-38
Conveyor Chains	30-50
Meat Hooks	38-50

2.5. Types of Electroless coating

Various types of electroless coatings have been developed over the years to fulfil different industrial requirements. Apart from coating with pure nickel, various other elements can be co deposited for achieving desired physical and mechanical property of the coating. Metals such as Cu, Co, Pd, W, Au or Ag are used in the alloy coating. Additionally, researchers are focusing on co-deposition of various soft or hard particles in the electroless coating matrix. This is known as composite coating.

2.5.1 Nickel alloy

The addition of another metal element into the electroless coating in order to enhance its properties for some particular applications, is called alloy coating. Sometimes, when a single metal is co-deposited along with the electroless deposits, it is known as Binary coating. When more than one metal is co-deposited, it is called ternary or quaternary alloy coating.

2.5.2 Binary alloy coating

In general, there are two types of binary coating- Nickel phosphorus and Nickel boron coatings. It mainly depends upon the reducing agent. For sodium hypophosphite baths, Ni-P coating is obtained. When borohydride or amine borane acts as the reducing agent, Ni-B coating is obtained.

Ni-P coating can be obtained with two types of baths-Acidic bath and Alkaline bath. Hot acid baths are used exclusively for thick deposits. A normal coating bath consists of- nickel sulphate (30-35 g/l), sodium hypophosphite (20-25 g/l), lactic acid (25-30 g/l), sodium succinate (15-20 g/l), and lead (0.002-0.005 g/l). And the other parameters are 5–6 pH level and 85–95 ^{o}C temperature. At high temperatures, alkaline baths are unstable. However, alkaline bath can be used at low temperature for depositing nickel on plastic. A standard alkaline bath's ingredients could comprise 20-25 g/l nickel chloride, 20-25 g/l sodium hypophosphite, 45-48 g/l sodium citrate, and 30-35 g/l ammonium chloride. A pH of 8–9 and temperature of 30–40 ^{o}C is to be maintained. A lot of work has been done on NiP electroless coating by different researchers (Li. Z. H,.*et al*.,2009 ; Palaniappa & Seshadri., 2008 ; Sahoo., 2009; Yan. M., *et al*., 2008) . Similarly, Ni-B coatings can also be obtained on acidic as well as

alkaline baths. A hot acidic bath is more stable and melting point of the deposits are very high of the order of 1350 ^{o}C. An acidic bath's usual makeup has nickel chloride (30=35 g/l), diethylamine borane (3-5 g/l), methanol (40-45 g/l), dimethylamine borane (DMAB) (4-6 g/l), sodium acetate (20=25 g/l), sodium succinate (20=25 g/l), and sodium citrate (10-15 g/l). 50–60 ^{o}C temperature and 5–6 pH is to be maintained. Because the as-plated hardness of nickel bromide coatings is higher than that of nickel paraffin coatings, nickel bromide coatings are more frequently employed for industrial wear applications. An alkaline cold bath composition consists of: nickel sulphate (30-35 g/l), dimethylamine borane (3-5 g/l), ammonium citrate (15-20 g/l), ammonium chloride (15-20 g/l), and 2-metcaptobenzothiazole (0.0002-.00005 g/l). And a pH 7-8, and temperature of 25–30 ^{o}C. Alkaline baths are used at low temperatures as they are very unstable at high temperatures. (Krishnaveni. K., *et al*., 2005; Oraon. B., *et al*., 2008; Vitry. V., *et al*., 2008) have worked on Ni-B alloy coatings.

2.5.3 Ternary and Quaternary alloy coating

Ternary and quaternary alloy coatings find applications in places where excellent resistance to temperature characteristics, electrical properties, either non-magnetic or magnetic qualities are required. Mixture of various elements are coated over the substrate for different applications with desired physical and mechanical properties. Economic viability and sustainability are the two key criteria that determine which alloy is best for coating.

Balaraju and Rajam developed Ni–Cu–P and Ni–W–P alloy coatings and investigated how tungsten and copper affected the NiP coating. It was found from the study that due to the addition of tungsten into the bath, there was a little rise in grain size and a decrease in the amount of phosphorus. Quaternary coating, Ni–W–Cu–P, was also developed by adding Cu in Ni-W-P bath. Coarse nodules were identified in the ternary Ni–Cu–P and Ni–W–P deposits by the SEM analysis, but after the quaternary bath developed, the deposit became extremely smooth (Balaraju & Rajam., 2005). For nanowire arrays, uniform electroless Ni–W–P alloy coatings were created in large-scale (Yuan. X.Y., *et al*., 2004). The findings demonstrated that adding tungsten to the Ni–P coating improved its mechanical and thermal stability. Wang developed ternary Ni–Fe–P alloy coatings. The buffering agent and

complexant employed by the author were boric acid and sodium citrate. The study revealed that the deposition of the alloy was restricted by the production of ferrous sulphate in the coating bath. The iron percentage in the coating was found to be not more than 15.6 atomic percentage. However, the addition of iron improved the coatings' mechanical qualities since the content increased., the phosphorus content decreased (Wang. S.L, 2004) . Duhin suggested a unique methodology for developing Ni-Si coatings. The author electrolessly plated Ni-alloys (Ni-P, Ni-W-P, and Ni-W-B) on p-type Silicon using amino propyl triethoxysilane (APTS) activated with Pd citrate (Duhin. A., *et al*., 2009). Valova developed hybrid multilayered Ni–Cu–P/Ti/ TiN deposits on mild steel, It was observed that the hybrid coatings exhibited improved values of friction coefficient and nano-hardness as compared to binary Ni–Cu–P on mild steel **(**Valova. E**.,** *et al***.,** 2010). So, according to the scientists, these kinds of hybrid multilayered coatings, when the right materials are added, can simultaneously improve mechanical and corrosion resistance.

2.5.4 Nickel composite

Electroless composite coatings are created by co-depositing non-metals with electroless coatings. To obtain the necessary qualities, electroless coating is co-deposited with solid lubricants like polytetrafluoroethylene (PTFE) and hard particles like silicon carbide, diamond, and aluminium oxide. Earlier, it was difficult to develop electroless composite coatings due to bath decomposition. However, the addition of surfactants, which disperse the small particles, increased the electroless bath's surface area by around 700–800 times compared to a typical electroless bath, causing the bath to become unstable. However, electroless nickel composite coatings were effectively created with the aid of appropriate stabilizers.

Co-deposition of dispersible SiO_2 nanoparticles and electroless Ni-P coating was developed on steel (Grade AISI 1045) substrates without the use of surfactants in the plating solution (Dong. D., *et al*., 2009). The resulting composite coatings are subjected to three different temperatures—200°C, 400°C, and 600°C—for a whole hour. The investigation revealed that the adding of SiO_2 particles enhanced the electroless Ni–P coating's hardness and wear resistance., and maximum hardness and wear resistance was obtained when heat-treated at about 400°C. On an Al–10Si–

0.3Mg substrate, the electroless Ni-P and Ni-P-Al_2O_3 composite coatings' tribological properties were investigated. The coated samples were heated at 400–550 ° C for 1–8 h. After performing all the experiments, the optimal heat treatment regime which gives the best coating properties was found to be 400 °C for 1 h. The authors came to the conclusion that heating above 450° produced intermetallic compounds, which reduced the coating's ability to withstand wear (Novák. M., *et al*., 2010). Winowlin developed NiP/diamond composite coating and examined its wear properties both prior to and following heat treatment. The results showed that due to formation of phosphides after heat treatment at around 350 °C, a significant increase in wear resistance was observed (Winowlin. J., *et al*., 2009) .Hosseinabadi incorporated B_4C into Ni-P matrix to increase its wear resistance properties. The results showed that the optimal amount of Boron carbide to achieve best wear properties was found to be 25 volume percentage (Hosseinabadi. E., *et al*., 2006). Srinivasan & John investigated the impact of adding PTFE to an acidic bath with no electroless nickel. The maximum wear resistivity was achieved by the authors by incorporating 18–25 percent PTFE into electroless nickel deposits. This wear resistivity was then further enhanced by heat treating the material at 400°C (Srinivasan & John, 2005). The properties of composite coatings made of nickel and carbon nanotubes (Ni/CNTs) on carbon steel substrates. via electroless deposition was investigated. Examining the wear and friction characteristics in dry sliding circumstances was done with a ball-on-disk arrangement. The microhardness of the Ni/CNT coating was found to be 865 HV. The authors concluded that due to typical structure of the hollow nanotubes, the composite coating resulted to enhanced mechanical properties (Chen X. H. *et al*.,2006).

2.5.5 Nano coating

Nanocoating are defined in two ways. One type is to have the thickness of the coatings in nanoscale and the second type is when the nano sized particles are being dispersed into the matrix. In the last ten years, several researchers have focused on regulating the parameters of the Ni-P electroless composite coating to co-deposit second phase nanoparticles in the NiP matrix. The most important ones amidst them are Al_2O_3, SiC, CeO_2, $ZnSiO_3$, $ZnSnO_3$ and nanometre diamond (ND). In order to create Ni-P-SiC composite coatings, Jiaqiang created superfine silicon carbide (SiC) particles. Because superfine particles were present, the Ni–P alloy coating was not as

microhard as the electroless composite coating (Jiaqiang, G., et al., 2006). After one hour of annealing at 400 °C, the microhardness increased even further (1200 HV50). Two types of NiP composite coatings was developed by Sarret. The authors attempted to include SiC and Si3N4 particles in the NiP matrix. The sizes of the particles range from 30 nm to 2 μm. After performing the experiments, the author found that for inclusion of micron-sized particles, the inclusion of carbide and nitride differs minimally. But, for nano-particles, the difference in the properties are significant enough (Sarret. M., *et al*., 2006). Dong attempted to coat AISI 1045 steel substrates with dispersible SiO_2 nanoparticles in a NiP matrix without the use of surfactants in the coating solution. The as coated composite coatings were heat-treated for 1 h at three different temperatures such as 200 °C, 400 °C, and 600 °C, respectively. The coating's hardness and wear resistance were increased by the addition of SiO_2 nanoparticles. Maximum hardness and wear resistance the composite coating was achieved when annealed at about 400 °C (Dong. D., *et al*., 2009).

2.6. Properties of Electroless Coating

Electroless coating method is an efficient method to produce different types of coatings according to requirement. Depending upon the bath composition of binary alloy coating, varying percentage of phosphorus (2-14%) and boron (1-10%) can be deposited. This variation in percentage of phosphorus or boron can significantly affect the properties of the deposited film. NiP coatings exhibit good hardness, good lubricity, good corrosion resistivity and are solderable. NiB coatings have almost same properties as that of NiP coatings except a few. Heat treated NiB coatings have very high hardness. They have excellent resistance to wear and abrasion. However, their corrosion resistivity is less than that of NiP coatings. Typical properties of electroless coatings are discussed in details in the following sections.

2.6.1 Physical properties

Structure

At low (3-5%) and medium (6-9%) phosphorous level, the structure of the coatings is generally amorphous in nature, however, sometimes they also show micro crystallinity in their structure. However, at high phosphorous level (10-14%), the structure is purely amorphous in nature (Dong.D., *et al*., 2009). After heat treatment above 400^{o}C, Ni_3P phase is obtained. It has been discovered that Ni-P begins transition from an amorphous to a crystalline form at temperatures over 220–260 ^{o}C. However, Ni_3P phase starts forming at a temperature above 320 ^{o}C and transforms into fully crystalline structure after heating at temperature above 400 ^{o}C for 1 h (Palaniappa & Seshadri, 2008). A matrix of nickel phosphite is formed when phosphorus content is above 9%, however at low phosphorus content, the dominant phase in the deposit is found to be pure nickel. For achieving higher hardness, corrosion resistance and wear resistance, heat treatment is required. In case of NiB coatings, Ni_2B phase having glass structure mixed with crystalline nickel is obtained, when the boron content is about 5**%** (Krishnaveni. K., *et al*., 2005). A study done by Yu and Zhang concludes that NiB also starts to crystallize above 250 ^{o}C and transforms to fully crystalline structure at 370–380 ^{o}C (Yu & Zhang, 1994a).

For nickel composite coatings, the structure is not much altered by adding Si_3N_4, CeO_2 and TiO_2 (Balaraju. J., *et al*., 2006)**.** It was observed that Ni-P-CNT, Ni-P-SiC and Ni-P-graphite coatings are amorphous in nature and change to purely crystalline form after heat treatment (Chen. X., *et al*., 2006). Also, few authors studied the effect of addition of Si_3N_4 particles in Ni–P matrix. It was found from the study that the addition of Si_3N_4 particles did not significantly alter the composite coating's structure. However, it did help to increase the number of nucleation sites, the degree of crystallization, and microstructural stability (Balaraju & Rajam., 2007 ; Pancrecious. M., *et al*., 2018) .

Melting Point

Electroless NiP deposits have melting range instead of a particular melting point. The melting point of pure nickel is about 1455 ^{o}C but in a study, it was concluded that the coatings' melting point drops as the phosphorus level rises.
The coatings have the highest melting points, approximately 1200 ^{o}C, at low

phosphorus levels (less than 3%), whereas the deposits have the lowest melting points, approximately 880 ^{o}C, with high phosphorous contents, approximately 11% or more (Balaraju J., *et al*., 2003). It has been observed that Ni–B coatings have relatively higher melting points. The coatings have a melting point of roughly 1080 ^{o}C when sodium borohydride is used as the reducing agent, and between 1350 and 1360 ^{o}C when DMAB is utilized.

Electrical property

Electroless nickel alloys possess high electrical resistivity compared to that of pure nickel coating (Keong & Sha, 2002). Pure nickel coating has electrical resistivity of $7.8x10^{-6}$ Ω cm. In alloy coating, resistivity increases with the increase in phosphorus content and ranges within 30-100 $x10^{-6}$ Ω cm (Sudagar. J.,*et al.*, 2013). However, upon heat treatment, the conductivity of the deposits increases. The electrical resistivity of NiB coatings for 5% boron is about 89 $x10^{-6}$ Ω cm. Due to high conductivity, NiB coatings are widely used in electronic industries.

2.6.2 Mechanical Properties

A coating's mechanical qualities are mostly determined by the deposit's phosphorus or boron concentration. In case of alloy coatings, the properties depend on the third metal added to the NiP matrix. In case of composite coating, addition of third element into the matrix results in varied properties of the coating to a large extent. Addition of hard particles such as diamond, SiC, TiO_2 results in increase of the wear resistance, whilst inclusion of soft materials like polytetrafluorethylene (PTFE) increases the lubricity of the coating. Here, the mechanical properties on electroless nickel coatings have been discussed in details.

Hardness

The hardness of as-deposited electroless NiP and NiB coatings lie in the range 550-700 $HV_{0.1}$ which is equivalent to the hardness of many hardened alloy steels. On the contrary, as-deposited electrolytically deposited nickel lies in the range 150–400 $HV_{0.1}$, which is much lower (Keong. K., *et al*., 2003). The hardness of electroless nickel coatings reach up to 1200 $HV_{0.1}$ after heat treatment. Yan developed a NiP coating of 8% phosphorus content with hardness value of 910 $HV_{0.1}$ in as-deposited condition, The bath's lactic acid to acetic acid ratio was adjusted by the authors. The

hardness of the heat-treated coatings increases due precipitation of nickel phosphide phase. The hardness is increased because the phosphides act as barriers to dislocation movement (Yan M.,*et al*.,2008). However, excessive annealing causes grain coarsening, which decreases hardness by increasing dislocation propagation and causing surface brittleness. (Dong. D., *et al*., 2009; Palaniappa & Seshadri, 2008). The as-deposited electroless nickel boron deposits posses' high hardness and excellent mechanical wear resistance. A parametric optimization was performed by B Oraon and achieved a hardness of 1400 $HV_{0.1}$ of NiB coating at the optimized parameter setting (Oraon. B., *et al*., 2008). Also, nitridation was done for Ni–B coating by placing the samples in pure nitrogen vacuum. The hardness increased up to 1500 $HV_{0.1}$ for the nitrided samples (Vitry. V., *et al*., 2008). The hot hardness ability of the coatings depends upon the percentage of phosphorus or boron. It increases with increase of P/B content. Since the composite coatings posses very high hardness values, they are widely used in various fields such as metal patterns like moulds, extruders for plastics, forging dies, core boxes, etc. Incorporation of hard ceramic particles results in increase of hardness whereas for soft particles, the hardness decreases. The hardness of the coatings mainly depends on three important factors: The proportion of the additional element, the matrix's phosphorus level, and the heat treatment.

A new Ni-P-TiO2 composite coating was produced by incorporating transparent TiO2 sol into the electroless solution. Microhardness levels were found to have significantly increased. The traditional Ni-P-TiO2 coating's microhardness value increased to 1025 HV0.2 from 710 HV0.2 (Chen, W., et al. (2010). The Ni-Zn-P-TiO2 composite coatings produced by Ranganatha were shown to have a substantially higher hardness than pure Ni-Zn-P alloy (Ranganatha. S., et al., 2010.

Friction

Friction is aversion to sliding motion. It is a very vital factor which decides effectiveness of any mechanism involving sliding movement. It also effects wear of any component to some extent. Coatings allow the surface to spontaneously lubricate itself. Electroless NiP coatings itself possess very good lubrication property due to the presence of phosphorus and also their unique nodular cauliflower like

microstructure (Delaunois & Lienard., 2002), (Balaraju. J., *et al*., 2006). However, incorporation of some other particles or element results in improved lubrication properties of the coatings. The addition of hard particles like B_4C, SiC, etc show poor lubricating characteristics as compared to electroless Ni–P deposits. However, soft particles like MoS_2, PTFE, and graphite can inhibit adhesion between the mating surfaces, which makes them effective lubricants. The effect of addition of PTFE in NiP matrix was studied and it was concluded reason behind the low coefficient of friction is mainly because of scraping and the formation of PTFE transfer film (Yu & Zhang, 1994).Another author also found from their investigation that smaller coefficient of friction value for composite coatings is much lower than electroless Ni-P deposits, as-plated condition and also when heat treated at 400 ^oC for 1 h. Thay also concluded that friction decreases with increasing percentage of PTFE (Ramalho & Miranda, 2005). When PTFE was added, the electroless Ni-P-PTFE composite coating that Liu produced showed a 70% decrease in the NiP coating's friction coefficient (Liu. W., et al., 2006). Wu created a hybrid composite coating of Ni–P–Gr–SiC that also displayed a decreased coefficient of friction because graphite-rich mechanical mixed layer (GRMML) formed on the contact surface. They found that the temperature rise of the hybrid coating is much less than that of Ni-P-SiC composite coating which means good anti friction property of the hybrid coating (Wu, Shen, *et al*., 2006). Ni-P-MoS_2 nano composite coating was developed by Hu and they found that coefficient of friction value of the composite coating is much lesser than that of Ni-P electroless coatings (Hu.X., *et al.*, 2009). The authored also prepared Ni-P-CNT composite coatings on carbon steel substrate by electroless deposition. In comparison to Ni-P and Ni-SiC-P coatings, it was found that the Ni-P-CNT composite coating has a substantially reduced friction coefficient.

Wear resistance

The enhancement of wear resistivity is a crucial component of electroless Ni-P composite coating. The three main parameters that determine wear resistivity of composite deposits are similar to those that determine hardness: the kind, size, and quantity of the inserted particles. Straffelini investigated and compared the nature of wear of several electroless Ni–P composite deposits. With reference to Ni-P deposit,

composite coatings containing SiC, PTFE, MoS_2 and B_4N particles were developed. When the sliding behaviour of the Ni-P deposit was examined, it was found that the deposits wear down gradually. The deposit experiences mild abrasive wear in the first stage, followed by acute wear and debris separation in the second stage. The best sliding behaviour was shown by the Ni-P-PTFE and Ni-P-MoS_2 coatings and the wear rate for both the coatings was almost negligible in the first stage (Straffelini. G., *et al*., 1999). The Ni-P-SiC composite coating was created by (Broszeit, E., 1982). It was found that the wear of the composite coatings is much less than that of NiP coatings until 350 °C. Further rise in temperature results in weight loss and reaches to a maximum at 650°C. However, the wear rate starts to decrease once the temperature goes above 650 °C. But, above that temperature, again an increase in wear rate is seen. The authors concluded that around 580 ^oC, a reaction takes place between nickel and SiC due to which wear rate increases. Above 650^oC, when the temperature reaches to 880^o, Ni-P reaches its eutectic point due to which partial melting occurs and so an increase in wear rate is seen. Another researcher developed Ni–P–B_4N composite coating on AISI 316L stainless steel substrate and examined its wear behaviour by conducting sliding wear tests at room temperature using a pin-on-disc setup. The researchers discovered that up to 11 volume percent of the coatings exhibit a wear mechanism that combines abrasive and adhesive wear. Considerable plastic strain and a gentle adhesive wear mechanism of the coatings were noted as the B_4N content increased beyond 11 volume percentage. The authors also reported that the wear decreased by half of its magnitude when 33 volume percentage of B_4N is incorporated the Ni–P matrix (León. O., *et al*., 2005). Reddy studied the wear behaviour of the Ni-P-diamond composite coating. The effect of heat treatment, phosphorus content and particle size were studied. The results showed that the thickness to particle size ratio had a substantial impact on the coating's wear resistance. The authors also found that the wear resistance was higher when the diamond particles are finer (3–6μm) rather than coarse diamond particles. It was also observed that phosphorus content is directly proportional to wear resistance. However, in all cases, the coatings showed higher wear resistance after heat treatment above 350 ^oC, due to better diffusion of nickel into the matrix (Reddy. V., *et al*., 2000).

2.6.3 Corrosion properties

NiP coatings have good corrosion resistivity and has got many applications in different environments where corrosion is a problem. By acting as a barrier, the coating keeps the substrate's surface from oxidizing. In contrast to pure nickel or chromium alloys, The coating resists corrosion to a considerable degree because of its amorphous nature. Polycrystalline materials are less resistant to corrosion than amorphous alloys. Islam performed a comparative study of corrosion resistance behaviour of NiP and composite coating. The author studied the corrosion behaviour in a 4wt% NaCl salt solution using the EIS approach. For pure Ni–P coatings, it is evident that NiP coating with medium phosphorus content offers good corrosion resistivity. However, the results showed that the addition of second phase element resulted in decrease of corrosion resistivity (Islam. M., *et al*., 2013). Ni-P-Al_2O_3 and Ni-P-SiC are the two composite coatings with the best qualities overall. However, after many days in a NaCl solution, the Ni-P-CNT coating shows the least amount of structural damage. Another author observed that phosphorus content plays an important role on the corrosion resistive property of NiP coating. The authors performed corrosion test of NiP coatings for various percentage of phosphorus. The corrosion resistance is ranked as follows: Ni-high P, Ni-medium P, and Ni-low P. The reason behind the difference in corrosion resistivity with varying amount of phosphorus content is due to the difference in the structure (Narayanan. S., *et al*., 2006). As low phosphorus coating has a crystalline, inhomogeneous structure, it possesses low corrosion resistivity whereas for a high phosphorus content, the structure is amorphous and homogeneous in nature due to which it has good corrosion resistivity. Besides structure and homogeneity, electronic effects are also considered to be responsible. It has been observed that even at the open circuit potential, dissolution of nickel occurs which leads to enriched phosphorus at surface. A layer of hypophosphite anions ($H_2PO_2^-$) is formed when phosphorus layer reacts with water. This layer acts as a hindrance due to which water does not reach the electrode surface, whereby preventing nickel to get hydrated. This is the reason behind higher corrosion resistivity of high phosphorus percentage Ni-P coating. This phenomenon is not able to occur when the phosphorus content is low. A 3.5% NaCl solution as the electrolyte and the conventional salt spray test was used to look at the high phosphorous (12% to 14%) content of Ni-P deposits' resistance to corrosion. After an

immersion period of 0.5-hour, EIS test was performed followed by polarization test. On the deposit, a disintegrating passivation film began to form at the beginning of immersion. Immersion time was slowly increased from 2 days to 6 days, then 13 days and at last 29 days. Slowly, with increasing immersion periods, passivation phenomenon also increased. Two-time constants that were obtained from the EIS spectra also represented the creation of the passivation film. The XRD and FE-SEM data verified the deposits' amorphous nature. Pinholes appeared on the deposit after a normal salt spray test lasting 15 days, and the surface of the deposit appeared to have a higher pH, which caused a passivation coating to form (Gao et al., 2007). Compared to Ni-P coatings, electroless Ni-B coatings are less corrosion resistant (Baskaran.L., *et al*., 2009). Chen studied the effect of Cu on corrosion resistivity of Ni-Cu-P alloy coating using electrochemical examination. The authors found that the Ni–Cu–P alloy has higher corrosion resistance than that of Ni-P alloy. It was observed that the passivation layer that was produced on ternary Ni-Cu-P exhibited p-n type bipolar semiconductor behaviour, In contrast, in a 3.5 weight percent NaCl solution, the Ni-P coating exhibited a passivation film with just one p-type semiconductor characteristic Chen. J., *et al*., 2019).

In general, the corrosion resistivity of Ni-P alloy coating is higher than that of composite coating. The second phase element present in the nickel matrix results in lower passivity and corrosion resistance. Researchers came up with another way of coating, known as duplex coating, which could give better results in terms of corrosion resistivity and also other enhanced properties. In duplex coating, the substrate is firstly coated with electroless Ni–P coating and after that, composite layer of coating is applied. **(**Balaraju. J., *et al*., 2006**)**. However, reviewers have noted that certain researchers have achieved good corrosion resistance with electroless Ni–P composite coatings.

(Dhakal.D., *et al.,* 2020) developed electroless Ni-P-TaC composite coating with almost 12 weight percent of TaC in the coating matrix on copper substrate. The author reported that 10g/L of TaC particles were used for plating. A study was conducted to compare the various properties of coating and electroless Ni-P. surface morphology, microhardness, and coating corrosion behaviour were the characteristics that were examined. After heat treatment, the results indicated that the Ni-P-TaC composite coating produced the best outcomes. The reason behind good corrosion resistivity

was compactness of the deposit. Also, incorporation of TaC led to reduction of inter-nodular spaces. And the formation of Ni_3P phase after heat treatment also increases the corrosion resistivity (Dhakal.D., *et al.,* 2020). Farzaneh studied the effect of the introducing SiC nanoparticles on corrosion properties both before and after and heat treatment of electroless Ni-P-SiC coating. The authors have used Bode plots and Nyquist plots to study the electrochemical nature of the coatings. It was observed that corrosion performance was enhanced by co-deposition of SiC nanoparticles. The reason may be un availability of effective metallic surface due to introduction of SiC particles into the matrix. However, it was found that when the concentration of SiC is increased beyond 2g/lit, the corrosion resistance starts to deteriorate. As in most of the cases, amorphous structure can be seen for as deposited coating and after heat treatment, the structure becomes crystalline in nature. In case of Ni-P-SiC also, the corrosion resistivity increased after heat treatment (Farzaneh.A., *et al.,* 2013). In terms of corrosion resistivity, heat treatment at 400 ◦C produced better results than as-deposited coating and coating heat treated at 700 ◦C. (Araghi & Paydar, 2010) studied the corrosion behaviour of electroless Ni-P-B_4C composite coating on AZ91D alloy substrate by extrapolating polarization curves to assess corrosion current densities, It was found that 350 $\mu A/cm^2$ was the corrosion current density for an untreated substrate. The current density for the composite coating dropped to 84 $\mu A/cm^2$, whereas the current density for the basic NiP coating was determined to be 7 $\mu A/cm^2$. From the polarization tests, the authors concluded that though composite coating showed better results than the uncoated substrate, but, the best corrosion performance was shown by NiP coating (Araghi & Paydar, 2010).

Chapter 3

Statistical Tools and Techniques

Outline of the chapter: *3.1 Introduction 3.2 Design of Experiment (DOE) 3.3 Basic principles of experimental design 3.4 Factorial design of experiments 3.5 Central Composite design (CCD) 3.6 Response Surface Methodology (RSM) 3.7 ANN Modelling 3..7.1 Parameters of ANN Model 3.8 Optimization techniques 3.8.1 Non dominated sorting Genetic Algorithm (NSGA)*

3.1 Introduction

In this study, the steel substrate's surface qualities have been improved through the application of Ni-based electroless coating. A variety of statistical modeling and optimization techniques have been applied to obtain the intended outcomes. In this chapter, the statistical tools and techniques used in this work has been discussed.

3.2 Design of Experiment (DOE)

A crucial component of the scientific (or technical) method is experimentation. A carefully planned experiment is crucial since the way the data were gathered has a significant impact on the findings and inferences that may be made from it. Systems and process performance is studied through experiments. The model depicted in Figure 3.1 can be used to illustrate the system or process. A process is any method that converts an input, usually a material, into an output that has any number of response variables that can be seen. While some process variables and material characteristics (x1, x2,, xp) are changeable, some variables (z1, z2,..., zq) are not (although they may be controllable for testing reasons). ((Montgomery, D. C., 2012).). The following could be among the experiment's goals:

1. Figuring out which factors have the most effects on the reaction y.

2. Figuring out where to put the significant x's such that y is nearly always close to the intended nominal value.

3. Figuring out where to place the influential x's to minimize y's variability .

4. Figuring out where to put the important x's to minimize the impact of the uncontrollable factors z1, z2,..., zq.

Design of experiment's is a technique for conducting tests, or a set of tests, with deliberate modifications made to the system's or process's controllable input variables. It makes it easier to watch and pinpoint the causes of variations in the answers. Planning experiments should adhere to the Design of Experiments (DOE), which is a scientific and systematic approach. The process of organizing an experiment to ensure that relevant data are gathered, evaluated, and reported using statistical techniques to produce reliable and impartial results is known as statistical design of experiments. Statistics must be applied to the experimental design in order to get meaningful conclusions from the data.

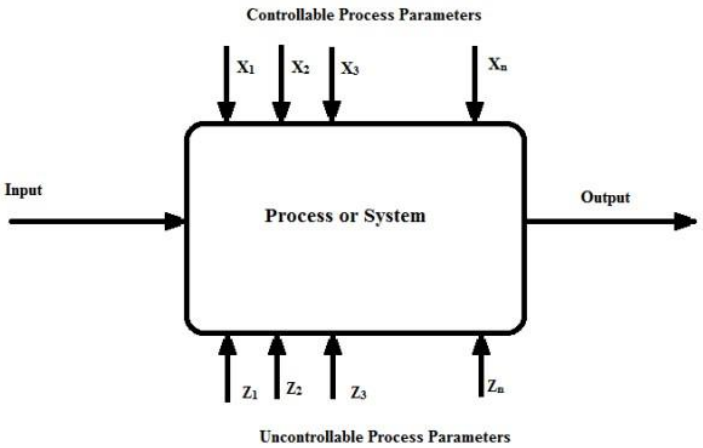

Fig.3.1: General Model of the process or system for Design of Experiment(Montgomery, D. C., 2012).

3.3 Basic principles of experimental design

1. **Randomization**: The distribution of the experimental materials and the sequencing of the various experiment runs are both subject to randomization. For statistical procedures to work, the data must be random variables with independent distributions. When randomization is done correctly, the impacts of any extraneous elements are "averaged out."

2. **Replication**: It denotes a separate iteration of every factor combination. Replication has two key characteristics. The first benefit is that it makes it possible to estimate the experimental error. It acts as a basic unit of measurement for determining the statistical significance of the observed differences in the data. Second, replication enables the researcher to determine a parameter with greater accuracy. provided the genuine mean response for one of the experiment's factor levels is estimated using the sample mean.

3. **Blocking**: It's a design technique meant to increase the accuracy of comparisons between the relevant factors. By lowering or getting rid of annoyance factors, or other influences that might have an impact on the experimental response but aren't specifically related to our study—we can minimize or completely remove the variability they transmit.

3.4 Factorial design of experiments

Multiple factors are involved simultaneously in factorial studies, and each component has two or more levels. The factorial design is used to examine both the primary effects and the interactions between many components. Full factorial designs (FFDs) are powerful tools that offers the most thorough understanding of a system's behavior because they take into account the impacts of all factors (major effects) and their interactions with one another. The total number of runs equals n^k if every factor k has the same number of levels.

The three key ideas of fractional factorial designs are as follows.

• The principle of sparseness of effects: It states that in situations when a large number of variables are present, preferably, a few major impacts with low order interactions should predominate when determining the systems or processes.

• The projection property: In the subset of significant factors, fractional factorial designs can be combined to create stronger designs.

• Sequential experimentation: To put together a larger design in order to assess the relevant factor effects and consequences, we must combine the runs of two or more fractional factorials.

3.5 Central Composite design (CCD)

The CCD architecture is a very good fit for the second-order model. Utilizing nF factorial runs, nC centre runs, and 2k axial or star runs, the CCD comprises of two thousand factorials. The CCD for k = 2 and k = 3 factors is displayed in Figure 3.2.

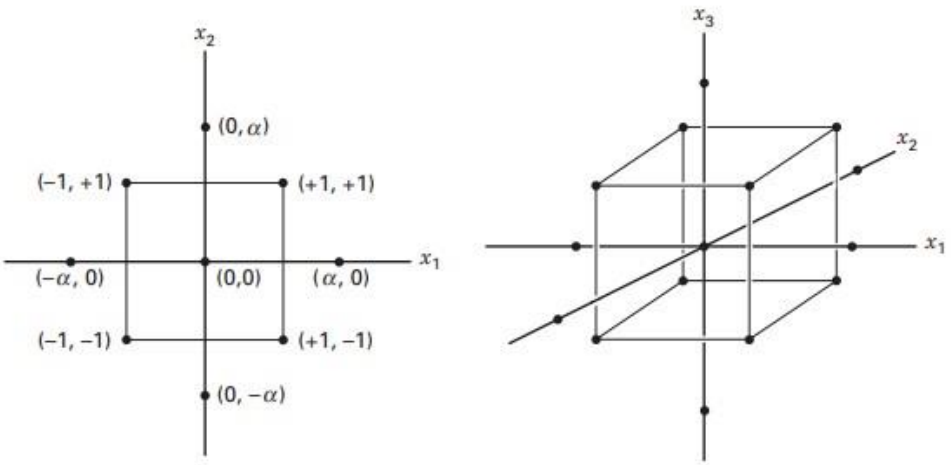

Figure 3.2: Points of Central composite design

Two design criteria that must be specified are the number of centre points and the axial runs' separation from the conceptual centre. The selection of α allows for the rotation of a central composite design. The value of α for rotatability is determined by the quantity of points in the design's factorial stage. It is chosen as follows (Montgomery, D. C., 2012):

$\alpha = \pm\sqrt[4]{n_f}$

where,

n_f = number of factorial points = 2^k

n_a = number of axial points = 2k

n_c = number of central points, (should be adopted)

Transformation from Actual to Coded values may be established in the following way (Oraon, B. et al., 2006.):

Let, Z_i = actual value of the i th process parameter.

X_i = coded value of the i th process parameter.

Z_i^{max}= maximum actual value of the i th process parameter.

Z_i^{min}= minimum actual value of the i th process parameter.

Z_i^0 = central point of the design or the basic level i th parameter.

ΔZ_i^0 = unit or interval of variation on the $Z_i$axis

Therefore,

$$Z_i^0 = \frac{Z_i^{max} + Z_i^{min}}{2}$$

$$\Delta Z_i^0 = \frac{Z_i^{max} - Z_i^{min}}{2}$$

$$X_i = \frac{Z_i - Z_i^0}{\Delta Z_i^0}$$

3.6 Response Surface Methodology (RSM)

A collection of mathematical and statistical techniques referred to as response surface methodology, or RSM, are used to model and evaluate scenarios where the objective is to optimize a response and where a number of variables affect the response. It is uncertain how the response and the input variables relate to one another in the majority of RSM instances. Thus, the first step in the RSM process is to identify a functional relationship between the response and the set of independent variables. Typically, a low-order polynomial is used initially. A function is a first-order model if it can accurately represent the answer as a linear function of the independent variables:

$$y = \beta_0 + \beta_1 x_1 + \beta_2 x_2 + ,,, + \beta_i x_i + \varepsilon \quad (3.1)$$

A polynomial of higher degree is required for a more complicated problem; an example of this would be the second-order model, such as

$$y = \beta_i + \sum_{i=1}^{k} \beta_i x_i + \sum_{i=1}^{k} \beta_{ii} x_i^2 + \sum_{i<j} \sum \beta_{ij} x_i x_j + \varepsilon \quad (3.2)$$

Modelling

Linear Regression Model

A Linear regression model can be expressed as

$$y = \beta_0 + \beta_1 x_1 + \beta_2 x_2 + \ldots + \beta_i x_i + \varepsilon \quad (3.3)$$

where,

y = response variable

i = numbers of regressor variables.

Ɛ = Error

β_j = Regression coefficients where *j* = (0,1,…..,k) .

The predicted change in response y per unit change in xj is represented by the parameter β_j, where every other independent factor x_i (i = j) is kept constant. The first order regression equation with two variables can be expressed as:

$$y = \beta_0 + \beta_1 x_1 + \beta_2 x_2 + \varepsilon \quad (3.4)$$

When you include an interaction term in the two-variable first-order model, the equation becomes

$$y = \beta_0 + \beta_1 x_1 + \beta_2 x_2 + \beta_{12} x_1 x_2 + \varepsilon \quad (3.5)$$

If we let $x_3 = x_1 x_2$ and $\beta_{12} = \beta_3$, then Equation can be written as

$$y = \beta_0 + \beta_1 x_1 + \beta_2 x_2 + \beta_3 x_3 + \varepsilon \quad (3.6)$$

This has three regressors and is a typical multiple linear regression model.

3.7 ANN Modelling

The biological nervous system, the brain, is the model for artificial neural networks (ANNs). It is made up of a vast network of interconnected units called neurons. The brain modifies the neuronal connections in order to store and process information. (Kant & Sangwan, 2015) . Artificial Neural Networks (ANN) are a widely recognized technology that provides a different approach to simulating complicated issues in recent years. This method works with nonlinear issues and can handle incomplete data. After

training, ANNs are capable of making accurate predictions and generalizations. (Betiku *et al*., 2014). In ANN, the network created by connecting the neurons resembles the operation of a biological nervous system. The weights (connections) between the neurons in a neural network are adjusted to train it to do a particular task. When a neural network is trained, it learns to associate a given input with a target output. A network is trained using numerous input and target pairings in artificial intelligence learning. Until the network's output matches the target, the weights of the network are changed based on its outcome and the target. A computational model with three layers is called an artificial neural network (ANN), each with a distinct number of neurons. The input layer, hidden layers, and output layer are the three layers. Every neuron in one layer is related to every other layer's neuron through the interconnection of these layers. Figure 3.3 displays the diagram for a network with a single neuron.

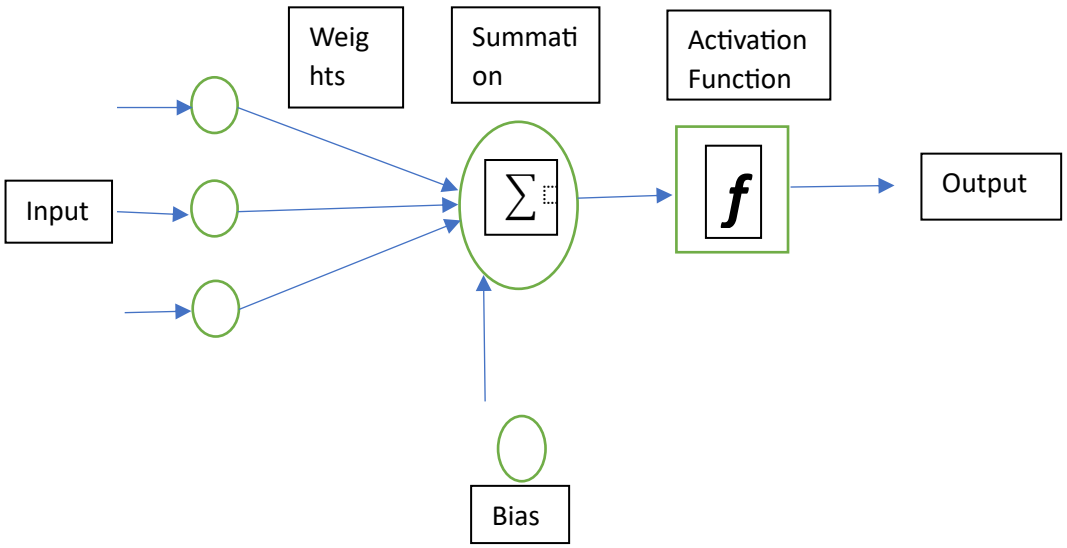

Figure 3.3: ANN network

Artificial neural networks consist of input nodes that receive signals, hidden layer nodes that analyse these signals, and output layer units that process the hidden layer's outputs using activation functions to produce the final output. It computes the net input from the processing neurons through the use of an activation function and a summation function. The weighted input of the neuron is converted to the activation of its output

via the activation function. Nonlinear interactions between input and output can be stored by a neural network with an activation function since it is made up of both linear and nonlinear algebraic equations. Neurons are transferred to other neurons once an activation function has weighted and altered them. The activation function's findings are accepted by output, which then displays them to the appropriate processing neuron or to other network nodes. Every input that is fed into the network, the target and network output are compared. The discrepancy between the desired result and the network's output is known as an error.

Choosing a neural network design requires choosing a lot of different factors. These factors include how many layers there are, how many neurons there are in each layer, how many training iterations there are, etc. Activation function and learning rate are two of the more crucial factors for training and network capacity (Kant G. G & Sangwan K. S., 2015).

3.7.1 Parameters of ANN Model

Several topologies were examined in order to establish the optimal number of training iterations, hidden layers, and neurons in each hidden layer.

Activation function (Transfer function)

Before being transferred to the following layer, every neuron in the hidden and output layers processes its output using the activation function. With the exception of "identity," these non-linear activation functions enable the neural network to discover non-linear correlations between the input and output data. All of the activation functions may be worth attempting during training to see which produces the best outcome because they all alter values in different ways and will result in different learning mappings, training procedures, and output predictions in a neural network. It is crucial to take into account each activation function's output ranges and how they relate to the training set of data when selecting one. Various types of activation functions are explained below and shown in Figure 3.4:

- "Identity": applies f(x) = x (any value can be in the output range).
- "Sigmoid": this function utilizes the logistic sigmoid function, which is f(x) = 1 / (1 + exp(-x)); the output will always fall between 0 and 1.
- “Relu”: With the rectified linear unit function, f(x) = max(x,0), the "Relu" function yields an output that is always larger than or equal to 0.

- “tanh”: The hyperbolic tan function is used by "tanh": f(x) = tanh(x) (the result is always larger than -1 and less than 1).

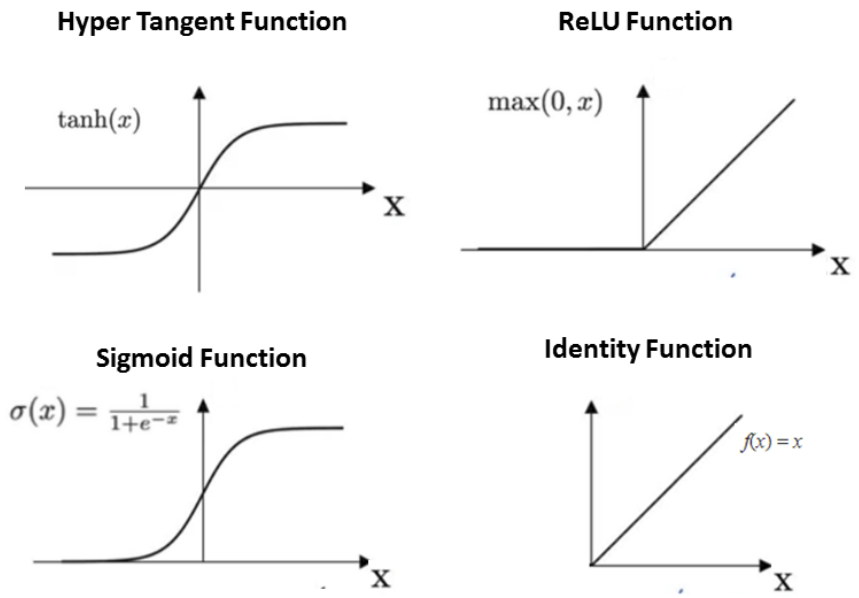

Figure 3.4: Activation functions

Learning rate

The amount by which the neural network's internal parameters should be adjusted during training is indicated by the learning rate, which is a scalar. The most crucial parameter to change when training a neural network is this one. To be more precise, learning rate is a small positive number, typically in the range of 0.0 and 1.0, that is a customizable hyper parameter used in neural network training. The learning rate determines how fast the model adjusts to the problem. In order to achieve reduced learning rates, more training epochs are needed because of the smaller weight changes with each update, while bigger learning rates provide faster changes and require fewer training epochs. A learning rate that is too high could lead the model towards convergence too soon to a less-than-ideal outcome, However, an excessively low learning rate can stall the process.

3.8 Optimization techniques

Genetic Algorithm

The Genetic Algorithm (GA) is a population-based stochastic search and optimization method that relies on Darwin's theory of natural selection and the mechanism of natural genetics. In 1965, Professor John Holland of the University of Michigan in the United States introduced GA. It is an iterative search method built around probability. There are five key steps in the operation of GA.

Step 1: Population Generation: A population of initial solution is generated randomly.

Step 2: Fitness Evaluation: Using the objective function, the fitness value for every solution in the population is determined. GA is typically applied to issues involving maximizing,

Step 3: Reproduction: Based on the fitness information calculated in the previous step, the good ones are selected from the population, There are different reproduction methods. In this work, Roulette Wheel Selection method has been used,

Roullete Wheel selection: Also known as the fitness-proportion selection, is a way of randomly selecting from a given list of weighted inputs, based on the spin result. In response to the fundamental values, The wheel's upper surface is split into n equal sections. A fixed pointer is used to show the winning area once the wheel stops when it is revolved in a specific direction. A certain subarea is selected as the winner.

Step 4: Crossover: Crossover is the process of two parents exchanging properties to create two new children. In order to do this, two parents or mating pairs are randomly selected from the mating pool. Thus, from ‘N’ no of population, ‘N/2’ number of mating pairs are formed.

Step 5: Mutation: In this case, the idea of biological mutation is simulated in order to alter the local answer.

One generation of GA is considered to be finished once the population has been altered utilizing these five methods. Until the termination criteria is met, this cycle continues.

3.8.1 Non dominated sorting Genetic Algorithm (NSGA)

Several optimal solutions, or Pareto optimal solutions, can be found in a multi-objective problem. One objective optimization replaces the multi-objective optimization problem using the classical optimization method.

By solving this type of optimization problem, each time one particular Pareto optimal solution is achieved. However, NSGA II can be used to evaluate a set of Pareto optimal solutions. (Deb, K. *et al*., 2002). The steps of NSGA II are discussed below:

- **Step 1**: A population size of 2N is considered by combination of the parent and the offspring. First, a combined population R_t is created, and a rapid non-domination process is used to sort R_t. This leads to other non-dominated fronts, such as F1, F2, etc.
- **Step 2**: The best non-dominated solution set F1 is also the best solution in the combined population. In the combined population, this needs to be recommended more than any other approach. All members of F1 will be chosen for the new population and represented by $P_{(t+1)}$ if the size of F1 is less than N. The solutions from the first front F1 are added to create the new parent population. This keeps on till the size is more than N.
- **Step 3**: A crowded comparison criterion is used to sort the accepted front solutions, and N points in total are selected.
- **Step 4**: To build the new population $Q_{(t+1)}$ of size N, the population $P_{(t+1)}$ of size N is used. This process is also carried out for other generations.

Chapter 4

Experimental Details

***Outline of the Chapter**: 4.1 Introduction 4.2 Development of Ni-P coating 4.3 Ni-P-PTFE composite coating 4.4 Instruments used in bath preparation 4.5 Hardness Measurement 4.5.1 Microhardness measurement 4.5.2 Nano hardness measurement 4.6 Surface Morphology and Compositional Analysis 4.6.1 Scanning electron Microscopy 4.6.2 Energy dispersive X-ray 4.6.3 X-ray diffraction 4.6.4 Transmission electron microscopy 4.7 Corrosion measurement*

4.1. Introduction

Experiment is a scientific procedure which is carried out under controlled conditions in order to understand and learn about a phenomenon. The present chapter deals with the preparation and characterization of electroless NiP coatings and its variants. In the present work, two types of coatings have been developed, which could be a probable solution to the existing problem discussed in the earlier chapters. Electroless NiP coating and electroless Ni-P-PTFE composite coating has been developed over martensitic stainless steel (AISI 420). The method of substrate preparation has been discussed. Also, various characterization techniques used to study the surface morphology, phase identification, elemental component analysis, hardness and corrosion characteristics of the coatings have been discussed in this chapter.

The electroless Nickel phosphorous coating is deposited onto martensitic steel substrate with size (10 × 10) mm^2 with 2mm thickness. The grade of steel used for the experiment is AISI 420 martensitic stainless steel. The Chemical composition of AISI 420 is given in Table 4.1. This was obtained by optical emission spectrometer.

Table 4.1 Chemical composition of AISI 420

	Chemical composition (%)							
	C	Mn	Si	P	S	Cr	Ni	
AISI 420	>0.15	1	1	0.04	0.03	12-14	0	

4.2. Development of Ni-P coating

- **Substrate preparation**

AISI 420 steel is used as the substrate. Firstly, the samples are cut using wire EDM into required size (10 mm ×10 mm × 2 mm). Before starting the coating procedure, samples are put through rigorous cleaning processes to remove any foreign particles present on the surface. Firstly, the specimen are finished with 400 grit size SiC paper. In order to clean the surface, it is degreased in acetone by immersing the samples in acetone for 5 minutes, washed in distilled water and then dried in dry air. After this, cleaning is done in de-ionized water using magnetic stirrer. Before plating, acid etching in 10% H_2SO_4 is done for 10 seconds followed by rinsing with acetone and then, with deionized water.

- **Activation of substrate**

In order to cross the energy barrier in the beginning and instigate the coating process, the samples are activated by dipping in Palladium chloride solution for 10 seconds at 55 ºC. Thereafter, they were rinsed with distilled water before coating.

- **Bath preparation of NiP bath**

The bath composition and its range was decided from a broad and detailed study of earlier literature (Selvi V., et al., 2014 ; Ali S., et al, 2021, Apachitei L.,et al, 1998; Salicio-Paz A et al, 2019) and also from many trial experiments. The condition for electroless Ni-P deposition is given in Table 4.2. The source of metal ion comes from nickel sulphate while sodium hypophosphite serves as the agent that reduces. This electroless bath also contains Tri-Sodium Citrate, dihydrate ($Na_3C_6H_5O_7$, $2H_2O$) as complexant, and Sodium Acetate (CH_3COONa, $3H_2O$) as buffering Agent. Then, a pH meter is used for continuous monitoring of pH and a thermometer is used for constant supervision of temperature. The coating is carried out for desired duration for achieving a substantial coating thickness. The bath volume and duration of coating were kept same for all the specimen. The samples are removed from the bath and washed with distilled water after the coating synthesis was done for the necessary amount of time. For annealing of some of the samples, the samples are put in a furnace at 400ºC for 1 hour and then furnace cooled.

Table 4.2 Conditions of electroless Ni-P coating deposition.

FACTORS		**Amount**
Nickel sulphate ($NiSO_4$)	Source of Ni ions	30 (g/L)
Nickel chloride ($NiCl_2$)	Source of Ni ions	30 (g/L)
Sodium hypophosphite ($NaPO_2H_2$)	Reducing agent	12 (g/L)
Trisodium citrate dehydrate ($C_6H_9Na_3O_9$)	Complexent	70 (g/L)
Ammonium chloride (NH_4Cl)	Buffering agent	50 (g/L)
Bath Volume		250 ml
Activation Temperature		55^o C
pH value		4.8
Temperature		90^o C
Deposition time		2 hours

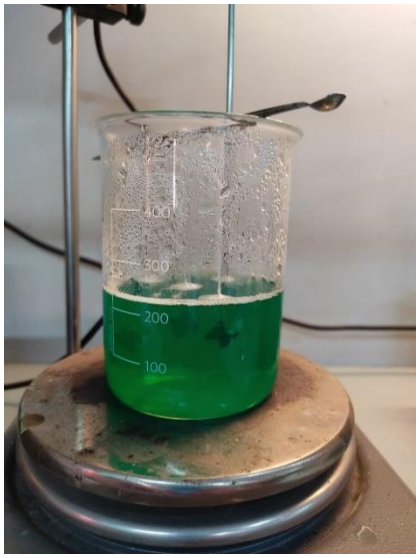

Figure 4.1: Schematic representation of setup for electroless nickel deposition

4.3 Development of Ni-P-PTFE composite coating

- **Substrate Preparation**

Here, AISI 420 steel substrate has been used for coating. The samples are first cut into required size (10 mm ×10 mm ×2 mm) and degreased using acetone for two minutes. It is followed by cleaning with distilled water for one minute. Acid pickling is very essential for removing the oxide layer from the surfaces to be coated. So, the samples are immersed into the 30% diluted H_2SO_4 solution. After 15 minutes, the substrates are again cleaned by distilled water and dried.

Activation of substrate

In order to cross the energy barrier in the beginning and instigate the coating process, the samples are activated by dipping in Palladium chloride solution for 10 seconds at 55 ºC. Thereafter, they were rinsed with distilled water before coating

Bath preparation of Ni-PTFE-P bath

The bath composition has been finalised after a rigorous literature survey ((Dhakal D *et al*,2020, Jiang W., *et al*, 2019; Huang Y.S., *et al*., 2003, Leon O., *et al*., 2003; Srinivasan K. N & John S., 2005; Wu Y., *et al*., 2006) and experiments. The condition for electroless Ni-PTFE-P deposition is given in Table 4.3. This electroless bath also contains nickel sulphate which is supplier of metal ion, sodium hypophosphite is the reducing agent, Tri-Sodium Citrate, dihydrate ($Na_3C_6H_5O_7$, $2H_2O$) as complexant, and Sodium Acetate (CH_3COONa, $3H_2O$) as buffering Agent. A 60% PTFE emulsion from Sigma, Aldrich was used for the composite coating. For better particle dispersion and surface charge adjustment, hexadecyl trimethyl ammonium bromide (HTAB) was used as a surfactant. The PTFE and the surfactant are mixed together with demineralised water in a separate portion by magnetic stirring for 30 minutes. Firstly, the specimen was introduced into the main Ni-P bath when the bath temperature reached 90^{o}C. After coating in the NiP bath for 30 minutes, the PTFE and the surfactant mixture was added to the main bath. Then, the final coating was carried out for 1 hour with the plating conditions of pH-4.8 and temperature, T= 90^{o}C. The bath composition and coating conditions are given in Table 4.3. A schematic of the coating procedure is shown in Figure 4.2.

Table 4.3: Conditions of electroless Ni-PTFE-P coating deposition

FACTORS		**Amount**
Nickel sulphate	Source of Ni ions	35-45 g/lit
Nickel chloride	Source of Ni ions	30 g/lit
Sodium hypophosphite	Reducing agent	25-35 g/lit
Trisodium citrate dehydrate	Complexent	70 g/lit
Ammonium chloride	Buffering agent	50 g/lit
PTFE	Source of composite	4-9.266 ml/lit
HTAB	surfactant	0.734-9.266 g/lit
Bath Volume		250 ml
Activation Temperature		55^{o} C
pH value		4.8
Temperature		71.835^{o}C-88.165^{o} C
Deposition time		1.5 hours

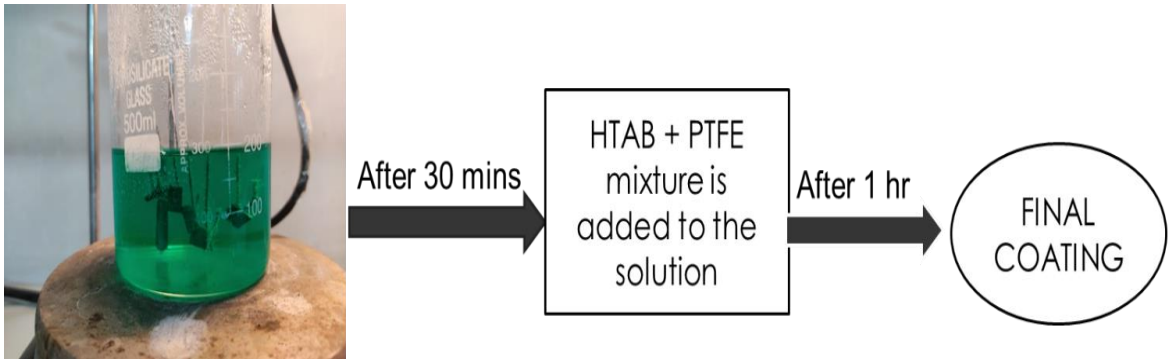

Figure 4.2: Schematic of electroless composite coating procedure

4.4 Instrument used in bath preparation

Electronic weighing balance: High precision electronic balance for weighing the chemicals. Sartorius (Model: BSA 224 S-CW) Max 220 g d=0.1 mg 32790312. (Figure 4.3)

Magnetic stirrer: Magnetic stirrer is used for proper mixing of bath solution (2MLH Magnetic stirrer, Manufactured by Remi Instruments). (Figure 4.4)

pH meter: A digital pH meter is used to measure the pH of the electroless bath (Eutech Instruments Part of Thermo Fisher Scientific; Made in Singapore P/N: 54 × 002606C; S/N 2351165; pH Tutor; pH/^{o}C meter) (Figure 4.6)

Mercury in glass Thermometer: For continuous measurement of temperature.

Tube furnace: For annealing. (Maximum Range 1200^{o}C) (M/s lokenath scientific concern`) (Figure 4.5)

Glass beaker: Used to hold the electroless bath solution. (Merk)

Figure 4.3: Electronic weighing balance

Figure 4.4: Magnetic stirrer

Figure 4.5: Tube furnace

Figure 4.6: pH meter

Chemicals used in the coating

- Nickel (II) Sulphate Hexahydrate **($NiSO_4.6H_2O$)** Merck Life Sciences Private Limited
- Nickel Chloride **($NiCl_2.6H_2O$) ,** Merck Life Sciences Private Limited
- Sodium Hypophosphite **($NaH_2PO_2.H_2O$),** LOBA CHEMIE
- Trisodium Citrate Dihydrate **($Na_3C_6H_5O_7.2H_2O$),** Merck Life Sciences Pvt. Ltd.
- Ammonium Chloride **(NH_4Cl)** , Merck Life Sciences Private Limited
- **PTFE EMULSION,** Sigma Aldrich
- **HTAB,** Sigma Aldrich
- Palladium (II) Chloride Anhydrous **($PdCl_2$),** Merck Life Sciences Pvt. Ltd**.**
- Water Distilled **(H_2O),** Merck Life Sciences Pvt. Ltd.
- Sulphuric Acid **(H_2SO_4) about 10%,** Merck Life Sciences Pvt. Ltd

4.5 Hardness Measurement

4.5.1 Microhardness measurement

This method is used to determine a material's hardness or aversion to indentation. Microhardness test mainly used to measure hardness of very thin samples, components with complex shapes and surface coatings. Different hardness testing techniques are available with various load ranges and scales, but Vickers hardness test is the most

widely used method because of its wide load range facility. The Vickers microhardness test uses Vickers type indenter, at a microscopic level, whose shape is square-pyramidal. In order to perform the test, the indenter is pressed into the surface of the material for 10-12 seconds. Vicker's microhardness tester (UHL VMHT) was used in the current work to measure the coatings' hardness at a speed of 25 µm/s, a weight of 50 g, and a dwell duration of 10 s. The final result is calculated as the mean of five observations for each sample.

Figure 4.7: Vicker's Microhardness Tester

4.5.2 Nano hardness measurement

Apart from nano hardness, this test is used for measuring many other useful mechanical properties (such as elastic modulus, stiffness and viscoelasticity) of various type of materials ranging from soft materials to hard alloys. Two main parameters of the test are loading force and indentation depth. In this work, this test was done using a standard

Berkovich indenter on fully calibrated Nano indenter (XP). Experiment was conducted using a load-time pattern. The tests were performed under controlled load condition, the maximum applied load was 8 mN, loading and unloading rate was 20 mN/min, and a dwell time of 5 s. A total of 10 indentations per sample was done at randomly selected positions of the surface, and the average values were calculated.

4.6 Surface Morphology, Compositional Analysis and Crystal orientation

4.6.1 Scanning electron Microscopy, EDX, XRD

Scanning electron microscopy (SEM) is the most important method for studying the surface characteristics and throws light on grain size and morphology. In SEM technique, a focused beam of electrons scans the sample and interacts with the atoms of the sample in order to provide image of the surface topography. In this work, scanning electron microscopy (SEM) is used to analyze the surface morphology of the samples and also study the changes that occurs in microstructure of the coatings, both in as coated and heat-treated condition.

4.6.2 Energy Dispersive X-ray

The sample's chemical characterization and elemental research are done using energy dispersive X-ray analysis, or EDX. In this study, the mass deposition of the coated particles is determined using EDX.

4.6.3 X-Ray Diffraction

X-Ray diffraction (XRD) CuKα analysis is used to identify the primary phases of the coating both before and after heat treatment. X-Ray diffraction analysis (XRD) provides comprehensive information about the crystal structure and elemental composition of a material. The method operates based on the idea that monochromatic X-rays in a crystalline material might interfere constructively.

4.6.4 Transmission electron microscopy

Transmission electron microscopy (TEM) is used to visualize the tiniest structures in matter which are not visible by SEM. The speciality of transmission electron microscopy (TEM) lies in its ability to form images of atomic positions of localized regions in the material. The detailed nature of the microstructure is visible by TEM, that

is, any change in the microstructure from one region to another, and the interfaces between them. Transmission electron microscopy images of the microstructure were captured using a FEI Tecnai F30-ST microscope which operates at 300 kV. The scanning unit, high angle annular dark-field (HAADF) detector, and energy-dispersive X-ray (EDX) detector are the three components that make up the microscope. Cross-sectional TEM sample was prepared by mechanical thinning followed by Air ion milling using Precision Ion Polishing System (Gatan), shown in the Figure 4.8(a,b).

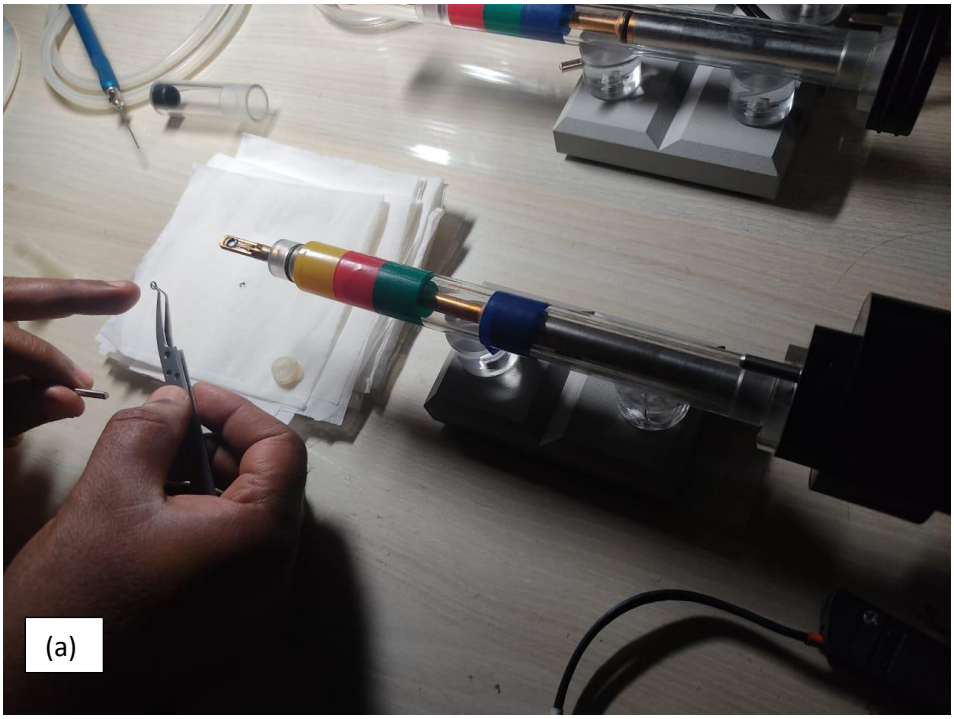

Figure 4.8 (a): Sample preparation by Air Ion Milling for TEM.

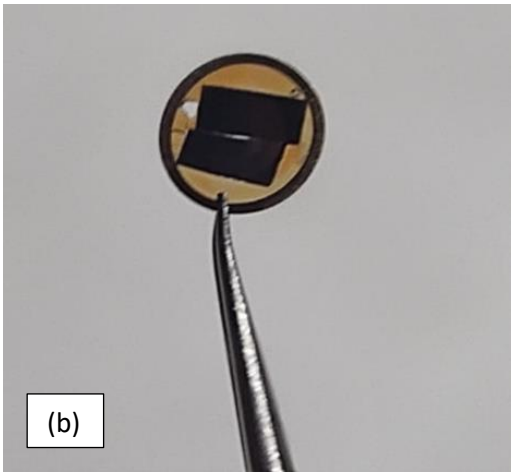

Figure 4.8 (b): Prepared sample for TEM

4.7 Corrosion measurement

Electron impedance spectroscopy (EIS) is one of the most powerful techniques to study the corrosion mechanism of any material. It can accurately measure the corrosion rates. Nevertheless, the findings of the EIS are modelled using software that is integrated into the interface for the measurement of charge transfer resistance or polarization resistance, which is proportionate to corrosion rate. Using the potentiodynamic polarization approach, current is applied through the electrolyte to change the electrode's potential at a steady rate. For polarization study, the working electrode's voltage must be changed, and the current generated by this potential shift must be measured. Polarization testing method is the most frequently used technique for corrosion resistance measurement.

In this work, corrosion has been studied by both the techniques. The corrosion tests were performed in CH Instruments (Electrochemical workstation) (Figure 4.9). Here, artificial and real blood plasma has been used as the electrolyte obtained from Calcutta Medical College. A saturated Ag/AgCl electrode served as the reference electrode, and a platinum electrode served as the counter electrode. About 1 cm^2 was the electrode's surface area that was in contact with the electrolyte. In order to assess the open circuit potential (OCP) of steel in real blood plasma solution for the polarization experiments, experimental settings were adjusted. A scan rate of 0.5 mv/s was chosen. Additionally, the frequency range used for the EIS test was 10KHz to 10mHz.

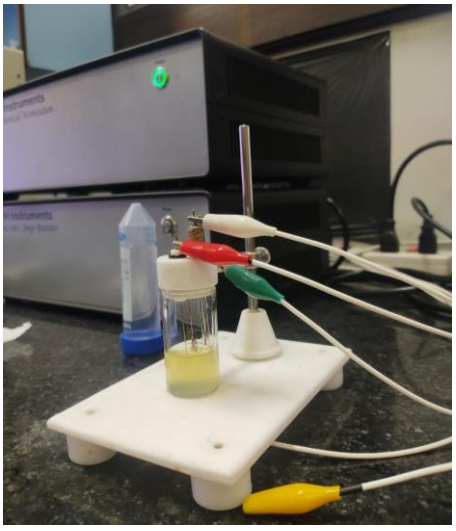

Figure 4.9: Electrochemical workstation

Chapter 5

Characterization Results

Outline of the Chapter: *5.1. Introduction 5.2. Characterization of steel substrate 5.2.1. Surface morphology and composition Analysis of substrate 5.2.2. Electrochemical Study of steel substrate 5.3 Characterization of optimized electroless Ni-P coating sample 5.3.1. Surface morphology and composition Analysis of Ni-P coating Corrosion study of Ni-P-PTFE coating 5.3.2 XRD analysis of optimized Ni-P electroless coating 5.3.3 Mechanical Characterization 5.3.4 Electrochemical Characterization of Ni-P coating 5.4. Characterization of electroless Ni-PTFE-P Composite Coating 5.4.1, Surface morphology and composition analysis of Ni-PTFE-P composite coating 5.4.2. Transmission electron microscope analysis 5.4.3. Nano hardness Test 5.4.4. Electrochemical Characterization of Ni-PTFE-P composite coating*

5.1 Introduction

The physical properties such as toughness, corrosion resistance, strength, ductility, hardness, etc are affected by the microstructure of a material. Microstructure analysis is an important process used to assess the coatings' properties. This type of analysis examines the microscopic structure, for a better understanding of its physical and mechanical properties. By understanding the microstructure of the coatings, we can develop ways to improve its properties. Various information such as coating thickness, grain size, grain growth development, crack initiation, defect can be obtained from microstructure study. With the advent of newer technologies, instruments with higher accuracy and resolution are now available which can give minute details such as the phase of the coatings, information about the interfaces, etc. In the present study, a combination of techniques viz. X-ray diffraction analysis (XRD), energy dispersive X-ray analysis (EDX), scanning electron microscopy (SEM) and Transmission electron microscopy (TEM) has been employed to characterize the coatings.

When metal interacts with oxygen, hydrogen, or hydroxide, it undergoes electrochemical oxidation, or corrosion. It is common phenomenon which occurs in most metals when subjected to corrosive environment. Corrosion has been recognized

as the most widespread problem in medical instruments. To sterilize the instruments, autoclaves are used with pressurized saturated steam at 121^{o}C for 30 minutes to 60 minutes at a pressure of 15 psi. After 5-6 autoclaves, the instrument starts to corrode and cannot be used any further. Martensitic stainless steel is more prone to corrosion compared to other stainless steels. Also, as we know that blood being a good electrolyte, propels the rate of corrosion in the instruments.

5.2. Characterization of steel substrate

5.2.1. Surface morphology and composition Analysis of substrate

AISI 420 steel was obtained from Baruipur surgical instrument cluster, Baruipur which is used by the cluster for manufacturing instruments. Figure 5.1 shows the SEM image of an unetched substrate. From the image, it can be observed that deformation lines in textural form are visible without any further details. The results of the EDAX given in Figure 5.2 gives the compositional details of the substrate. Table 5.1 shows the percentage weight of each composition of AISI 420.

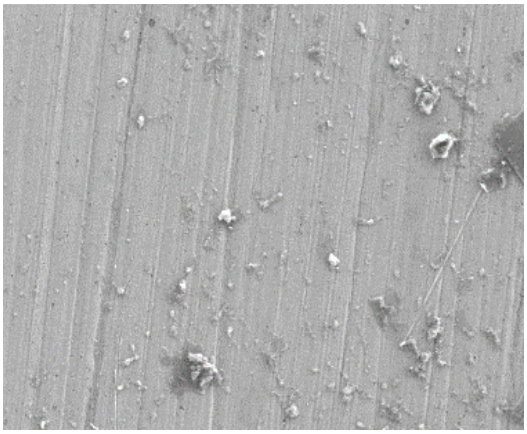

Figure 5.1: SEM image of unetched substrate

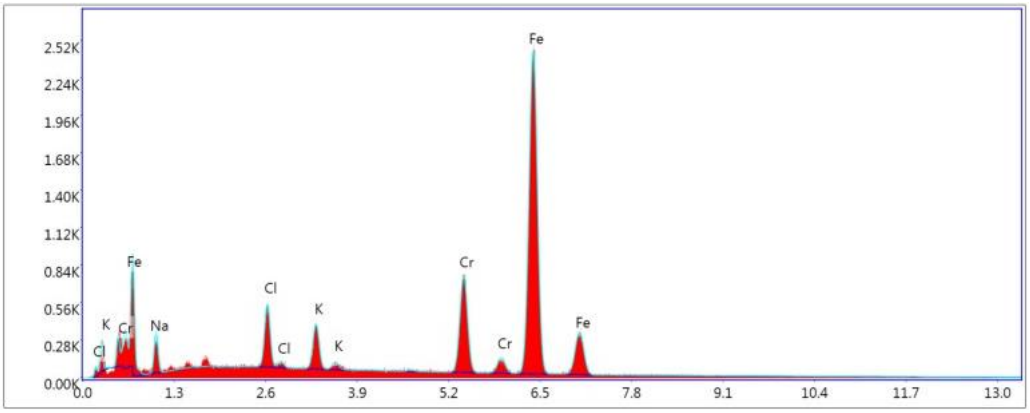

Figure 5.2: EDAX analysis of steel substrate

Table 5.1 Elemental composition of steel substrate

Element	Weight %	Atomic %
Na	8.07	16.85
Cl	5.17	5.63
K	3.52	5.32
Cr	13.82	12.75
Fe	70.51	60.56

5.2.2 Electrochemical Study of steel substrate.

Both electrochemical impedance study and potentiodynamic polarization test has been carried out for corrosion study of the samples. For performing the corrosion studies, three samples of martensitic stainless steel of three different grades namely, AISI 420, Custom 455 and Custom 630 has been considered for this study. A comparison of the corrosion properties has been performed for better understanding of martensitic stainless steel. The chemical composition of the three samples are given in Table 5.2. which is obtained from Optical emission spectrometer (OES). The experiments have been carried out with artificial blood plasma as the corrosive media. The chemical composition of the artificial blood plasma is given in Table 5.3. The experimental details have been discussed in Section 4 .7

Table 5.2 Chemical composition of the martensitic stainless steel (AISI 420, Custom 630 & 455) used in this study

.	Chemical composition (%)						
	C	Mn	Si	P	S	Cr	Ni
AISI 420	>0.15	1	1	0.05	0.03	12-15	0
Custom 630	0.05	0.5	0.5	0.05	0.03	15-17.5	3-5
Custom 455	0.05	0.5	0.5	0.05	0.03	11-12	7.5-9.5

Table 5.3 Chemical composition of Artificial Blood Plasma (Saha. N., *et al*, 2019)

Components	***Amount in distilled water (g/L)***
KCl	0.5
$CaCl_2$	0.2
$NaHCO_3$	2.2
NaCl	6.8
$MgSO_5$	0.1
NaH_2PO_5	0.026
Na_2HPO_5	0.126

- ***Electrochemical impedance analysis***

The 10 kHz to 10 mHz frequency range and 5 mV potential amplitude were used in the EIS research, which was conducted at OCP throughout a range of time intervals from 15 minutes to 25 hours. Figure 5.3 (a,b and c) displays the Nyquist plot of the samples at varying immersion times, i.e., 15 minutes to 25 hours, for Custom 630, Custom 455, and AISI 420, respectively. According to the impedance spectra, the high frequency region is represented by a tiny semicircle, while the low frequency region is by a vertical line. Internal resistance (Rs) is the value obtained from the semicircle's high-frequency intercept with the real axis (Z'). Three variables can cause internal resistance: (i) the electrolyte's (artificial blood plasma) ionic resistance; (ii) the electrode materials' intrinsic resistance; and (iii) the resistance across the interface between the current collector and electrode. The charge transfer resistance is measured at the real axis (Z') beginning of the semicircle. R_{ct} typically equates to corrosion resistance. (Mareci D., *et al*. 2017, Rustandi A.,*et al* 2018). The instrument's fitting software (AUTOLAB-30) was used to evaluate the impedance spectra, and the Randles equivalent circuit

modelling displayed in Figure 5.5 was used. The electrode-electrolyte interface constant phase element (CPE), internal resistance (Rs), and charge transfer resistance (R_{ct}) are the three main parts of the model circuit. The modulus error is ± 1% on average. Table 5.4 provides the values of R_s, CPE, and R_{ct}. AISI 420 (R_{ct} = 135 kΩ-cm^2) has a lower charge transfer resistance than Custom 630 (R_{ct} = 421 kΩ-cm^2) and Custom 455 (R_{ct} = 483 kΩ-cm^2). This demonstrates that as compared to AISI 420, Custom 630 and Custom 455 are more resistant to corrosion when it comes to blood. For all the three samples, respectively, the phase angles (Ø) and impedance modulus (|Z|) are plotted against frequency in Figure 5.4 (a, b, and c). The phase angles (Ø) of the AISI 420 (78.590^o), Custom 455 (76.170^o), and Custom 630 (79.770^o) are similar to one another in the Bode plot. The Custom 630's greater impedance value (5.27 Ω) in relation to the AISI 420 (5.87 Ω) and Custom 455 (5.97 Ω) is what drives its stronger resistance to blood plasma behaviour.

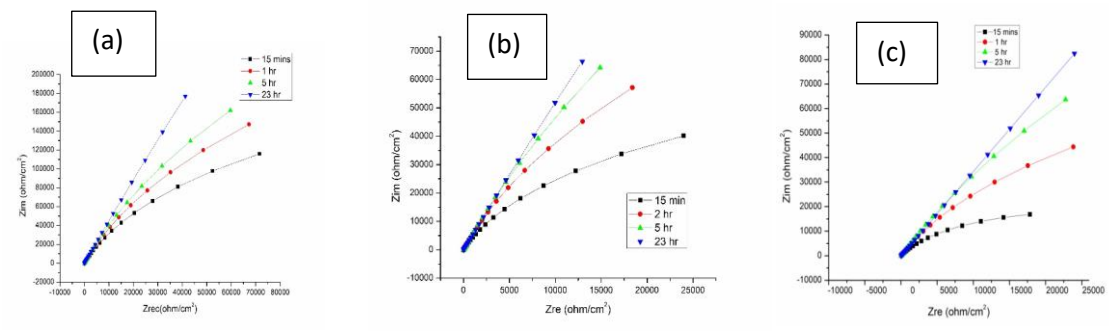

Figure 5.3 (a,b,c) : Nyquist diagrams in artificial blood plasma solution at 25 °C for AISI 420, Custom 630, and Custom 455, respectively, recorded after varying immersion periods,

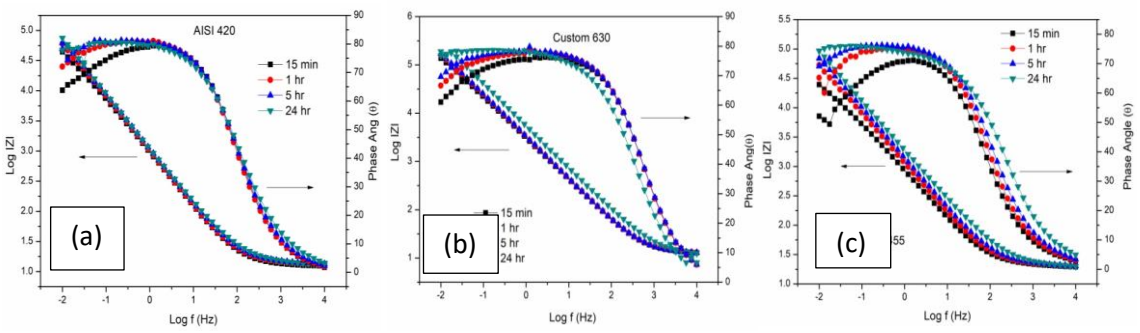

Figure 5.4 (a, b, c): Bode graphs were acquired at 25°C in fake blood plasma solution for AISI 420, Custom 630, and Custom 455, respectively, following varying immersion periods

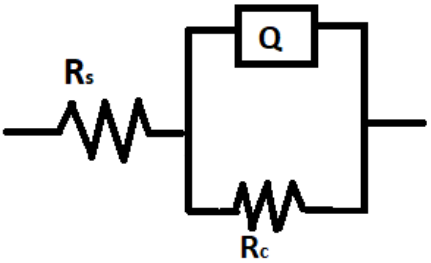

Figure 5.5: Electric equivalent circuit

Table 5.4. Electrochemical parameters obtained from equivalent circuit (for steel substrate)

Grade	R_s (ohm-cm^2)	R_{ct} (kΩ-cm^2)	CPE	
			Yo (F)	n
AISI 420	12.93	135	$0.2126x10^{-3}$	0.8783
Custom 630	12.92	521	0.6789×10^{-5}	0.8521
Custom 455	20.26	583	$0..2723 \times 10^{-3}$	0.8025

- ***Potentiodynamic polarization study***

The Custom 630, Custom 455, and AISI 420 samples were subjected to polarization (Tafel) studies to investigate their corrosion behaviour in blood plasma (Figure 5.6). Following a 25-hour immersion in the electrolyte, the polarization tests were carried out. Table 5.5 shows the corrosion parameters- E_{corr}, I_{corr}, R_p and Corrosion rate—obtained from the polarization tests. In fact, these corrosion metrics accurately reflect the level of deterioration in each sample. At I_{corr} = 1.135 µA/cm^2, the maximum current density of the AISI 420 shows that its corrosion resistance property is lowest (R_p = 0.6001 mΩ). The AISI 420's high corrosion current and rate could be caused by the zero Ni percentage in the material. Conversely, the Custom 630 and Custom 455 may be immune to corrosion because of a passive layer of nickel oxide that developed on their surface. The zero current potential, or E_{corr}, in the current situation is in line with the corrosion rate (R_{corr}) and corrosion current (I_{corr}). In comparison to the AISI 420 (0.006 V) and the Custom 455 (0.075 V), the Custom 630's maximum break down potential (E_b) of 0.275 V demonstrates its remarkable resistance to pitting corrosion.

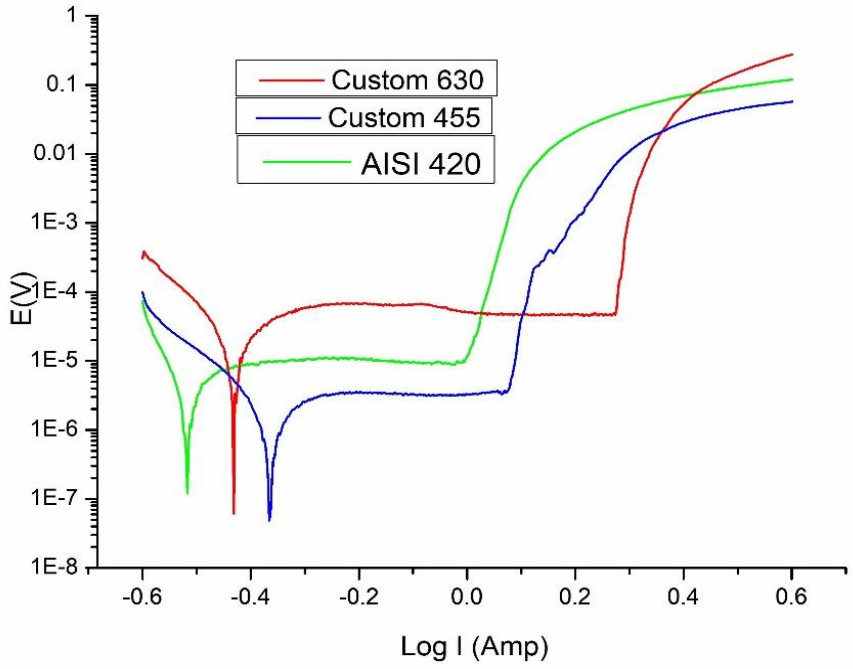

Figure 5.6: Potentiodynamic polarization curves obtained after 25 hours

Table 5.5 Electrochemical parameters obtained from potentiodynamic polarization test (for steel substrate)

	E_{corr} (V)	**I_{corr} ($x10^{-6}$) $A.cm^2$**	**R_p ($x10^{-3}$) Ω**	**Corrosion rate ($x10^{-3}$) mm/year**
AISI 420	-0.517 V	1.135	0.6016	13.18
CUSTOM 630	-0.532 V	0.5739	1.811	6.665
CUSTOM 455	-0.365 V	0.529	2.58	5.975

Within the electrochemical investigations, the Custom 630 exhibits the greatest impedance value [5.27 ohm] and a greater charge transfer resistance [Rct = 421 kΩ-cm^2]. Their resistance to corrosion can be attributed mostly to these reasons. The Tafel plot for the linear potentiodynamic polarization experiment shows that the Custom 455 has the lowest E_{corr} value (-0.365V), whereas the Custom 630 has the highest break down potential (E_b) (E_b=0.275 V), which causes pitting corrosion. Therefore, it can be said that over time, Custom 630 would be a more effective corrosion-resistant material.

5.3 Characterization of electroless Ni-P coating sample

5.3.1 Surface morphology and Composition Analysis of Ni-P coating

The SEM images of the as coated sample is shown in Figure 5.7. The coating exhibits a nodular structure with uniform distribution of the grains all over the substrate. The EDS plot provides assurance that Nickel (Ni) and Phosphorous (P) are present in the coating, shown in Figure 5.9. Also, elemental distribution is shown in Figure 5.10. The grains of the coating is spherical with varying diameter ranging from 1 μm to 5 μm. The coating appears to be uniform and crack free.

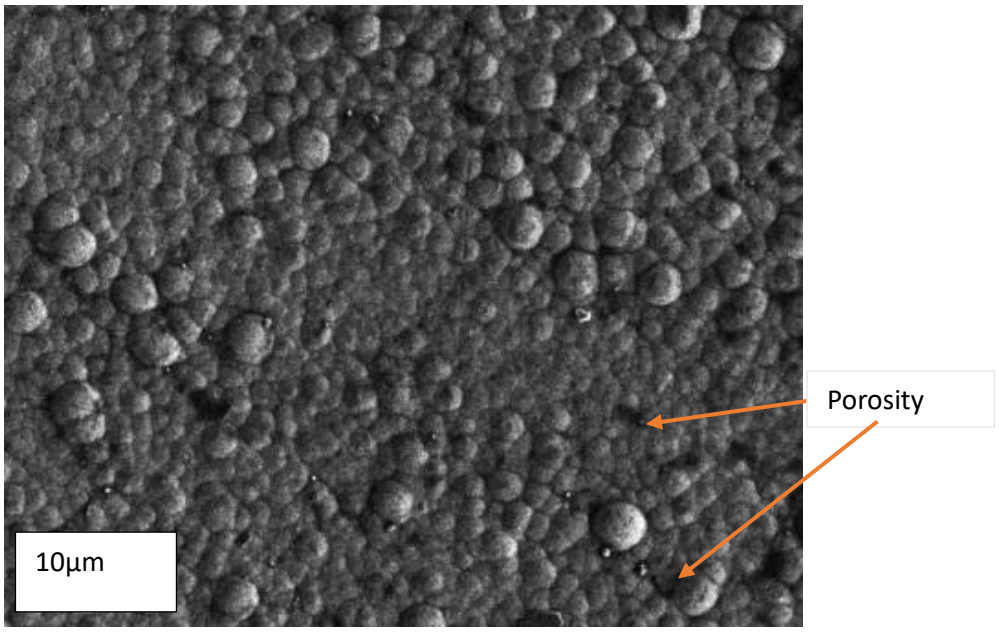

Figure 5.7: SEM image of NiP coating

After annealing, a slight change in the structure of the coating is visible. Fine equiaxed grains can be seen and the coating seems to be more homogenous and denser, as shown in Figure 5.8

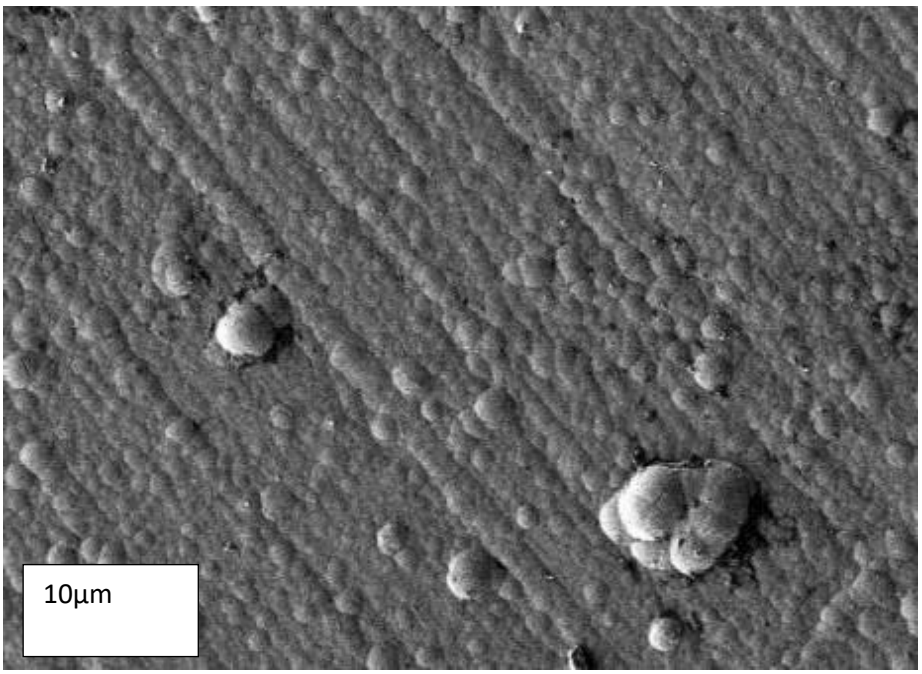

Figure 5.8: SEM image of coated sample after heat treatment at 300°C

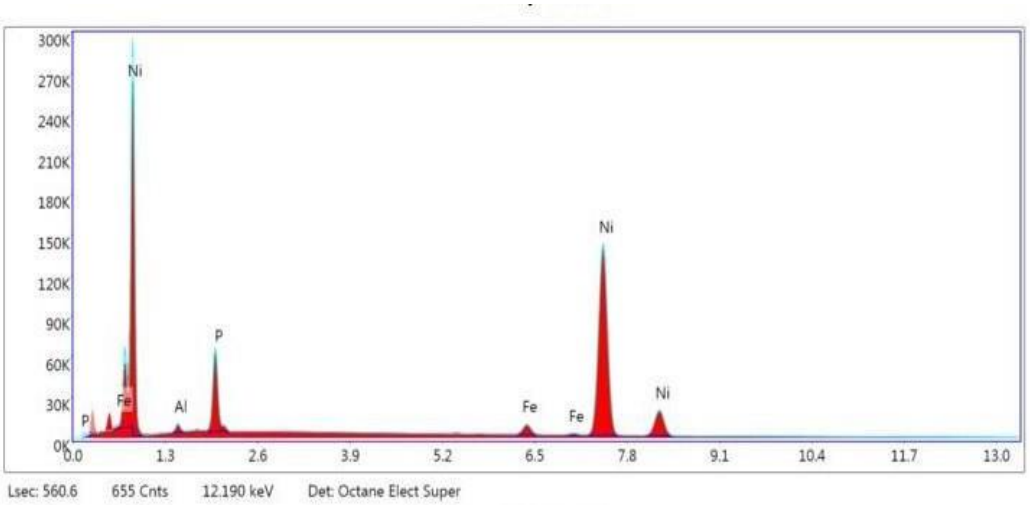

Figure 5.9: EDS plot of NiP coated sample

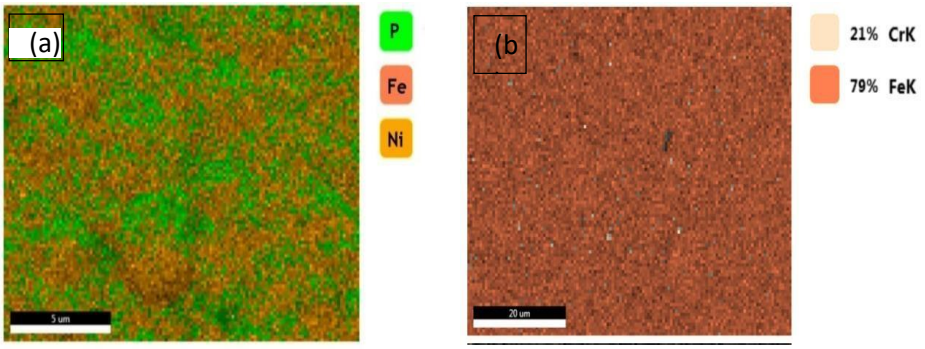

Figure 5.10: Elemental distribution MAP (a) As deposited NiP coating (b) AISI 420 steel substrate

Table 5.6 EDX results of NiP coating

Element	P	Fe	Ni
Weight%	13.75	1.67	85.58
Atomic %	23.19	1.56	75.25

EDAX analysis shown in Table 5.6 gives the different compositional weight percentage in Ni-P coating. The weight percentage of phosphorus was determined to be 13.75%, whereas 85.58% of the weight of nickel had been detected to have been deposited on the surface. From the weight % of phosphorous, the coating can be characterized as having a high phosphorus content.

In order to investigate the substrate-coating interface, Transmission Electron microscope has been employed. The TEM image (Figure 5.11) shows that there is no gap between the substrate and the coating and the coating layer seems to adhere to the substrate quite well. Also, no new phase can be seen to coexist at the interface between the two layers. So, it can be said that the bonding between the two layers is purely physical in nature.

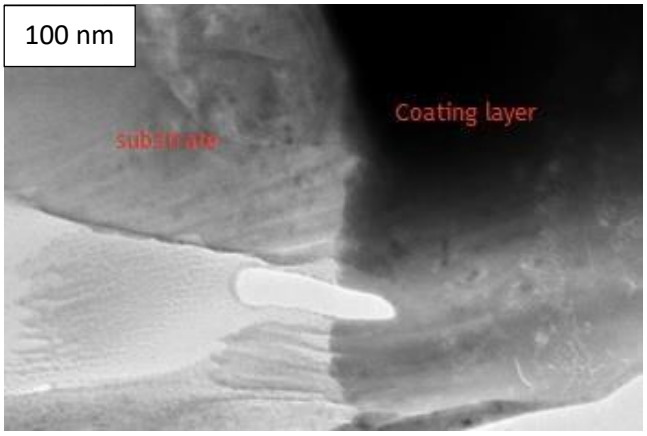

Figure 5.11: TEM image showing interface

5.3.2 XRD analysis of Ni-P electroless coating

The heat-treated and as-deposited samples' coatings' XRD patterns are displayed in Figure 5.12. The broad peak at 55.5° visible in the XRD plot for the as-deposited coating suggests that the coating matrix is amorphous.

Both Ni and Ni_3P, two types of crystalline diffraction peaks, are visible following an hour-long heat treatment at 300°C. This suggests that heat treatment causes the amorphous covering to change into a crystalline phase.

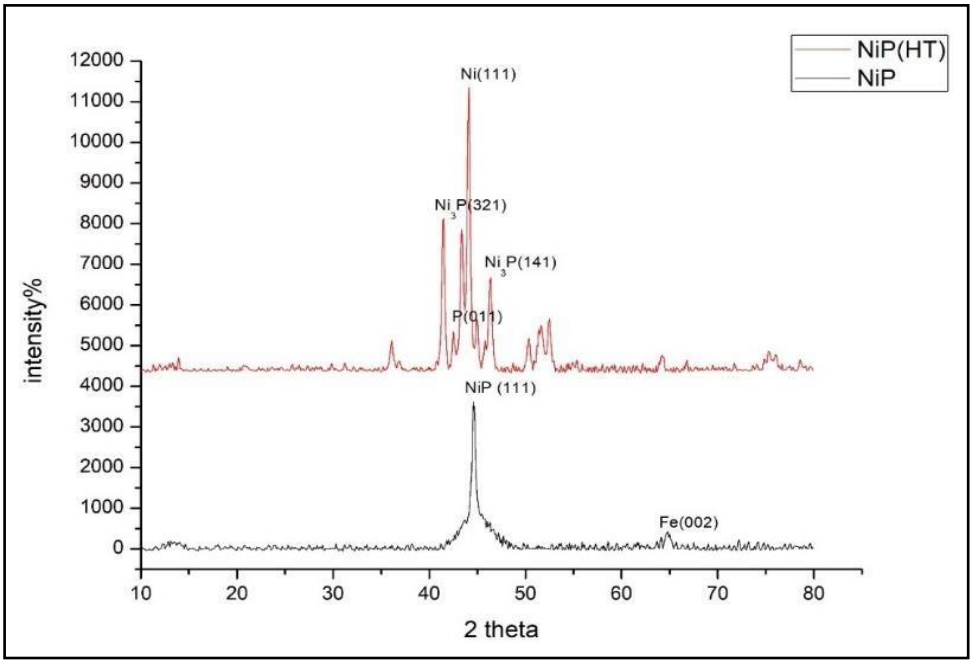

Figure 5.12: XRD pattern of NiP (as coated) and NiP (heat treated at 300°C for 2 hr)

5.3.3 Mechanical Characterization

The microhardness results are tabulated in Table 5.7. The hardness of the uncoated AISI 420 stainless steel substrate is 396 HV. After Ni-P coating, the hardness value increased to 592 HV. Upon heat treatment of the coated samples to 300°C for 1 hour. Further increase in hardness to 677 HV has been observed. Precipitation hardening, which results from the precipitation of a hard Ni_3P intermetallic phase, is primarily to blame for this rise (seen by XRD, Figure. 5.12). Same phenomenon has been observed in several studies [Luo H., *et al*,2015, Zhang L., *et al*, 2008]. All the values are average of five readings taken for each sample.

Table 5.7 Microhardness values

Samples	Uncoated AISI 520	As- deposited	Heat treated (300°C)
Hardness	396 HV0.5	592 HV0.5	677 HV0.5

5.3.4 Electrochemical Characterization of Ni-P coating

- **Electron impedance spectroscopy study**

An analogous circuit concept that utilizes the Randles circuit (Figure 5.5) was used to explain the corrosion behaviour of the electroless Ni-P coatings at their respective open circuit voltages, made up of charge transfer resistance (R_{ct}), double layer capacitance (C_{dl}), and solution resistance (R_s), where the R_{ct} and C_{dl} are parallel to one another, has been modelled. A similar model was employed by (Ali. S., et al, 2021, Dhakal. D. R., et al, 2019) to examine the electrochemical impedance behaviour of electroless NiP coatings in salt water solution. Table 5.8 compiles the C_{dl} and R_{ct} values following data fitting using the semi-quantitative software (AUTOLAB 30) that the device offers for the samples. The heat-treated sample in blood appears to have a higher level of corrosion resistance than the other samples, based on its high charge transfer resistance (R_{ct} = 553 Ω) and low capacitance (C_{dl} = 0.7598 x 10^{-5} F). The coating's porosity is connected to the C_{dl} values. (Sankara Narayanan T S N et al, 2011). A high C_{dl} value for as plated Ni-P coating indicates higher porosity than the annealed Ni-P coating. This is supported by the observation that the annealed NiP coating is more resistant to corrosion than the as-plated NiP coating.

.

Table 5.8 Results of the electrochemical study (for Ni-P coating)

Grade	**Rs (ohm-cm^2)**	**Rct (kΩ-cm^2)**	**CPE**	
			Yo (F)	**n**
Uncoated	23.57	170	0.5731x10^{-5}	0.8885
NiP Coated	33.33	521	0.5563 x 10^{-5}	0.8521
Heat treated	57.01	553	0.7598 x 10^{-5}	0.8218

- **Polarization study**

The polarization curves of the uncoated and Ni-P coated AISI 420 samples are shown in Figure 5.13 both before and after heat treatment, obtained from potentiodynamic polarization test which was performed after 25 h immersion of the samples in

artificial blood plasma (electrolyte). With a scan rate of 0.5 mV/s, the linear potentiodynamic polarization study is conducted from -1.0 VSCE to +1.0 VSCE.The results of the polarization test are shown in tabulated form in Table 5.9. It can be observed that the corrosion rate has rather increased after NiP coating than bare AISI 420 sample. This is explained by the coating's porous structure. The electrolyte enters via the pores in the coating when it is exposed to a corrosive liquid, reaching the substrate and creating a galvanic couple between Fe and Ni, which speeds up the corrosion process. Similar kind of observation is reported by (Taheri R., *et al*, 2001). In contrast to the Ni-P coating, the authors discovered that heat-treated Ni-P (up to 200°C) had better corrosion resistance. (Farzaneh A., *et al*, 2013) noted an increase in Ni-P and Ni-W-P alloys' corrosion resistance. when annealed at 300^{o} C but many studies have found that heating beyond 300°C has adverse effects on corrosion property of Ni-P coating, as observed by (Mafi Iman R and Changiz D.2011, Selvi V et al,2015). However, [Gao Y., *et al*.,2004] found better corrosive properties of NiP coatings after heating up to 500^{o}C. Figure 5.14 shows the Tafel plot, which indicates a movement in the corrosion potential towards a more negative zone (-0.270 V) and current density has increased to 3.752 X 10^{-7} for the coated sample which indicates that as plated Ni-P coating is least corrosion resistant among the three samples. Additionally, it is evident that the corrosion current (I_{corr}) and corrosion rate are in line with the zero current potential, or E_{corr}.

Table 5.9 Results of polarization test (for Ni-P coating)

Sample	**E_{corr}(V)**	**I_{corr}(A/cm)**	**Rp(ohm)**	**Corrosion rate(mm/year)**
Uncoated	-0.259 V	5.051 X 10^{-8}	1.531 X 10^{6}	5.695 X 10^{-5}
NiP coated	-0.270 V	3.752 X 10^{-7}	7.505 X 10^{5}	5.590 X 10^{-3}
Heat treated	-0.011 V	3.533 X 10^{-9}	1.165 X 10^{7}	5.105 X 10^{-5}

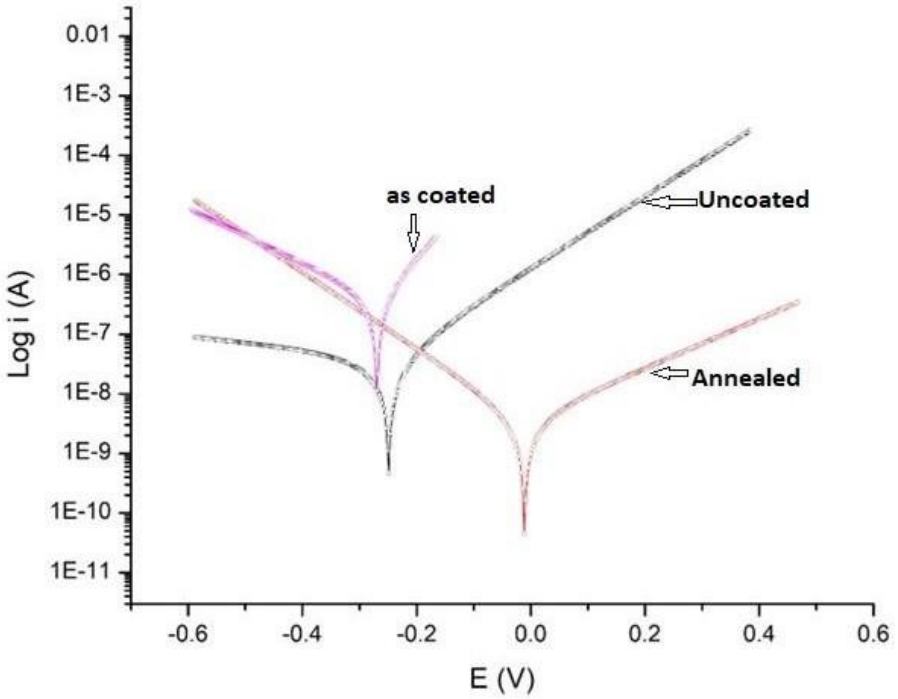

Figure 5.13: Tafel plot- Potentiodynamic polarization curves for uncoated, as coated and annealed electroless Ni–P coatings, in artificial blood plasma solution

The results of electrochemical study and potentiodynamic polarization test can be correlated with the SEM images obtained for NiP (as coated) and NiP (heat treated). As was previously said, the as-deposited coatings are amorphous in nature and include a lot of grain boundaries, which serve as active locations for the corrosive attack to progress. Again, the coating's porous nature accelerates the rate of corrosion (refer Figure 5.7). However, after heat treatment, the coatings transformed to crystalline nature which results in decrease of density of grain boundaries. Also, porosity decreased after heat treatment. Corrosion resistance has therefore improved.

5.4 Characterization of electroless Ni-PTFE-P Composite Coating

5.4.1 Surface morphology and composition analysis of Ni-P-PTFE composite coating

The morphology of the Ni-P and Ni-P-PTFE coating surfaces are shown in Figure 5.14. and 5.15 respectively. Here, a comparison between the two coatings has been discussed. As illustrated in Figure 5.14, the coatings have globular structure. The grain size being uniform, as shown in Figure 5.14, infers to homogeneity of the structure. However,

some occasional heaps of particles can be seen to be formed in Figure 5.14, which probably identifies the position of nuclei of the coating. The surface morphology of the composite coating is displayed in Figure 5.15. It has fine structure with uniform distribution of PTFE over the matrix. The lack of discernible fractures validates the uniform distribution of PTFE particles throughout the NiP matrix. No agglomeration phenomena are visible on the surface. Similar observation was made by (Jiang W., et al., 2019). It may be stated that the kinetics of nucleation and grain development processes were altered by the PTFE addition to the NiP matrix. Inclusion of PTFE might have increased the number of nuclei, resulting in finer structure and smaller grains.

Figure 5.14: SEM images of as coated Ni-P

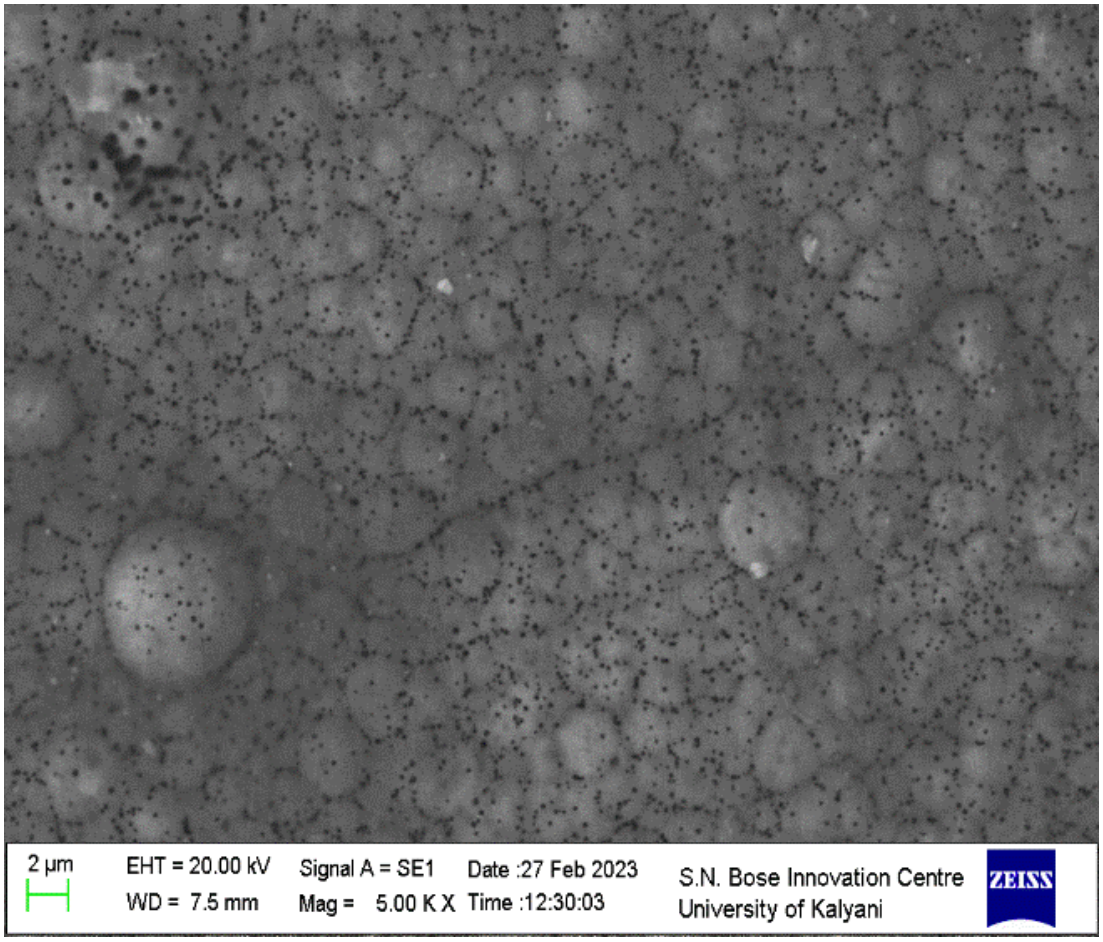

Figure 5.15: SEM images of as coated Ni-P-PTFE

5.4.2. Transmission electron microscope analysis

To investigate the growth and crystallographic structure of EN-PTFE composite coating film, TEM analysis was carried out. The cross-sectional TEM picture of the composite coating is displayed in Figure 5.16. It can be observed from the image that the three layers of the coating are distinctly visible. Furthermore, to confirm the observation, EDX was performed at three different points as shown in the figure. The EDX results are given in Figure 5.16 (b), (f), (g) and (h). It can be seen that the EDX at point 3, shows the presence of Iron (Fe) and Chromium (Cr). Therefore, the first layer (containing point O_3) is the substrate (AISI 420). Nickel (Ni) and phosphorus (P) are present, according to the EDX at point 2 (O_2). The is the middle layer where Ni-P was first deposited on the substrate before the addition of PTFE to the bath. The EDX at point 1 (O_1) shows the presence of Nickel (Ni) and Carbon (C) which proves the PTFE particles are present in the Ni matrix. Also, it can be seen that no new phase has been formed at the contact point of the Ni matrix and the PTFE particles. This indicates that

the Ni-P-PTFE bond is purely mechanical or physical in nature. The physical or chemical properties of a composite film is greatly affected by the type of interaction between the matrix and the third particle. Therefore, the study of the interface is of great importance. Figure 5.16 (a, c, e and f) shows the selected area electron diffraction (SAED) images of the Ni-P matrix incorporated with PTFE particles. The diffused circular rings with small white dots in the SAED pattern in Figure 5.16 (e) corresponds to the substrate layer which is purely crystalline in nature. Figure 5.16 (d) corresponds to Ni-P matrix with polycrystalline structure and Figure 5.16 (c) with purely circular rings confirm that the PTFE particles are purely amorphous in nature.

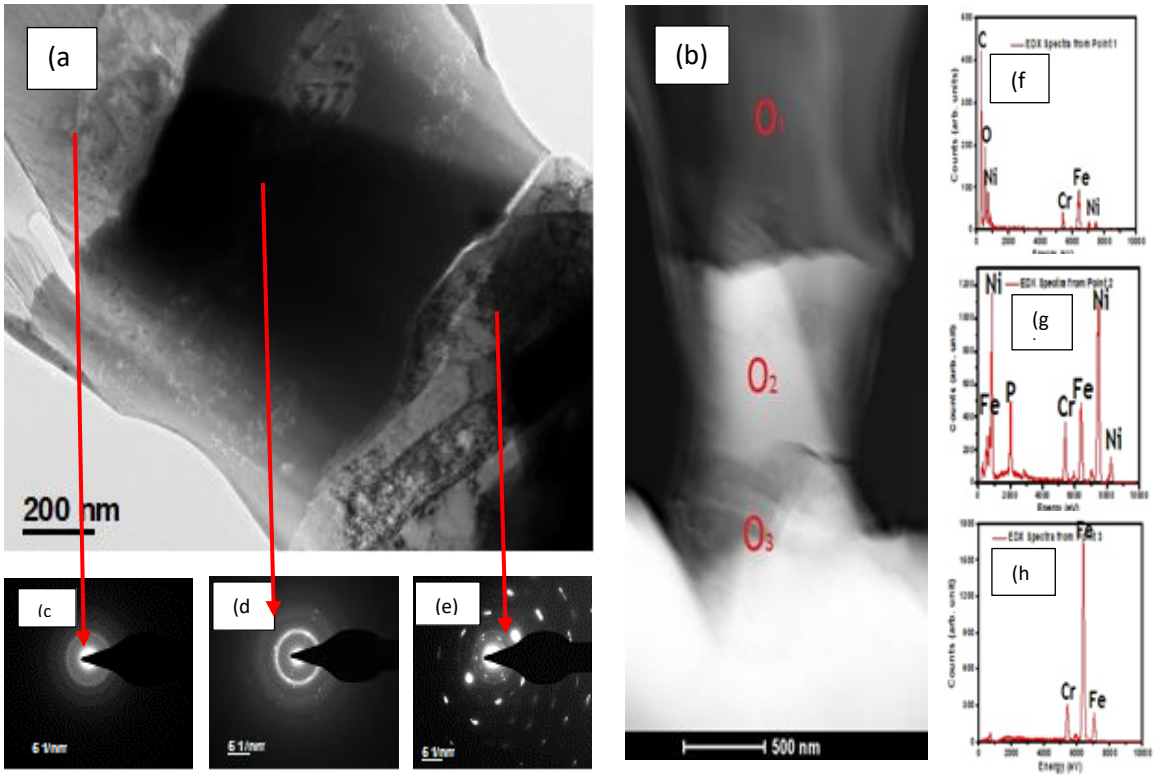

Figure 5.16 (a) Cross-sectional bright-field TEM image, (b) Scanning TEM-HAADF image, (c), (d),(e) are selected area electron diffraction pattern (SAED) taken from three different region marked with dotted circles in (a). (f), (g) and (h) are EDX spectra collected from three different region marked by point 1, 2 and 3

5.4.3. Nano hardness Test

The representative load versus displacement curve for NiP and Ni-P-PTFE composite coating are displayed in Figure 5.17. The average nano hardness value and elastic modulus for both the coatings are tabulated in Table 5.4.1. Also, the stiffness, elasticity and resistance to plastic deformation of the coatings has been calculated and given in Table 5.4.1. It can be observed that the hardness value has decreased after the addition of PTFE. Similar kind of hardness value of NiP coating was reported by (Sribalaji et al,2016). Since, elasticity increases with increase in hardness, it is clear that Ni-P-PTFE coating has a lower elasticity value than Ni-P coating. Due to lose structure and soft property of PTFE particles, coating gets easily deformed under external load (Yanhai C et al, 2019) . Therefore, the load versus displacement curve depicts a different behaviour for Ni-P-PTFE composite coating.

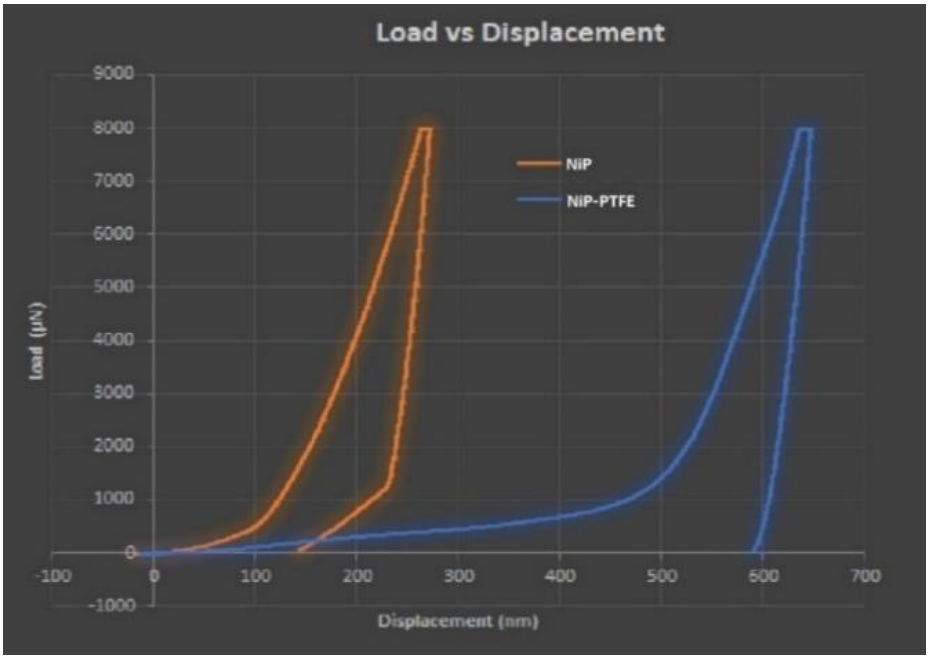

Figure 5.17: Load versus displacement curve for NiP and NiP-PTFE

Table 5.10 Nano hardness results

Coating	Hardness (GPa)	Young's Modulus (GPa)	Stiffness N/m	Elasticity	Plasticity Index
Ni-P	6.053	160.365	28.96 X 10^3	0.0377	0.0086
Ni-P-PTFE	1.536	72.296	7.87 X 10^3	0.0212	0.0007

Figure 5.18 shows that the Ni-P-PTFE deforms significantly more than the Ni-P coating when it is indented. Of the 10 indentations, the Ni-P coating yields a minimal amount of penetration depth, h_{max}= 187.78 nm while the load is at its highest 7.9 mN. And, for the same peak load, the Ni-P-PTFE coatings yields a minimum penetration depth, h_{max}= 315.0625 nm. Therefore, it can be inferred that the Ni-P coated surface is harder than the Ni-P-PTFE coated surface. Similar kind of conclusion was drawn by (Gong et al , 2005) . The stiffness value has been calculated by calculating the slope of the curves, given in Table 5.10.

5.4.5. Electrochemical Characterization of Ni-PTFE-P composite coating

The corrosion tests were performed in CH Instruments (Electrochemical workstation). Here, real blood plasma has been used as the electrolyte. The detailed test procedure has been discussed in Section 4.7. Here, a comparison between the corrosion behaviour of three samples namely, uncoated steel substrate, NiP coated sample and Ni-P-PTFE coated sample has been studied.

- **Electron impedance spectroscopy study**

The coatings' open circuit potentials are displayed in Figure 5.18. The surface potential of both the coatings is greater than the substrate's, which suggests enhanced anodic protection of the stainless-steel substrate after coating. The coating surface potentials seem to be stable. This suggests that the coatings are pore free and uniform.

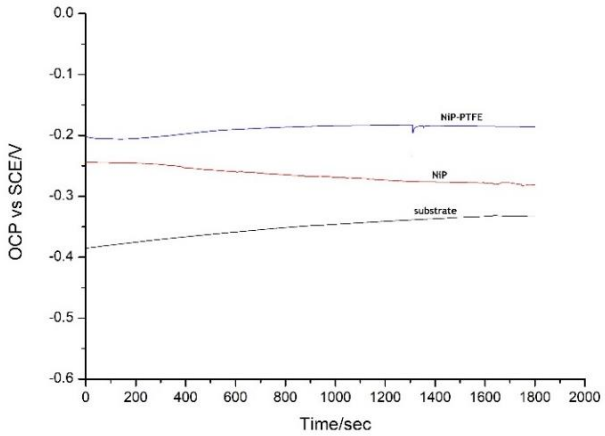

Figure 5.18: Open Circuit Potential vs time for substrate and the coatings, in real blood plasma

The Nyquist plots are given in Figure 5.19. It can be observed from the plots that all the curves are single semicircles which indicates that the coatings have single layer protective scale. However, the semicircle with the largest diameter is for Ni-P-PTFE coating which again confirms that Ni-P-PTFE coating shows the highest corrosion resistivity.

The coating electrochemical parameters were fitted using the analogous circuit depicted in Figure 5.20, where the constant phase element (CPE) is similar to a capacitor with a phase angle other than 90°. Here, the system's inhomogeneity is explained by the use of CPE instead of a capacitor. Table 5.11 is a list of the fitted results.

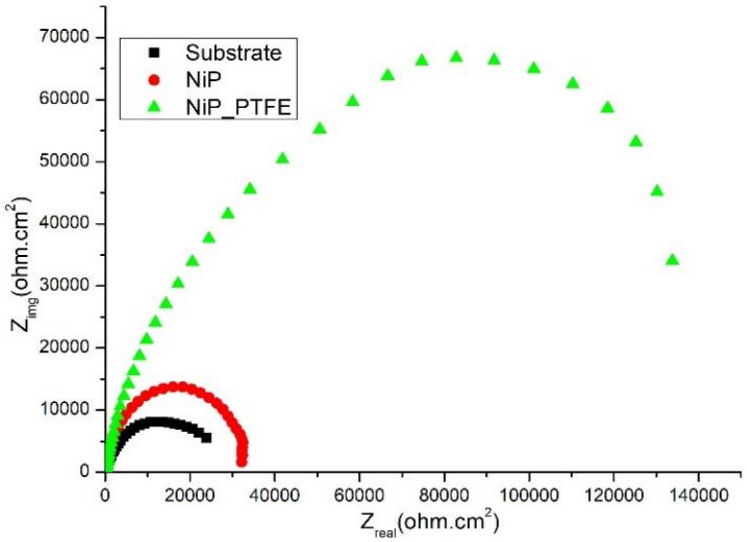

Figure 5.19: Nyquist plot obtained for substrate and the coatings, in real blood plasma

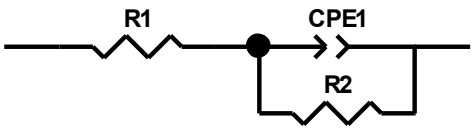

R1- Solution resistance
R2- Resistance of the capacitive layer
CPE1- Constant phase element

Figure 5.20: Randles equivalent circuit model

Table 5.11 Fitted values from Randles equivalent circuit model (for Ni-P-PTFE)

SAMPLE	R1 (Ω-cm^2)	R2 (kΩ-cm^2)	CPE (F)	
			CPE-T	CPE-P
Substrate	35.97	10570	1.25X10^{-5}	0.73858
NiP	36.56	26381	2.132X10^{-5}	0.92516
PTFE	35.03	59055	2.95X10^{-5}	0.86259

- **Polarization Study**

The polarization curves (Tafel plots) for the composite coatings Ni-P and Ni-P-PTFE are displayed in Figure 5.21. It is observed that the current density has decreased from 0.535 µA of the substrate to 0.188 µA of the EN coating and E_{corr} value increased from -0.587 to -0.323, which indicates an improvement of the corrosion properties. Similar result was obtained by (Salicio-Paz et al.2019) NiP coatings serve as a protective layer over the substrate which acts as a barrier to diffusion of the corrosive ions to the metal surface (Mafi I R and Dehghanian C, 2011) . With a positive corrosion potential (Ecorr= -0.226 V) and a low corrosion current (Icorr= 0.0585 µA), the coatings containing PTFE, however, exhibit the best corrosion resistance. This is explained by the PTFE particles' homogeneous dispersion throughout the NiP matrix (Figure 5. 15) which acts as an additional layer to block the corrosive ions to reach the substrate. The PTFE particles aid in further improving the corrosion-resistant qualities of the EN coatings because they are inert by nature and have very little electrical conductivity.

Table 5.12 shows the results of the polarization test for all the specimen. The Ni-P-PTFE coating exhibits a corrosion rate of 9.91×10^(-3) mm/year, a significantly lower rate than that of the EN coatings..

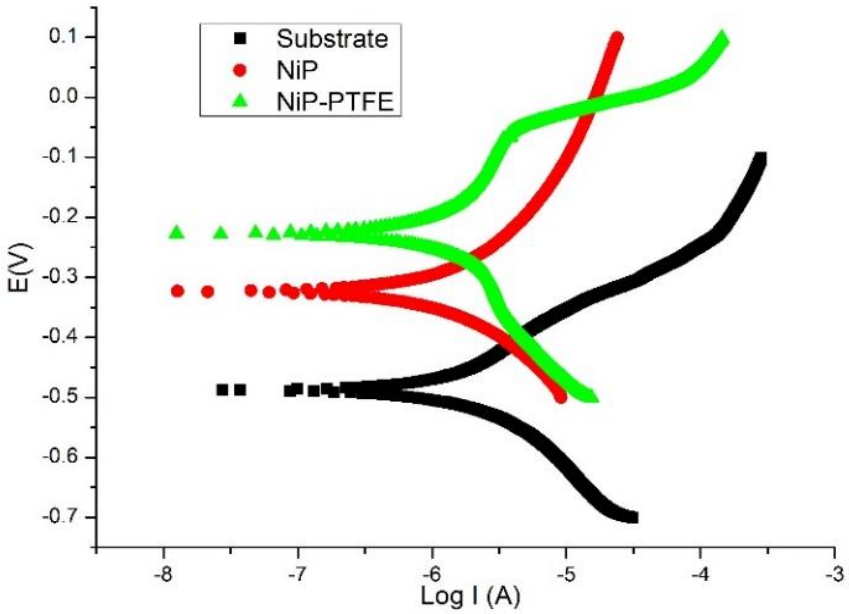

Figure 5.21: Potentiodynamic polarization curve obtained for substrate and the coatings, in real blood plasma

Table 5.12: Polarization test results (for Ni-P-PTFE)

Sample	**Corrosion rate** $(\times 10^{-3}$ **mm/year)**	**E_{corr} (V)**	**I_{corr}(µA/cm^2)**
Substrate	16.31	-0.587	5.35×10^{-1}
EN	15.89	-0.323	1.88×10^{-1}
EN-PTFE	9.91	-0.226	5.85×10^{-2}

Chapter 6

Data Analysis and Optimization

Outline of the chapter*: 6.1 Introduction 6.2 Analysis of deposited mass per unit 6.2.1 Calculated Mass deposited per unit area 6.2.2 Statistical analysis of mass deposition per unit area for Ni –PTFE –P electroless coating 6.2.3 Test of significance of the process parameters 6.2.4 Second order response surface model 6.2.5 Reliability test for the second-order response surface equation with the help of F- test 6.2.6 Contour plots for mass deposition 6.2.7 Optimization of process parameters for maximum mass deposition per unit area using Genetic Algorithm 6.3 Analysis of Hardness of Ni-PTFE-P composite coating 6.3.1 Statistical analysis of micro hardness for Ni –PTFE –P electroless coating. 6.3.2 Test of significance of the process parameters 6.3.3 Second order response surface model 6.3.4 Reliability test for the second-order response surface equation with the help of F- test 6.3.5 Surface plots for mass deposition 6.3.6 Modelling with Artificial neural Network 6.3.7 Performance test of ANN and RSM Model 6.3.8 Performance evaluation of ANN and RSM*

6.1 Introduction

The deposited mass per unit area and hardness of Ni-P-PTFE coating have been studied statistically in this chapter. The electroless coating process is affected by various parameters like concentration of coating components in the bath, temperature of deposition, etc. Some of the parameters are controllable and some are uncontrollable. The effects of uncontrollable variables on the response are assumed as error in statistical analysis. Amongst the controllable parameters, significant process parameters can be identified for a particular response. Improvement of some property of the coating is possible by optimizing the values of the process parameters. A regression equation can be developed using design of experiment to study the main effects and also the interactions. To determine the important process parameters, a student's t-test is run. Here, the experiment was created utilizing a central composite design, followed by response surface methodology for modelling. Genetic Algorithm has been used for optimization purpose. Also, a comparison between the results obtained from two

different modelling process namely, Linear regression, Response surface and Artificial neural network has been performed.

6.2 Analysis of deposited mass per unit area

Maximizing the bulk deposition rate of the electroless Ni-P-PTFE coating while taking into account the components of the chemical bath is the goal. Electroless Ni–P–PTFE coating has been deposited onto stainless steel substrate (AISI 420) with variations in concentrations of surfactant (HTAB), PTFE and temperature. The response variable has been determined to be the rate of deposition per unit area of the substrate. An examination of the significance of the input process variables and how they interact is carried out using a full factorial design of trials with Central composite design. The condition of the electroless Ni-P-PTFE coating is stated in Table 4.3. Response surface methodology (RSM) was followed for modelling of the process using MINITAB 16 software (Table 6.1). A fitted regression equation has been created to assess the importance of each process parameter separately as well as the interactions between them, followed by student t-test. A second order equation has been developed using RSM. The best input process parameter values that maximize the rate of coating deposition have been determined using the genetic algorithm (GA).. The design table for the experiment, with varying amounts of the three input factors, is displayed in Table 6.1.

Table 6.1. CCD design table for experiment

Input parameters	Unit	Axial point value -α	Low level	Central point	High level	Axial point value +α
HTAB (X_1)	g/lit	0.734	2	4	6	7.266
PTFE (X_2)	ml/lit	2.734	4	6	8	9.266
Temperature (X_3)	^oC	71.835	75	80	85	88.165

6.2.1 Calculated Mass deposited per unir area

Before and after the electroless deposition, the specimen's weight was recorded using a digital balance (model: Sartorius BSA 224 S-CW) with a resolution of 0.0001 g. The coating deposition rate per unit area was calculated using the following equation:

$$W = \frac{W_o - W_d}{2A} = y \text{ x } 10^{-4}\ g/cm^2 \qquad (6.1)$$

where the specimen's mass is indicated by W_O and W_d, respectively, preceding and following electroless deposition. In equation 6.1, A denotes the deposition area. For eg, if W_0= 0.7904 g, W_d= 0.8064 g and 2A= 3.28 cm^2, then W = 48.78 x 10^{-4} g/cm^2. The value of y for the experiment is shown in the subsequent table (**Table 6.2**).

Table 6.2. Observed data considering CCD

Sequence no		HTAB (g/lit)	PTFE (ml/lit)	Temp (°C)	Mass Deposition (x 10^{-4}g/cm^2)
		X_1	**X_2**	**X_3**	**D**
1	Factorial points	6	8	75	396.006
2		6	4	85	276.258
3		6	8	85	282.341
4		2	8	85	492.222
5		2	4	75	336.266
4		2	4	85	372.314
7		6	4	75	228.421
8		2	8	75	456.366

9	Central Points	4	6	80	372.281
10		4	6	80	300.396
11		4	6	80	282.259
12		4	6	80	270.247
13		4	6	80	312.546
14		4	6	80	336.455
15	Axial points	0.734	6	80	312.652
16		7.266	6	80	168.285
17		4	9.266	80	480.355
18		4	2.734	80	138.146
19		4	6	71.835	294.258
20		4	6	88.165	504.658

6.2.2 Statistical analysis of mass deposition per unit area for Ni-P-PTFE electroless coating

A fitted regression equation has been established to assess the impact of each process parameter and its interactions on the mass deposited per unit area of electroless Ni-P-PTFE coating. It gives a correlation between the response (amount of coating-mass accumulated per unit area) and the input process parameters viz. concentrations of PTFE, HTAB and Temperature. A first order fitted equation has been developed by MINITAB 16 software, shown in Equation 6.2:

$$\acute{D} = -1776.41 + 124.155\,X_1 + 266.465X_2 + 24.31X_3 - 2.062X_1X_2 - 1.725X_1X_3 - 2.025X_2X_3 \quad (6.2)$$

6.2.3 Test of significance of the process parameters

Replication variance = Estimate of error = $\sigma_e^2 = \sum_{n_c=1}^{6} \frac{(D_{act}-D_{avg})^2}{(n_c-1)}$ (6.3)

where,

D_{act}= Actual value of mass deposition per unit area for the i^{th}central point.

D_{avg} = Average value of mass deposition per unit area for six the central points.

n_c= No. of central points = 6 and Degrees of freedom (DOF) =n_c– 1 = 6–1 = 5

$$D_{avg} = \frac{(372.281+300.396+282.259+270.247+312.546+336.455)}{6} = 312.364 \quad (6.4)$$

Now, from eqn 6.3,

$$\sigma_e^2 = \frac{3590.04 + 143.233 + 906.111 + 1773.842 + 0.033 + 580.376}{5} = 1398.768$$

Now. $\sigma_\beta^2 = \frac{\sigma_e^2}{n_f}$ (6.5)

Where, n_f *is number of factorial points* $= 8$

Therefore, $\sigma_\beta^2 = \frac{1398.768}{8} = 174.846$

And $\sigma_\beta = 13.222$

Equation (6.6) can be used to determine the estimated "t" values for a given process parameter.

$$t_{esrimated} = \frac{|co-eff\ of\ process\ parameters|}{\sigma_\beta} = \frac{|\beta|}{\sigma_\beta} \quad (6.6)$$

where the coefficient of process parameter has been obtained from the regression equation (6.2).

It has been observed that at a 5% level of significance, the 't' value at five degrees of freedom (v = n_c − 1 = 5) is $t_{0.05,5}$ = 2.015. Table 6.3 shows the significance level of all individual parameters and the interactions. If $t_{estimated} > t_{0.05,5}$ for a certain regression

coefficient, then all of the individual parameters and the factor interaction relating to that specific regression coefficient are significant.

Table 6.3 t-values of the co-efficient vs student's t distribution considering mass per unit area as response

Student's t co-efficient	$t_{estimated}$ values	Significance
t_1	28.154	**Significant**
t_2	22.717	**Significant**
t_3	21.346	**Significant**
t_{12}	20.437	**Significant**
t_{13}	21.636	**Significant**
t_{23}	25.444	**Significant**

It can be seen from table 6.4, at 5% significance level, all the main effects and the interaction effects are significant.

6.2.4 Second order response surface model

In order to obtain a more precise correlation between the input elements and the response, response surface methodology was used. Equation (6.7) displays the response surface equation:

$$\acute{D} = 8811.68 + 160.128X_1 + 183.612X_2 - 241.006X_3 - 4.54X_1^2 + 1.92X_2^2 + 1.65X_3^2 - 2.06X_1X_2 - 1.73X_2X_3 - 2.025X_1X_3 \quad (6.7)$$

Where,

$\acute{D}\ is\ mass\ deposited\ per\ unit\ area$ in x 10^{-4}g/cm^2

$X_1\ is\ concentration\ of\ HTAB$ in g/lit

$X_2\ is\ concentration\ of\ PTFE$ in g/lit

$X_3\ is\ Temperature$ in ^{o}C

6.2.5 Reliability test for the second-order response surface equation with the help of F- test

An effective method for evaluating the dependability of the second order response surface equation that is used to predict the output is the Fisher's Variance Ratio, or F-Test. Equation (6.8) can be used to get the F-ratio. Table 6.4 gives the values of F-ratio:

$$F = \frac{\sigma_{res}^2}{\sigma_e^2} \tag{6.8}$$

where,

σ_e^2 is called the replication variance

σ_{res}^2 is called the residual variance which is given by Eqn (6.9)

$$\sigma_{res}^2 = \sum_{i=1}^{20} \frac{(Dact_i - Dest_i)^2}{(Z-n)} \tag{6.9}$$

where,

D_{act_i} is the actual mass deposition at i^{th} point.

D_{est_i} is the estimated mass deposition at the i^{th} point.

Table 6.4 Estimation of Fisher's F ratio

Predicting Response Surface Equation	Residual Variance	Replication Variance	Estimated F-value
D = f (X_1,X_2,X_3)	7329.544	1398.768	5.24

Regarding the current problem, the upper degree of freedom (v1 = Z-n) and lower degrees of freedom (v2 = n_c-1) are 10 and 5, respectively. From the critical values of F distribution table, the F-value for 1% significance level (for v1 = 10 and v2 = 5) is found to be $\boldsymbol{F_{0.05\,(10,5)}}$**= 10.051**. Regarding the equation for the response surface D = f (X1, X2, X3), the estimated F-value (5.24) is less than 10.051. It follows that the response surface model's predicted equation provides a good fit to the data that was seen.

6.2.6 Contour plots for mass deposition

Contour plots have been generated using Minitab 16 software, where the interaction of any two input parameters, keeping the third parameter constant at the zero value, on response has been shown. Figure 6.1 (a,b and c) show the contour plots of Mass deposition.

From Figure 6.1 (a), it can be said that the mass deposition is higher for high concentration of PTFE and low to medium concentration of HTAB. Figure 6.1(b) illustrates that mass deposition increases at low to medium HTAB values. From figure 6.1 (c), it can be said that temperature is an insignificant parameter as its effect on mass deposition is not prominent enough. However, mass deposition is maximum for high concentration of PTFE.

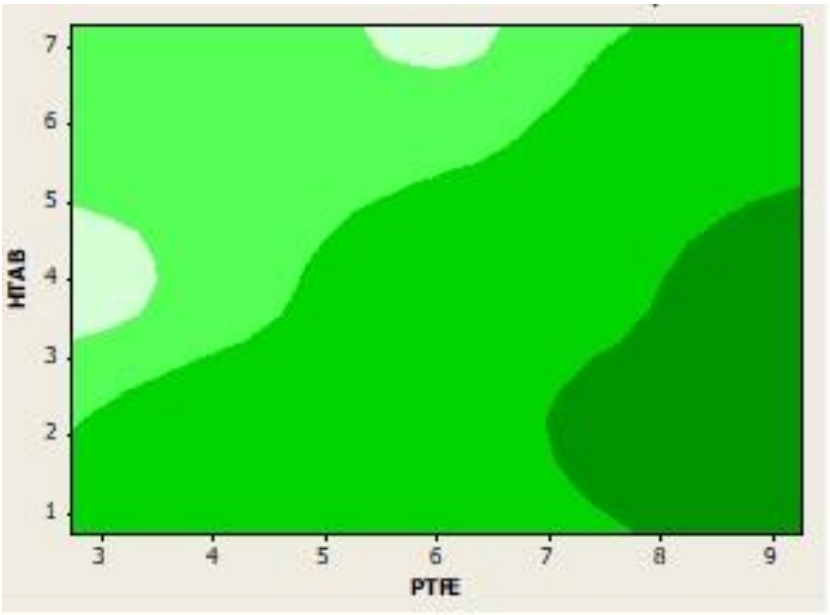

Figure 6.1 (a): Contour plot for D = $f(X_1,X_2)$ when hold value is $X_3 = 0$

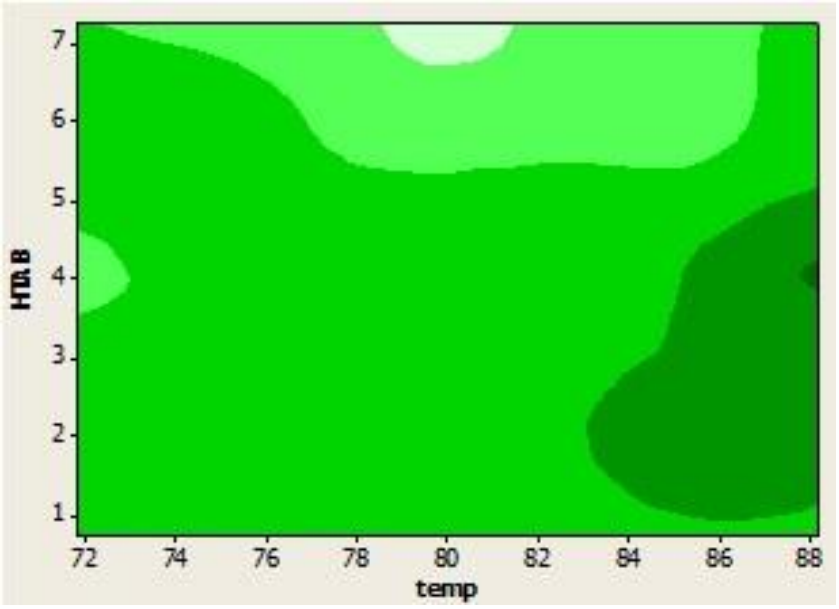

Figure 6.1 (b): Contour plot for D = $f(X_1,X_3)$ when hold value is $X_2 = 0$

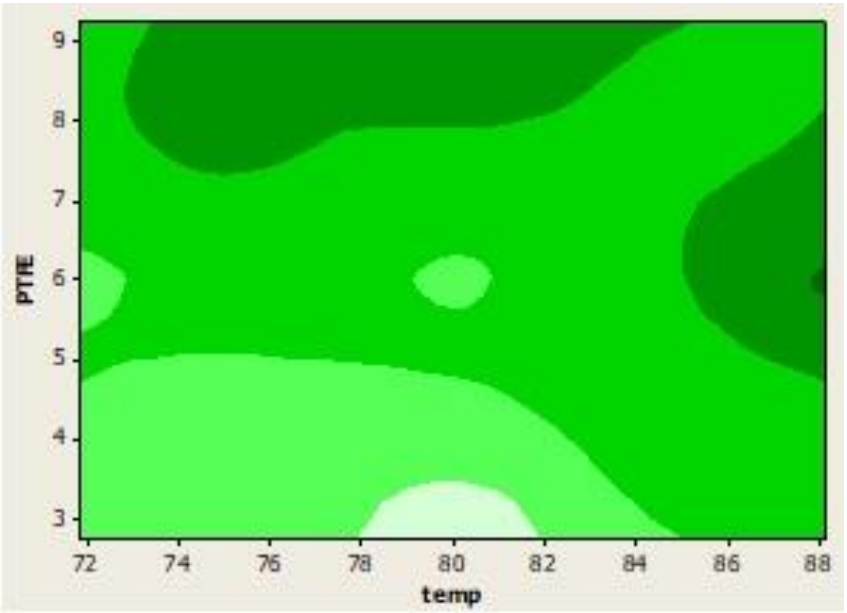

Figure 6.1 (c): Contour plot for D = $f(X_2,X_3)$ when hold value is $X_1 = 0$

6.2.7 Optimization of process parameters for maximum mass deposition per unit area using Genetic Algorithm.

A code in Python (Spider IDE 5.1.5) has been generated considering a set of 10 solutions designated as t = 0 to 10 inside the process parameters' search range, specifically X_1, X_2, and X_3. Equation 6.7, which is the second order response surface equation, has been identified as the target function. Maximizing the second order equation, as stated in equation 6.7, is the goal, using GA, subject to the process parameter ranges listed in Table 6.1. The parents were selected firstly using roulette wheel method based on their fitness value. The offspring solutions were generated following crossover between the parent chromosomes or solutions, and then followed by a mutation. To determine which of the offspring solutions was the fittest, their fitness values were compared to both of their parent solutions and to each other. To deal with the problems of local minima, the concept of elite chromosome was used. The number of generation or iteration was considered as 1000. The process parameters' ideal values viz concentration of HTAB, PTFE and Temperature were estimated as X_1 = **2.47** g/lit, X_2= **8** g/lit and X_3=**77.67** ^oC respectively which results into a mass deposition per unit area of $\mathbf{501.86\times 10^{-4}}$ g/cm^2**.** For confirmation, the coating has been deposited at the evaluated optimal condition and the result converges with mass deposition per unit area calculated using GA.

.

6.3 Analysis of Hardness of Ni-P-PTFE composite coating

The resistance a material shows to permanent distortion by the penetration of another harder substance is known as its hardness. Determining whether a material is appropriate for the specific application, is the main goal of the hardness test. The kind of indenter and its geometry, the load applied to the indenter, a particular loading time profile, and a particular load duration are all taken into consideration when determining the quantitative value of hardness. In this work, Vicker's hardness test is done for measuring the hardness of the substrate and coated samples.

Microhardness of the electroless coating depends on various factors such as bath composition, time of coating, etc. The correlation between hardness and various input parameters are not defined extensively in the earlier literatures. To comprehend the

significance of various input parameters on hardness, a statistical analysis has been performed. The effect of each input parameter is shown with the help of surface plots. In order to find the correlation between the input and the output, modelling has been performed. We have used Linear regression, Response surface methodology and Artificial neural network. A comparison has been done regarding the effectiveness of the methods to predict the output.

The experiments have been designed using central composite design. Here, the concentration of Nickel Sulphate ($NiSO_4$, $7H_2O$), PTFE and Sodium hypophosphite (NaH_2PO_2. H_2O) , have been considered as input parameters and hardness as the response parameter. Six central, six axial, and eight factorial points are enclosed by the CCD.The design factors along with their levels are shown in Table 6.6 and Table 6.7 shows the experimental data.

Table 6.5 Coded values of CCD design

Factor Name	Input parameters	Unit	-α	-1	0	1	α
A	Nickel Sulphate ($NiSO_4$, $7H_2O$)	g/lit	35	37.028	40	42.972	45
B	PTFE	ml/lit	2.734	4	6	8	9.266
C	Sodium Hypophosphite (NaH_2PO_2. H_2O)	g/lit	25	27.028	30	32.972	35

Table 6.6 Experimental results

Sequence no		$NiSO_4$,$7H_2O$ (g/lit)	PTFE (ml/lit)	NaH_2PO_2. H_2O (g/lit)	Hardness ($HV_{0.5}$)
		X_1	**X_2**	**X_3**	**H**

1	Factorial points	35	8	25	220.08
2		45	4	25	176.53
3		35	4	25	196.53
4		45	4	35	168.26
5		45	8	25	263.23
4		35	8	35	106.33
7		45	8	35	195.23
8		35	4	35	248.03
9	Central Points	40	6	30	183.52
10		40	6	30	186.44
11		40	6	30	179.29
12		40	6	30	178.58
13		40	6	30	188.53
14		40	6	30	186.98
15	Axial points	45	6	30	245.23
16		35	6	30	120.65
17		40	2.734	30	132.61
18		40	9.266	30	194.57
19		40	6	35	210.21
20		40	6	25	109.45

6.3.1 Statistical analysis of micro hardness for Ni-PTFE-P electroless coating.

An equation for first-order regression that has been fitted to determine the impact of each process parameter and their interactions on the micro hardness of electroless Ni-P-PTFE coating. It offers a correlation between the response (microhardness) and the input process parameters. (concentrations of sodium hypophosphite, PTFE, and nickel sulphate). A first order fitted equation has been developed by MINITAB 16 software, shown in Equation 6.8:

$$\acute{H} = -2759.59 + 57.68\,X_1 + 53.73X_2 + 73.35X_3 - 0.23X_1X_2 - 1.35X_1X_3 - 1.20X_2X_3 \quad (6.10)$$

6.3.2 Test of significance of the process parameters

Replication variance = Estimate of error = $\sigma_e^2 = \sum_{n_c=1}^{6} \frac{(H_{act}-H_{avg})^2}{(n_c-1)}$ (6.11)

Where,

H_{act}= Actual value of microhardnessfor the i^{th}central point.

H_{avg} = Average value of microhardness for six the central points.

n_c= No. of central points = 6 and DOF= n_c– 1 = 6–1 = 5

$$H_{avg} = \frac{(183.52+186.44+179.29+178.58+188.53+186.98)}{6} = 183.89 \quad (6.12)$$

Now, from eqn 6.11,

$$\sigma_e^2 = \frac{0.1369 + 6.5025 + 21.16 + 28.196 + 21.529 + 9.548}{5} = 17.414$$

We know. $\sigma_\beta^2 = \frac{\sigma_e^2}{n_f}$ (6.5)

Where, n_f *is number of factorial points* $= 8$

Therefore, $\sigma_\beta^2 = \frac{17.414}{8} = 2.176$

And $\sigma_\beta = 1.475$

Equation (Eqn 6.6) can be used to determine the estimated "t" values for a given process parameter.

$$t_{esrimated} = \frac{|co-eff\ of\ process\ parameters|}{\sigma_\beta} = \frac{|\beta|}{\sigma_\beta} \quad (6.6)$$

where the coefficient of process parameter has been obtained from the regression equation (6.10).

It has been noted that the "t" value at five degrees of freedom ($v = n_c - 1 = 5$) is $t_{0.05,5} = 2.015$ at a 5% level of significance. Table 6.8 shows the significance level of all individual parameters and the interactions. For a particular regression coefficient, if $t_{estimated} > t_{0.05,5}$, then every single parameter and every factor's interaction that corresponds to that specific regression coefficient is significant.

Table 6.7. t-values of the co-efficient vs student's t distribution considering mass per unit area as response

Student's t co-efficient	$t_{estimated}$ values	Significance
t_1	39.238	**Significant**
t_2	36.551	**Significant**
t_3	49.897	**Significant**
t_{12}	0.156	**Not Significant**
t_{13}	0.918	**Not Significant**
t_{23}	0.816	**Not Significant**

It can be seen from Table 6.8, at 5% significance level, all the main effects are significant but the interaction effects are insignificant.

6.3.3 Second order response surface model

In order to obtain a more precise correlation between the input elements and the response, RSM was used. Equation (6.10) displays the response surface equation:

$$\acute{H} = -705.054 - 84.195X_1 + 53.183X_2 + 117.428X_3 + 1.644X_1^2 - 1.826X_2^2 - 0.929X_3^2 + 0.137X_1X_2 - 1.130X_2X_3 - 0.954X_1X_3 \quad (6.13)$$

where,

$\acute{H}\ is\ microhardness$ in $HV_{0.5}$

$X_1\ is\ concentration\ of\ Nickel\ Sulphate$ ($NiSO4,7H2O$) in g/lit

$X_2\ is\ concentration\ of\ PTFE$ in g/lit

$X_3\ is\ the\ concentration\ of\ Sodium\ hypophospite$ ($NaH2PO2.H2O$) in g/lit

6.3.4 Reliability test for the second-order response surface equation with the help of F- test

An effective method for evaluating the dependability of the second order response surface equation that is used to predict the output is the Fisher's Variance Ratio, or F-Test. Equation (6.6) can be used to get the F-ratio. Table 6.9 gives the values of the estimated F-ratios:

$$F = \frac{\sigma_{res}^2}{\sigma_e^2} \quad (6.8)$$

Where,

σ_e^2 is called the replication variance

σ_{res}^2 is called the residual variance which is given by Eqn (6.7)

$$\sigma_{res}^2 = \sum_{i=1}^{20} \frac{(Hact_i - Hest_i)^2}{(Z-n)} \quad (6.14)$$

Where,

H_{act_i} is the actual microhardness at i^{th} point.

H_{est_i} is the estimated microhardness at the i^{th} point.

Table 6.8 Estimation of Fisher's F ratio

Predicting Response Surface Equation	Residual Variance	Replication Variance	Estimated F-value
$D = f(X_1, X_2, X_3)$	118.066	17.414	6.78

For the current problem, the upper (v1 = Z-n) and lower (v2 = nc-1) degrees of freedom are 10 and 5, respectively. From the critical values of F distribution table, the F-value for 1% significance level (for v1 = 10 and v2 = 5) is found to be $\boldsymbol{F_{0.01\,(10,5)} = 10.051}$. With respect to the response surface equation D = f (X1, X2, X3), the estimated F-value (6.78) is lower than 10.051. Therefore, it may be concluded that the response surface model's anticipated equation provides a satisfactory fit to the observed data.

6.3.5 Surface and Contour plots for mass deposition

3D surface plots have been generated in MATLAB to check the effects of interaction of the input variables to the response. Here, interaction of any two input parameters, with the third one as constant, has been generated. Figure 6.2 shows the 3D surface and contour plots. Figure 6.2 (a) shows the interaction effect of '$NiSO_4$' and 'PTFE'. Figure 6.2 (b) shows the interaction effects of parameter '$NiSO_4$' and 'NaH_2PO_2'. In the Figure 6.2 (b), it can be seen that microhardness increases with increase in 'X_3'. Hardness rises as both 'PTFE' and 'NaH_2PO_2' increase, as seen by the interaction plot between "PTFE" and 'NaH_2PO_2' (Figure. 6.2(c)).

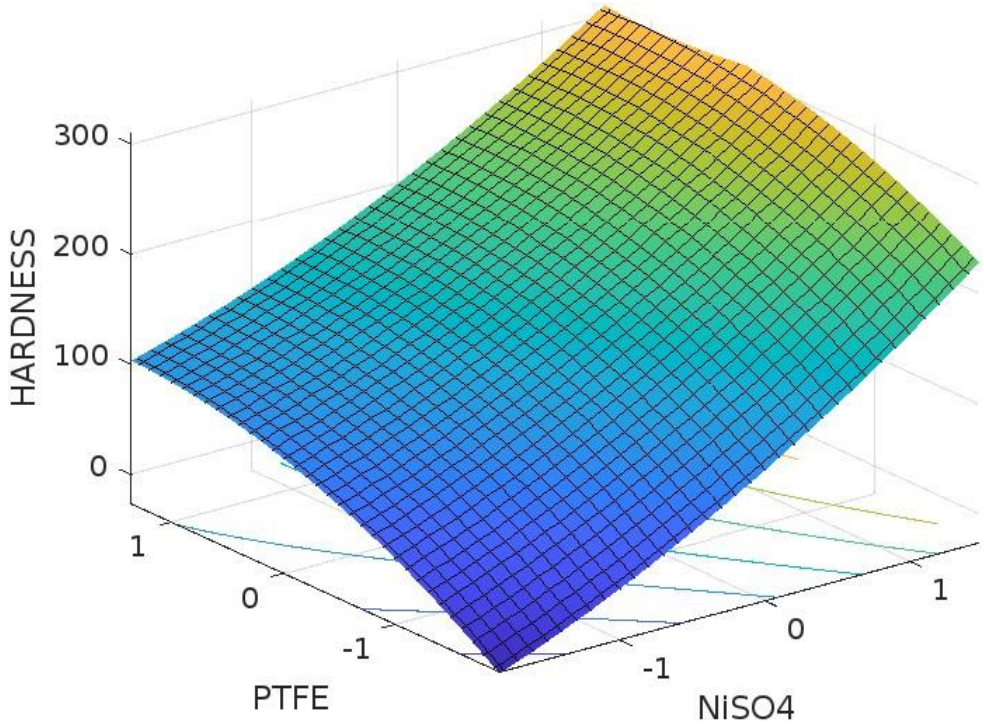

Figure 6.2 (a): Surface plots for microhardness with interaction of Nickel Sulphate (NiSO4,7H2O) and PTFE

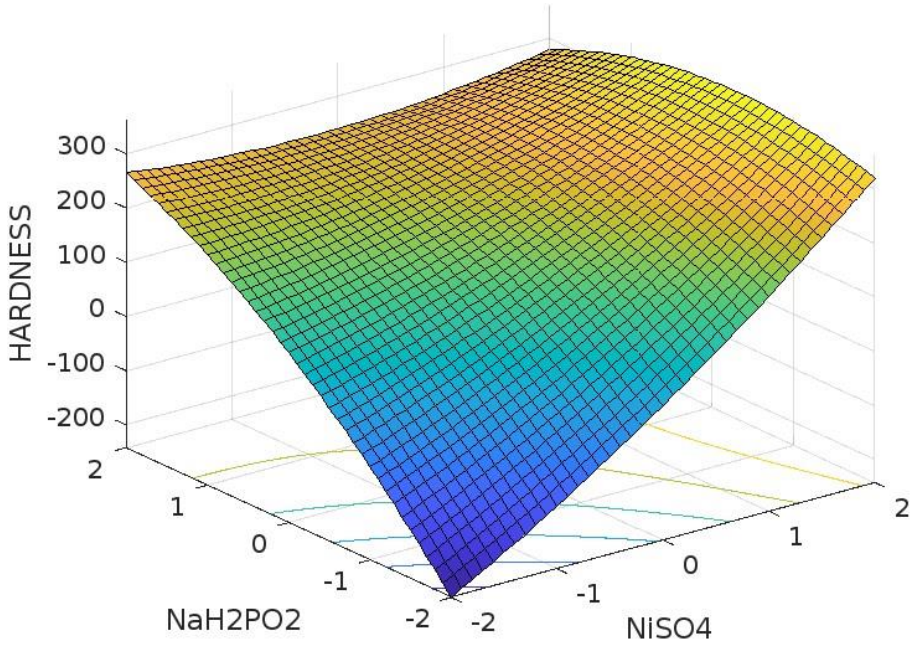

Figure 6.2 (b): Surface plots for microhardness with interaction of Nickel Sulphate (NiSO4,7H2O) and Sodium Hypophosphite (NaH_2PO_2. H_2O)

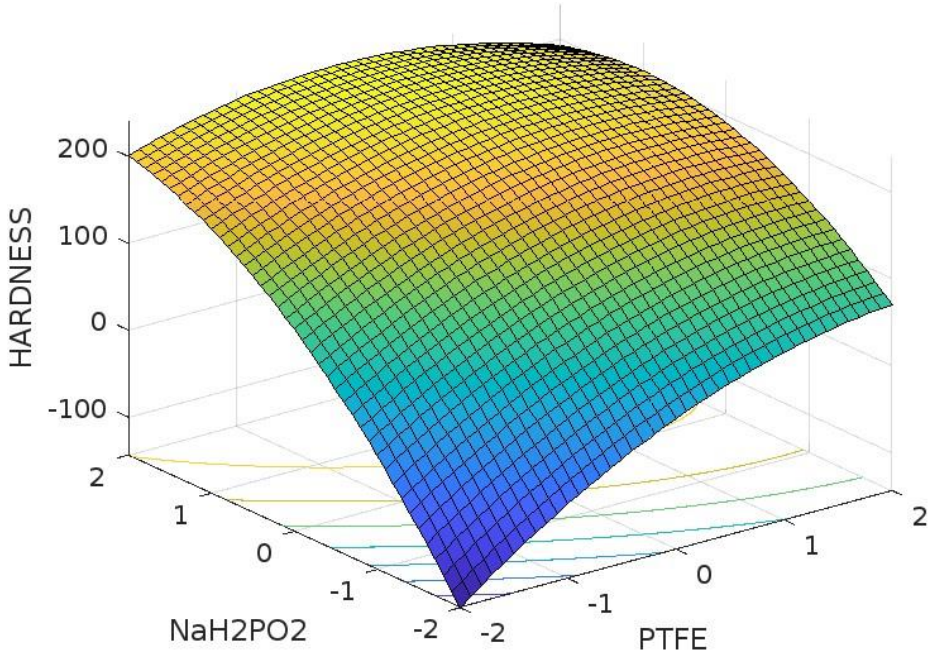

Figure 6.2 (c): Surface plots for microhardness with interaction of PTFE and Sodium Hypophosphite (NaH_2PO_2. H_2O)

6.3.6 Modelling with Artificial neural Network (ANN)

Python 3.8 has been used with various scientific libraries such as pandas and numpy for providing preprocessing methods of training the machine learning model.

This study evaluated a number of neural network topologies and architectures for the estimation and forecasting. After the neural network models were successfully trained, different ANN learning strategies and transfer function impacts were investigated. Many topologies with values ranging from 1 to 12 were examined in order to ascertain the optimal number of neurons in the hidden layer. Hardness is predicted using Multilayer Normal Feed Forward (MNFF) network, which is trained with Batch back propagation (BBP) learning algorithm. The ANN architecture consists of three layers. The input layer contains three neurons, the output layer contains one, and the buried layer contains four neurons. '*Tanh*' is the output layer's transfer function, and *'relu'* is the hidden layer's. After creating multiple networks and iteratively determining these parameters, the ideal topology was ultimately determined to be **3-4-1**. Figure 6.3 shows

the interface of the python program used in this work. All other parameters were chosen as default values of the program. There are two sections to the experimental data listed in Table 6.7: training and testing. Every ANN model is trained using a 500-iteration as the stopping criterion.

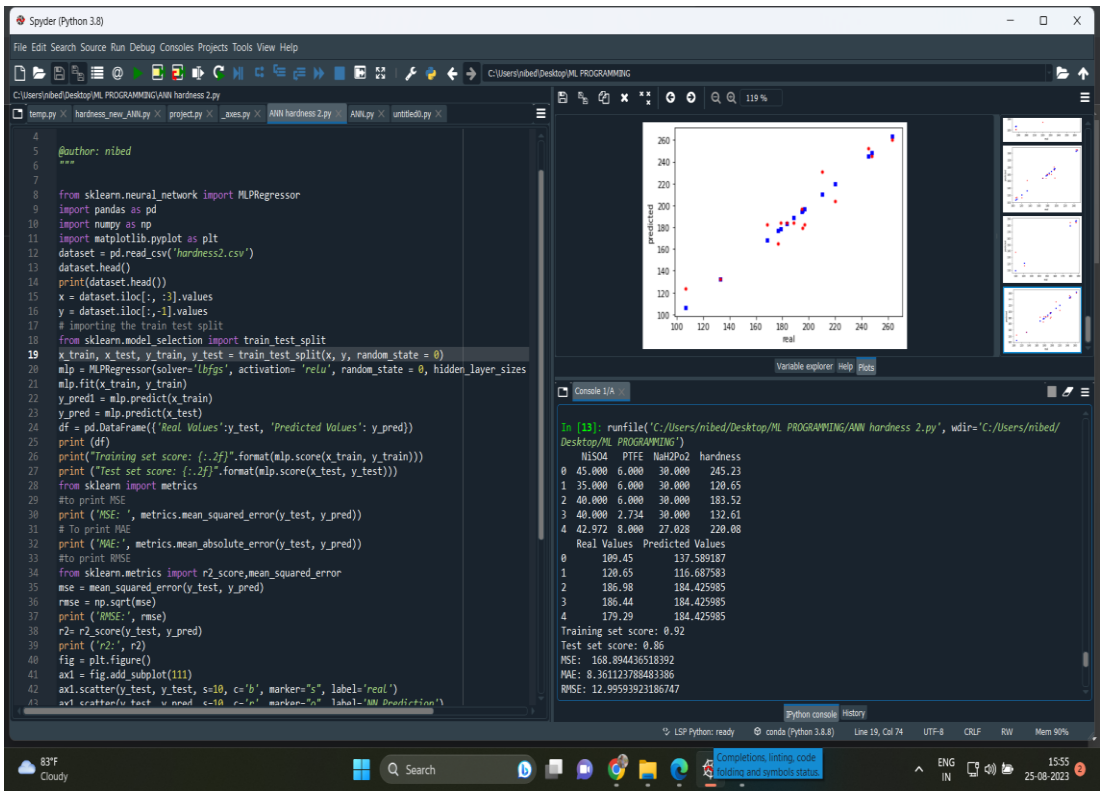

Figure 6.3: Python window showing ANN program and results

6.3.7 Performance test of ANN Model

Comparing the expected response with the actual experimental responses allowed for the evaluation of the ANN model's efficiency. The optimal model was chosen using the values of R^2 (coefficient of determination) and MSE (mean square error), which were computed. The R^2 and MSE values were evaluated by Eqn 6.15 and Eqn 6.16 :

$$R^2 = 1 - \sum_{i=1}^{n} \frac{(y_{i,pred} - y_{i,exp})^2}{(y_{avg,exp} - y_{i,exp})^2} \quad (6.15)$$

$$MSE = \frac{1}{n} \sum_{i=1}^{n} (y_{i,exp} - y_{i,pred})^2 \quad (6.16)$$

The R^2 value was calculated to be **0.855** and MSE value was **168.894**.

6.3.8 Performance evaluation of ANN and RSM

The correctness of the models predicted by ANN and RSM are checked by calculating the values of both R^2 and MSE. From Table 6.10, it can be observed that both the modelling shows good predictions, The value of R^2 and MSE for RSM is calculated to be 0.82 and 424.55 respectively. For ANN, R^2 and MSE value are evaluated as 0.85 and 168.89 respectively. However, ANN shows better results both in terms of R^2 and MSE. Figure 6.4(a.b) shows the fitting curves for both ANN and RSM obtained for modelling microhardness in electroless coating**.**

Table 6.9: Experimental and predicted values by RSM and ANN

Sl No	Experimental Hardness	RSM predicted	RSM deviation	ANN predicted	ANN deviation
1	248.03	280.922	-32.892	245.179	2.851
2	176.53	183.335	-6.805	164.652	11.878
3	263.23	280.521	-17.291	259.88	3.35
4	220.08	211.258	8.822	204.2	15.88
5	183.52	182.328	1.192	184.426	-0.906
6	194.57	172.161	22.409	196.429	-1.859
7	188.53	182.328	6.202	184.426	4.104
8	210.21	242.843	-32.633	231.263	-21.053
9	196.53	184.792	11.738	182.395	14.135
10	195.23	179.677	15.553	179.352	15.878
11	168.26	184.792	-16.532	182.395	-14.135
12	132.61	153.539	-20.929	132.61	0

13	245.23	280.922	-35.692	252.164	-6.934
14	106.33	76.708	29.622	123.673	-17.343
15	178.58	182.328	-3.748	184.426	-5.846

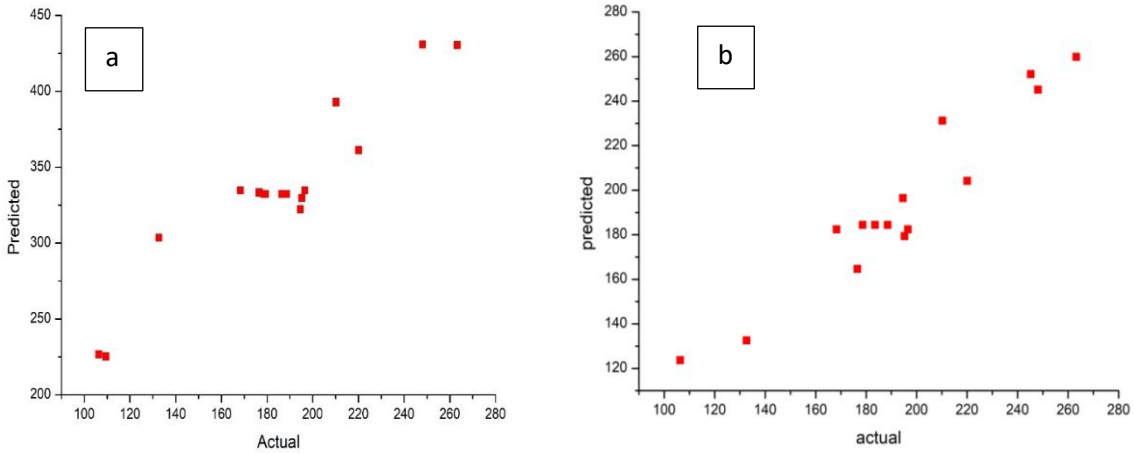

Figure 6.4(a,b) : Plot showing actual and expected values for RSM and ANN

Chapter 7

Conclusion, Summary and Future scope

***Outline of the Chapter*:** *7.1 Introduction 7.1.1 Crystallisation behaviour and compositional analysis of NiP coating 7.1.2 Corrosion behaviour of NiP coating 7.1.3 Crystallisation behaviour and compositional analysis of Ni-PTFE-P coating 7.1.4 Corrosion behaviour of Ni-PTFE-P coating 7.1.5 Nano hardness of NiP and Ni-PTFE-P coating 7.1.6 Statistical Analysis of Mass deposited per unit are of Ni-PTFE-P coating 7.1.7 Statistical Analysis of Hardness of Ni-PTFE-P coating 7.2 Summary 7.3 Future Scope of Work*

7.1 Introduction

This chapter is the summarization of analysis and results of the entire work presented in the preceding chapters. In the beginning of the thesis, the present scenario of the industrial clusters of India has been discussed. It has been concluded from the discussion that the condition of the rural industrial clusters of the country are in a vulnerable state and immediate measures have to be taken to save these clusters. Though Government has taken some measures regarding this, but they did not turn out to be of much benefit. According to author, Business-University-Business (B-U-B) Model can be of much benefit for the clusters in terms of technology transfer and assimilation. The B-U-B Model is a new model for technology transfer where the involvement of university to solve technology related problems, can be of great benefit. The scope of the B-U-B Model has been discussed in the first chapter. It has already been discussed that the present work is based on the philosophy of the B-U-B Model.

A Case study on Baruipur Surgical Instrument Cluster has been performed in the present Work. Baruipur surgical cluster is a self-grown cluster functioning since the beginning of 19th century. This cluster has been producing various types of surgical instruments since a long time. It has been fulfilling the local demand as well as exporting their products. But, after Globalization, this cluster has been losing its ground in international as well as local market. Nowadays, good quality products with international brands are easily accessible to everyone and with affordable price, In this competitive market, the

products produced by this cluster are not able to stand beside the international products. So, firstly, the author tried to find the main problem with the products produced in this cluster. In order to do so, the author has visited the cluster quite a few times and has studied the cluster very thoroughly. After studying the processes and practices followed by Baruipur Surgical instrument cluster, the author has done a thorough analysis of the problems faced by the cluster. After a detailed analysis, it has been found that, rust propagation in the instruments is the main problem. After studying the manufacturing procedure followed by the cluster and also the economic condition of the cluster, the author realized that it was not possible to make any changes in the manufacturing process. So, the author came up with an idea of surface modification of the instruments. After studying the various surface treatment techniques, electroless coating was chosen as the technique for surface modification as it is an efficient process which gives very good results and also economically cheaper than other surface treatment techniques.

From review of the previous literatures, it has been found that electroless coating is an efficient coating process. It gives excellent results in terms of hardness, corrosion resistance, fracture toughness and may more properties. The primary goal of this study is to make the instruments more resistant to corrosion. To achieve this, martensitic stainless steel (Grade AISI 420) has been coated with Ni-P alloy and Ni-P-PTFE composite coating. Since most surgical instruments are constructed of this grade of stainless steel, martensitic stainless steel of the specified grade is employed here as the substrate. After successful synthesis of Ni-P and Ni-P-PTFE composite coating, several physical, mechanical and electrochemical tests have been performed. The results are summarized in the preceding portion of this chapter. Also, modelling and optimization has been performed to obtain maximum microhardness and mass deposition per unit area. To create a mathematical model of the experiment, the experiment's Central Composite Design was carried out. The optimization of process parameters has been performed with different statistical tools which has also been summarized here.

7.1.1 Crystallisation behaviour and compositional analysis of NiP coating

X-ray diffraction tests and scanning electron microscopy have been used to analyse microstructure. The Nickel and phosphorous content have been measured with EDAX. The grains of the as-deposited NiP coating appeared spherical and the overall coating looked uniform and crack free. However, some porosity was visible in the as-deposited

coating. Following the 300^{o}C annealing process, the structure seemed denser and more homogeneous. The grains of the coating became finer and equiaxed. The EDX results show that 84.58 weight % of Nickel was deposited and 13.75 weight % of Phosphorous was deposited, Due to high phosphorus coating, the coating seemed amorphous in nature in the as-deposited condition. However, after heat treatment, the coating structure became crystalline in nature. This was confirmed from the results obtained from X-ray diffraction. From the XRD results, broad peaks at 44.5^{o} was seen for as-deposited coating which indicated amorphous nature of the coatings. However, after annealing, the peaks were narrow. Peaks of Ni and Ni_3P were visible which indicated crystalline nature of the heat-treated coating. TEM image was studied to understand the nature of interface of the substrate and coating. It was seen that no new phase was formed in between the two layers and the bonding between the two layers were purely physical in nature.

7.1.2 Corrosion behaviour of NiP coating

To investigate the as-deposited and heat-treated NiP coating's corrosion behaviour, both electron impedance spectroscopy and Potentiodynamic polarization tests were performed. More importantly, all the corrosion tests were carried with artificial blood plasma as the corrosion medium. As blood is a strong electrolyte, when the surgical instruments are in contact with blood for a long time, they start to corrode. So, author used artificial blood plasma for studying the corrosion behaviour of the coating. The high resistance to charge transfer (Rct =543 Ω) value and low capacitance (Cdl = 0.7498 x 10-5 F) implied that the heat-treated blood sample had improved corrosion resistance towards blood, than the uncoated and the as-deposited coating. After fitting the data using the device's semi-quantitative fitting software, an analogous circuit model based on the Randles circuit was created, consisting of solution resistance (R_s), charge transfer resistance (R_{ct}), and double layer capacitance (C_{dl}) (AUTOLAB 30). The results of the polarization tests show that the corrosion rate rather increased after NiP coating than uncoated substrate. This was explained by the coating's porous nature. But after heat treatment, corrosion resistivity significantly increased. The Tafel plot showed that for the heat-treated sample, the corrosion potential moved to the more positive side and the

current density reduced, which indicated that heat treated coating had the highest corrosion resistivity.

7.1.3 Crystallisation behaviour and compositional analysis of Ni-PTFE-P coating

It can be seen from the SEM analysis that the coating had fine structure with uniform distribution of PTFE all over the matrix. Uniform distribution of PTFE over the Ni-P matrix confirms uniform particle dispersion during the coating process. No visible cracks and no agglomeration phenomena were visible on the surface.

To investigate the development and crystalline structure of the Ni-P-PTFE composite coating film, TEM examination was performed. Three layers of the coating were distinctly visible from the image. Furthermore, to confirm the observation, EDX was performed at three different points. According to the EDX at point 2 in the middle layer, Nickel (Ni) and phosphorus (P) were present where Ni-P was first deposited on the substrate before the addition of PTFE to the bath. The topmost layer's EDX demonstrates the presence of carbon (C) and nickel (Ni), demonstrating that the Ni matrix contains PTFE particles. Absence of any new phase at the interface confirmed that the coating was totally physical in nature.

7.1.4 Corrosion behaviour of Ni-PTFE-P coating

A comparative study of the corrosion behaviour of three samples namely, uncoated steel substrate, Ni-P coated sample and Ni-P-PTFE coated sample was performed. The Open circuit potential (OCP) curves of the three samples seemed stable, which suggested that there are no pores and that the coatings were uniform. It can be seen from the Nyquist plot that all the curves were single semicircles which indicated that the coatings have single layer protective scale. The semicircle for EN-PTFE coating showed the largest diameter which indicated that Ni-P--PTFE coating had the highest corrosion resistivity. The Tafel plots obtained from the polarization tests showed that the current density decreased from 0.534 μA of the substrate to 0.188 μA of the Ni-P coating and E_{corr} value increased from -0.487 to -0.323, which indicated an improvement of the corrosion properties after Ni-P coating. PTFE-containing coatings, on the other hand, exhibited the best corrosion resistance, with the lowest corrosion current (I_{corr}= 0.0485 μA) and

positive corrosion potential (E_{corr}= -0.226 V). It was seen from the results of polarization test that the corrosion rate of the Ni-P-PTFE coating was 9.91×10^{-3} mm/year that is much slower than the Ni-P coating's rate of corrosion.

7.1.5 Nano hardness of NiP and Ni-PTFE-P coating

A load versus displacement curve was obtained for Ni-P and Ni-P-PTFE composite coating from the nano hardness test. It was observed that the hardness value decreased from 6.053 GPa to 1.536 GPa after the addition of PTFE. This could be attributed to the lose structure and soft property of PTFE particles due to which the coating gets easily deformed under external load. It was seen from the graph that for same amount of external load application, the deformation of the composite coating was much higher.

7.1.6 Statistical Analysis of Mass deposited per unit are of Ni-PTFE-P coating

The stainless steel ((AISI 420)) substrate has been coated with an electroless Ni-P-PTFE layer with variations in concentrations of surfactant (HTAB), PTFE and temperature. The impact of three distinct process parameters and their interplay have been examined, with the response being the amount of deposited mass per unit area. The experiment was designed using a Central Composite Design. A model of first order regression was developed in order to correlate the process parameters with the outcome. The regression model was developed to investigate the impact of specific process parameters as well as their combined effect. Mass deposition per unit area was used as the response in a student's t test. It has been concluded that the concentration PTFE, concentration of HTAB and Temperature and all their interactions are significant factors that influenced the mass deposition per unit area at 5% level of significance. Also, a response surface equation was formulated for better understanding of the process. When the response surface equation's reliability was assessed using Fisher's F-test, the results showed that the response surface equation's establishment and the observed data agree rather well. Response surfaces give graphical representation with Contour plots by varying the concentrations of the process parameters. From figure 6.1 (a), it was concluded that the mass deposition was maximum for high concentration of PTFE and low to medium concentration of HTAB. It was concluded from figure 6.1 (b) that mass deposition was maximum for low to medium value of HTAB. From figure 6.1 (c), it could be said that temperature was an insignificant parameter as its effect on mass deposition was not significant enough. However, mass deposition was maximum for

high concentration of PTFE. For optimization of the process parameters, Genetic Algorithm was used to get the optimized parameter set to maximise mass deposition per unit area. The ideal values for each process parameter, namely concentration of HTAB, PTFE and Temperature were estimated as X_1, = **2.47** g/lit, X_2= **8** g/lit and X_3=**77.67** ^oC respectively which resulted into a mass deposition per unit area of **501.86**$\times$ $\mathbf{10^{-4}}$ g/cm^2

7.1.7 Statistical Analysis of Hardness of Ni-PTFE-P coating

It has been investigated how various process variables and their interactions affect the electroless Ni-PTFE-P composite coating's microhardness. The variations in microhardness value were obtained by varying the process parameters (concentrations of Nickel Sulphate, PTFE and Sodium Hypophosphite)) within the range, following full factorial central composite design of experiment as shown in Table 6.6. A regression equation of first order was established to find relationship between the response, i.e. microhardness and the process parameters. Then, T-test was used to determine the relevance of each individual parameter and how they interact. It was found that concentration of each individual parameters was significant whereas their interaction effects were insignificant. The development of a second order response surface model and the use of Fisher's F-test to assess the response equation's dependability. The result of F-test confirmed that the equation was reliable enough in predicting the response i.e microhardness. To examine the effects of the interaction between the input variables and the response, MATLAB was used to create 3D surface plots using the response surface equation.

Also, modelling was done with Artificial neural network. An advanced multilayer feed forward network featuring backpropagation was used to design the network. A three layer model with Input layer consisting of three neurons, output layer with one neuron and hidden layer with four neurons that is 3-**4-1** was chosen to be the optimum model for predicting the response. . An analysis that compared the prediction effectiveness of RSM and ANN approaches was conducted. Python 3.8 was used to for the programming purpose of ANN. By computing the values of R^2 and MSE, the correctness of the models was verified. The value of R^2 and MSE for RSM was calculated to be 0.82 and 424.55 respectively. For ANN, R^2 and MSE value were evaluated as 0.85 and 168.89 respectively.

7.2 Summary

Finally, author would like to conclude that after successful completion of the coating process and testing, it was observed that corrosion resistivity had increased. So, it can be concluded that a new technology has been developed which may be a feasible and a sustainable solution for increasing the corrosion resistivity of the instruments. Steps has been taken to transfer this newly developed technology to the cluster members. An incubation of this technology at the Common Facility Centre of the cluster has been done so that there will be a scope for implementing this technology at a large scale.

7.3 Future Scope of Work

In the present work, to improve the steel substrate's ability to withstand corrosion, composite coating was created by including Particles of PTFE in the Ni matrix. The substrate used in the present study are used for manufacturing surgical instruments. The application of electroless coating can be of practical use in numerous other areas such as automotive, Textile, electronics, food processing, etc. A lot more research on different types of coating can be done to enhance new properties. Further investigation is needed into electroless coating of challenging substrates such as magnesium, aluminium, etc.

Although lot of work has been done in the field alloy coating and composite coating, the field of nano coating has lot of scope in the future. Since, electroless coating is biologically compatible, research in the field of biomaterial coatings can open many new ventures of electroless coating.

Most of the earlier work on electroless coating has been done on metallic substrates. Very few works have been done on non-metallic surface. Therefore, electroless coating on non-conductive surface could be of additional opportunity in the field of electroless coating.

The present work has addressed the Baruipur Surgical instrument cluster for technology transfer. In the similar manner, many other clusters can be addressed to solve their technology related problems in future. This is high time, when education has to be linked with industry for overall development of both sides. So, the importance of B-U-B model should be realized and more future work should be done in this regard.

REFERENCES

- Apachitei, I., Duszczyk, J., Katgerman, L., & Overkamp, P. J. B. (1998). Electroless Ni–P Composite Coatings: The Effect of Heat Treatment on the Microhardness of Substrate and Coating. *Scripta Materialia*, *38*(9), 1347–1353. https://doi.org/10.1016/S1359-6462(98)00054-2

- Aida Calderaa & Olivier Debande., 2010, Performance of Spanish universities in technology transfer: An empirical analysis, Research Policy (39) 1160–1173. DOI:10.1016/j.respol.2010.05.016

- Ali S , Meißner T.M. .Oskay ;Galetz M, C., 2021. Electroless Ni–P coatings on low- Cr steels: a costefficient solution for solar thermal applications. Sol Energy Mater Sol Cells (231). DOI: 10.1016/j.solmat.2021.111312

- Araghi, A., & Paydar, M. H. (2010). Electroless deposition of Ni-P-B4C composite coating on AZ91D magnesium alloy and investigation on its wear and corrosion resistance. *Materials and Design*, *31*(6), 3095–3099. https://doi.org/10.1016/j.matdes.2009.12.042

- Balaraju, J. N., & Rajam, K. S. (2005). Electroless deposition of Ni–Cu–P, Ni–W–P and Ni–W–Cu–P alloys. *Surface and Coatings Technology*, *195*(2–3), 154–161. https://doi.org/10.1016/J.SURFCOAT.2004.07.068

- Balaraju, J. N., & Rajam, K. S. (2007). Electroless Deposition and Characterization of High Phosphorus Ni-P-Si 3 N 4 Composite Coatings. In *Int. J. Electrochem. Sci* (Vol. 2). www.electrochemsci.org

- Balaraju, J., Sankara Narayanan, T. & Seshadri, S. Electroless (2003) Ni–P composite coatings. Journal of Applied Electrochemistry 33, 807–816 (2003). https://doi.org/10.1023/A:1025572410205

- Balaraju, J. N., Sankara Narayanan, T. S. N., & Seshadri, S. K. (2006). Structure and phase transformation behaviour of electroless Ni-P composite coatings. *Materials Research Bulletin*, *41*(4), 847–860. https://doi.org/10.1016/j.materresbull.2005.09.024

- Baskaran, I., Sankara Narayanan, T. S. N., & Stephen, A. (2009). Corrosion resistance of electroless Ni-low B coatings. *Transactions of the Institute of Metal Finishing*, *87*(4), 221–224.https://doi.org/10.1179/174591909X438848

- Basu J., Bhattacharyya A., Sarkar B., Business to University to Business (BUB) model: An Alternative Methodology for Technology Transfer to Rural Industrial Clusters in India,*Journal of Knowledge Globalization, 2(3),* 2010.

- Betiku E., Omilakin O.R., Ajala S.O., Adebisi Aminat Okeleye A.A., Taiwo A.E., Solomon B. O., Mathematical modeling and process parameters optimization studies by artificial neural network and response surface methodology: A case of non-edible neem (Azadirachta indica) seed oil biodiesel synthesis, *Energy, 72*, 266-273. https://doi.org/10.1016/j.energy.2014.05.033.

- Brenner, A., & Riddell, G. E. (1946). *Nickel Plating on Steel by Chemical Reduction* (Vol. 37).

- Broszeit, E. (1982). Mechanical, thermal and tribological properties of electro- and chemodeposited composite coatings. *Thin Solid Films*, *95*(2), 133–142. https://doi.org/10.1016/0040-6090(82)90235-8

- Chan, L., & Daim, T. U. (2011). Technology transfer in China: Literature review and policy implications. *Journal of Science and Technology Policy in China*, *2*(2), 122–145. https://doi.org/10.1108/17585521111155192

- Chen, J., Zhao, G., Matsuda, K., & Zou, Y. (2019). Microstructure evolution and corrosion resistance of Ni–Cu–P amorphous coating during crystallization process. *Applied Surface Science*, *484*, 835–844. https://doi.org/10.1016/J.APSUSC.2019.04.142

- Chen, W., Gao, W., & He, Y. (2010). A novel electroless plating of Ni–P–TiO2 nano-composite coatings. *Surface and Coatings Technology*, *204*(15), 2493–2498. https://doi.org/10.1016/J.SURFCOAT.2010.01.032

- Candelarias A.F and Pinedo C. E. (2002). Influence of the heat treatment on the corrosion resistance of the martensitic stainless steel type AISI 420. Journal of Materials Science Letters, 22, 1151 – 1153

- Chen, X. H., Chen, C. S., Xiao, H. N., Liu, H. B., Zhou, L. P., Li, S. L., & Zhang, G. (2006). Dry friction and wear characteristics of nickel/carbon nanotube electroless composite deposits. *Tribology International*, *39*(1), 22–28. https://doi.org/10.1016/J.TRIBOINT.2004.11.008

- Corsi A., Regina N. P., Kovaleski J. L.,Da Silva V. L., (2019), Technology transfer for sustainable development: social impacts depicted and some other

answers to a few questions., Journal of Cleaner Production https://doi.org/10.1016/j.jclepro.2019.118522

- Das R .and Das A. K., (2011) Industrial Cluster: An Approach for Rural Development in North East IndiaInternational Journal of Trade, Economics and Finance, Vol. 2, No. 2, DOI: 10.7763/IJTEF.2011.V2.96

- Deb, K., Pratap, A., Agarwal, S., & Meyarivan, T. A. M. T. (2002). A fast and elitist multiobjective genetic algorithm: NSGA-II. IEEE transactions on evolutionary computation, 6(2), 182-197.

- Delaunois, F., & Lienard, P. (2002). Heat treatments for electroless nickel–boron plating on aluminium alloys. *Surface and Coatings Technology*, *160*(2–3), 239–248. https://doi.org/10.1016/S0257-8972(02)00415-2

- Dhakal, D. R., Gyawali, G., Kshetri, Y. K., Choi, J. H., & Lee, S. W. (2020). Microstructural and electrochemical corrosion properties of electroless Ni-P-TaC composite coating. *Surface and Coatings Technology*, *381*. https://doi.org/10.1016/j.surfcoat.2019.125135

- Dong, D., Chen, X. H., Xiao, W. T., Yang, G. B., & Zhang, P. Y. (2009). Preparation and properties of electroless Ni–P–SiO2 composite coatings. *Applied Surface Science*, *255*(15), 7051–7055. https://doi.org/10.1016/J.APSUSC.2009.03.039

- Duhin, A., Sverdlov, Y., Feldman, Y., & Shacham-Diamand, Y. (2009). Electroless deposition of NiWB alloy on p-type Si(1 0 0) for NiSi contact metallization. *Electrochimica Acta*, *54*(25), 6036–6041. https://doi.org/10.1016/J.ELECTACTA.2009.01.062

- Fayyad E.M., Mohammad K. Hassan, Kashif Rasool, Khaled A. Mahmoud, Adel M.A. Mohamed, George Jarjoura, Zoheir Farhat, Aboubakr M. Abdullah, (2019) Novel electroless deposited corrosion resistant and anti-bacterial NiP–TiNi nanocomposite coatings. Surface and Coatings Technology, 369, 323-333. https://doi.org/10.1016/j.surfcoat.2019.04.064

- Farzaneh, A., Mohammadi, M., Ehteshamzadeh, M., & Mohammadi, F. (2013). Electrochemical and structural properties of electroless Ni-P-SiC nanocomposite coatings. *Applied Surface Science*, *276*, 697–704. https://doi.org/10.1016/j.apsusc.2013.03.156

- Gao, R., Du, M., Sun, X., & Pu, Y. (2007). Study of the corrosion resistance of electroless Ni-P deposits in a sodium chloride medium. *Journal of Ocean University of China*, *6*(4), 349–354. https://doi.org/10.1007/s11802-007-0349-2

- Gao Y, Zheng ZJ, Zhu M,luo C.P., 2004. Corrosion resistance of electrolessly deposited Ni–P and Ni– W–P alloys with various structures. *Mater Sci Eng A 381(1–2)*:98–103. DOI: 10.1016/j.msea.2004.04.077

- Gong J, Peng Z, Miao H (2005) Analysis of the nanoindentation load-displacement curves measured on high-purity fne-grained alumina. *J Eur Ceram Soc 25(5):*649–654. https://doi.org/10.1016/j.jeurceramsoc.2004.04.003

- Hosseinabadi E. M., Azari-Dorcheh, K., & Vaghefi, S. M. M. (2006). Wear behavior of electroless Ni–P–B4C composite coatings. *Wear*, *260*(1–2), 123–127. https://doi.org/10.1016/J.WEAR.2005.01.020

- Hu, X., Jiang, P., Wan, J., Xu, Y., & Sun, X. (2009). Study of corrosion and friction reduction of electroless Ni-P coating with molybdenum disulfide nanoparticles. *Journal of Coatings Technology and Research*, *6*(2), 275–281. https://doi.org/10.1007/s11998-008-9131-7

- Huang, Y. S., Zeng, X. T., Annergren, I., & Liu, F. M. (2003). Development of electroless NiP–PTFE–SiC composite coating. *Surface and Coatings Technology*, *167*(2–3), 207–211. https://doi.org/10.1016/S0257-8972(02)00899-X

- Islam, M., Azhar, M. R., Fredj, N., & Burleigh, T. D. (2013). Electrochemical impedance spectroscopy and indentation studies of pure and composite electroless Ni–P coatings. *Surface and Coatings Technology*, *236*, 262–268. https://doi.org/10.1016/J.SURFCOAT.2013.09.057

- Jiaqiang, G., Lei, L., Yating, W., Bin, S., & Wenbin, H. (2006). Electroless Ni–P–SiC composite coatings with superfine particles. *Surface and Coatings Technology*, *200*(20–21), 5836–5842. https://doi.org/10.1016/J.SURFCOAT.2005.08.134

- Jiang W, Shen L, Wang Z, Wang K, Xu M, Tian Z (2019) Wear resistance of a Ni-PTFE composite coating strengthened with nano-SiC particles. *Mater Res Express*. https://doi.org/10.1088/ 2053-1591/ab320b

- Kant Garg Girish & Sangwan Kuldip Singh. (2015). Predictive Modelling and Optimization of Machining Parameters to Minimize Surface Roughness using Artificial Neural Network Coupled with Genetic Algorithm. Procedia CIRP. 31. 453-458. 10.1016/j.procir.2015.03.043

- Keong, K. G., & Sha, W. (2002). Crystallisation and phase transformation behaviour of electroless nickel - Phosphorus deposits and their engineering properties. In *Surface Engineering* (Vol. 18, Issue 5, pp. 329–343). IOM Communications Ltd. https://doi.org/10.1179/026708402225010010

- Keong, K. G., Sha, W., & Malinov, S. (2003). Hardness evolution of electroless nickel–phosphorus deposits with thermal processing. *Surface and Coatings Technology*, *168*(2–3), 263–274. https://doi.org/10.1016/S0257-8972(03)00209

- Krishnaveni, K., Sankara Narayanan, T. S. N., & Seshadri, S. K. (2005a). Electroless Ni–B coatings: preparation and evaluation of hardness and wear resistance. *Surface and Coatings Technology*, *190*(1), 115–121. https://doi.org/10.1016/J.SURFCOAT.2004.01.038

- Leong C and Tugrul U. D.,2011., Technology transfer in China: literature review and policy implication Journal of Science and Technology Policy in China Vol. 2 No. 2, pp 122-145 DOI:10.1007/S10961-016-9487-2

- León, O. A., Staia, M. H., & Hintermann, H. E. (2003). High temperature wear of an electroless Ni–P–BN (h) composite coating. *Surface and Coatings Technology*, *163–164*, 578–584. https://doi.org/10.1016/S0257-8972(02)00663-1

- León, O. A., Staia, M. H., & Hintermann, H. E. (2005). Wear mechanism of Ni-P-BN(h) composite autocatalytic coatings. *Surface and Coatings Technology*, *200*(5–6), 1825–1829. https://doi.org/10.1016/j.surfcoat.2005.08.061

- Li, Z.-H., Chen, Z.-Y., Liu, S.-S., Feng, Z., & Dai, A.-G. (2009). *Corrosion and wear properties of electroless Ni-P plating layer on AZ91D magnesium alloy*.

- Luo H, Leitch M, Behnamian Y,,2015. Development of electroless Ni–P/nano-WC composite coatings and investigation on its properties. Surf Coat Technol ;277:99–106. DOI: 10.1016/j.surfcoat.2015.07.011

- Mafi IR and Dehghanian C (2011) Comparison of the coating properties and corrosion rates in electroless Ni-P/PTFE composites prepared by diferent types

of surfactants. Appl Surf Sci 257(20):8653–8658. https://doi.org/10.1016/j.apsusc.2011.05. 04

- Mareci D., Trinca L.C., Cotea V.V., Souto R.M., (2017) Electrochemical Studies on the Stability and Corrosion Resistance of Two Austenitic Stainless Steels for Soft Drinks Containers. *Int. J. Electrochem. Sci., 12* (2017) 5438 – 5449. doi: 10.20964/2017.06.35

- Mitra A., Sharma C., Veganzones-Varoudakis M. A., (2014) Trade liberalization, technology transfer, and firms' productive performance: The case of Indian manufacturing, Journal of Asian Economics 33 pp 1–15 http://dx.doi.org/10.1016/j.asieco.2014.04.001

- Montgomery, D. C., (2012). Design and Analysis of Experiments, 7th edition.Wiley India (P.) Ltd., ISBN: 978-81-265-2837-0.

- Narayanan T. S.., Baskaran, I., Krishnaveni, K., & Parthiban, S. (2006). Deposition of electroless Ni–P graded coatings and evaluation of their corrosion resistance. *Surface and Coatings Technology*, *200*(11), 3438–3445. https://doi.org/10.1016/J.SURFCOAT.2004.10.014

- N. Saha N., J. Basu J., P. Sen P., Majumdar G. (2019), Electrochemical behaviour of martensitic stainless steel with blood, Materials Today: Proceedings, https://doi.org/10.1016/j.matpr.2019.12.364

- Novák, M., Vojtěch, D., & Vítů, T. (2010). Influence of heat treatment on tribological properties of electroless Ni–P and Ni–P–Al2O3 coatings on Al–Si casting alloy. *Applied Surface Science*, *256*(9), 2956–2960. https://doi.org/10.1016/J.APSUSC.2009.11.057

- Oraon, B., Majumdar, G., & Ghosh, B. (2008a). Improving hardness of electroless Ni–B coatings using optimized deposition conditions and annealing. *Materials & Design*, *29*(7), 1412–1418. https://doi.org/10.1016/J.MATDES.2007.09.005

- Palaniappa, M., & Seshadri, S. K. (2008). Friction and wear behavior of electroless Ni–P and Ni–W–P alloy coatings. *Wear*, *265*(5–6), 735–740. https://doi.org/10.1016/J.WEAR.2008.01.002

- Pancrecious, J. K., Ulaeto, S. B., Ramya, R., Rajan, T. P. D., & Pai, B. C. (2018). Metallic composite coatings by electroless technique–a critical review. In *International Materials Reviews* (Vol. 63, Issue 8, pp. 488–512). Taylor and Francis Ltd. https://doi.org/10.1080/09506608.2018.1506692

- Ramalho, A., & Miranda, J. C. (2005). Friction and wear of electroless NiP and NiP + PTFE coatings. *Wear*, *259*(7–12), 828–834. https://doi.org/10.1016/j.wear.2005.02.052

- Ranganatha, S., Venkatesha, T. V., & Vathsala, K. (2010). Development of electroless Ni–Zn–P/nano-TiO2 composite coatings and their properties. *Applied Surface Science*, *256*(24), 7377–7383. https://doi.org/10.1016/J.APSUSC.2010.05.076

- Reddy, V. V. N., Ramamoorthy, B., & Nair, P. K. (2000). A study on the wear resistance of electroless Ni–P/Diamond composite coatings. *Wear*, *239*(1), 111–116. https://doi.org/10.1016/S0043-1648(00)00330-6

- Tour A., Matthieu G, Yan M., (2011), Innovation and international technology transfer: The case of the Chinese photovoltaic industry, Energy Policy 39 pp 761–770 DOI:10.1016/j.enpol.2010.10.050

- Rustandi, Andi & Sirait, Geraldo & Saputra, Andy & Sadeli, Yunita. (2018). The Use of Electrochemical Impedance Spectroscopy Method for Corrosion Resista Evaluation of 2205 and 410s Stainless Steels in Aqueous Sodium Chloride Solution. *IOP Conference Series: Materials Science and Engineering. 299.* 012-053. Doi: 10.1088/1757-899X/299/1/012053.

- Sahoo, P. (2009). Wear behaviour of electroless Ni–P coatings and optimization of process parameters using Taguchi method. *Materials & Design*, *30*(4), 1341–1349. https://doi.org/10.1016/J.MATDES.2008.06.031

- Salicio-Paz A, Grande H, Pellicer E, Sort J, Fornell J, Ofoiach R, Lekka M, García-Lecina E (2019) Monolayered versus multilayered electroless NiP coatings: Impact of the plating approach on the microstructure, mechanical and

corrosion properties of the coatings. Surf Coat Technol 368:138–146. https://doi.org/10. 1016/j.surfcoat.2019.04.013

- Sarret, M., Müller, C., & Amell, A. (2006). Electroless NiP micro- and nano-composite coatings. *Surface and Coatings Technology*, *201*(1–2), 389–395. https://doi.org/10.1016/J.SURFCOAT.2005.11.127

- Selvi V, Chatterji P, Subramanian S, Balaraju J.N., (2014). Autocatalytic duplex Ni–P/Ni–W–P coatings on AZ31B magnesium alloy. Surf Coat Technol. (240):103–109. DOI: https://doi.org/10.1016/j.surfcoat.2013.12.022

- Srinivasan, K. N., & John, S. (2005). Studies on electroless nickel-PTFE composite coatings. *Surface Engineering*, *21*(2), 156–160. https://doi.org/10.1179/174329405X40902

- Sribalaji M.,Asiq Rahman O.S., Laha T, Keshri A.K.(2016) Nanoindentation and nanoscratch behavior of electroless deposited nickel-phosphorous coating, *Materials Chemistry and Physics,* (177), 220-228. https://doi.org/10.1016/j.matchemphys.2016.04.022.

- Straffelini, G., Colombo, D., & Molinari, A. (1999). Surface durability of electroless Ni–P composite deposits. *Wear*, *236*(1–2), 179–188. https://doi.org/10.1016/S0043-1648(99)00273-2

- Sudagar, J., Lian, J., & Sha, W. (2013). Electroless nickel, alloy, composite and nano coatings - A critical review. In *Journal of Alloys and Compounds* (Vol. 571, pp. 183–204). https://doi.org/10.1016/j.jallcom.2013.03.107

- Taheri R, Oguocha I.N.A, Yannacopoulos S, 2001, The tribological characteristics of electroless NiP coatings,Wear 249 (5-6): 389-396, https://doi.org/10.1016/S0043-1648(01)00539-7.

- Valova, E., Georgieva, J., Armyanov, S., Avramova, I., Dille, J., Kubova, O., & Delplancke-Ogletree, M. P. (2010). Corrosion behavior of hybrid coatings: Electroless Ni–Cu–P and sputtered TiN. *Surface and Coatings Technology*, *204*(16–17), 2775–2781. https://doi.org/10.1016/J.SURFCOAT.2010.02.035

- Vitry, V., Delaunois, F., & Dumortier, C. (2008). Mechanical properties and scratch test resistance of nickel–boron coated aluminium alloy after heat

treatments. *Surface and Coatings Technology*, *202*(14), 3316–3324. https://doi.org/10.1016/J.SURFCOAT.2007.12.001

- Wang, L. Y., Tu, J. P., Chen, W. X., Wang, Y. C., Liu, X. K., Olk, C., Cheng, D. H., & Zhang, X. B. (2003). Friction and wear behavior of electroless Ni-based CNT composite coatings. *Wear*, *254*(12), 1289–1293. https://doi.org/10.1016/S0043-1648(03)00171-6

- Wang, S. L. (2004). Studies of electroless plating of Ni–Fe–P alloys and the influences of some deposition parameters on the properties of the deposits. *Surface and Coatings Technology*, *186*(3), 372–376. https://doi.org/10.1016/J.SURFCOAT.2004.01.017

- Wen-Hsiang Lai, (2011) Willingness-to-engage in technology transfer in industry–university collaborations, Journal of Business Research 64 pp 1218–1223 DOI: 10.1016/j.jbusres.2011.06.026

- Winowlin Jappes, J. T., Ramamoorthy, B., & Kesavan Nair, P. (2009). Novel approaches on the study of wear performance of electroless Ni–P/diamond composite deposites. *Journal of Materials Processing Technology*, *209*(2), 1004–1010. https://doi.org/10.1016/J.JMATPROTEC.2008.03.040

- Wu, Y., Liu, H., Shen, B., Liu, L., & Hu, W. (2006). The friction and wear of electroless Ni–P matrix with PTFE and/or SiC particles composite. *Tribology International*, *39*(6), 553–559. https://doi.org/10.1016/J.TRIBOINT.2005.04.032

- Wu, Y., Shen, B., Liu, L., & Hu, W. (2006). The tribological behaviour of electroless Ni–P–Gr–SiC composite. *Wear*, *261*(2), 201–207. https://doi.org/10.1016/J.WEAR.2005.09.008

- X.H. Chen, C.S. Chen, H.N. Xiao, H.B. Liu, L.P. Zhou, S.L. Li, G. Zhang (2006), Dry friction and wear characteristics of nickel/carbon nanotube electroless composite deposits, *Tribology International 39(1)* 22-28, https://doi.org/10.1016/j.triboint.2004.11.008.

- Yan, M., Ying, H. G., & Ma, T. Y. (2008). Improved microhardness and wear resistance of the as-deposited electroless Ni–P coating. *Surface and Coatings Technology*, *202*(24), 5909–5913. https://doi.org/10.1016/J.SURFCOAT.2008.06.180

- Yanhai C, Lu R, Xianliang M, Jinyong Y, Xianhua T (2019) The efect of PTFE addition on mechanical and anti-corrosion properties of coating of heat exchangers. Mater Res Express. https://doi. org/10.1088/2053-1591/ab2222

- Yu, L. G., & Zhang, X. S. (1994). The friction and wear properties of electroless Ni-polytetrafluoroethylene composite coating. *Thin Solid Films*, *245*(1–2), 98–103. https://doi.org/10.1016/0040-6090(94)90883-4

- Yuan, X. Y., Xie, T., Wu, G. S., Lin, Y., Meng, G. W., & Zhang, L. D. (2004). Fabrication of Ni–W–P nanowire arrays by electroless deposition and magnetic studies. *Physica E: Low-Dimensional Systems and Nanostructures*, *23*(1–2), 75–80. https://doi.org/10.1016/J.PHYSE.2004.01.011

- Zhang L, Yong J, Peng B, 2008. Effects of annealing temperature on the crystal structure and properties of electroless deposited Ni–W–Cr–P alloy coatings. *Appl Surface Sci. 255 (5):*1686–1691

Appendix

Table: 2.1 Components of Electroless Nickel bath and their functions

Component	Function	Chemicals
Nickel ions	metal source	Nickel chloride, Nickel sulphate
Hypophosphite ions	Reducing agents	Sodium hypophosphite, Sodium borohydride, Hydrazine
Complexants	• Acts as a pH buffer • Stabilizes the solution • prevent free Ni ion concentration \	Ammonia, Monocarboxylic acids, di carboxylic acids, hydroxycarboxylic acids,
Accelerators	• Activate hypophosphite ions • accelerate the deposition rate.	Anions of some mono & di carboxylic acids, fluorides, borates
Buffers	• controls the pH of the bath	Sodium salt of certain complexants
Stabilizers	• Prevents bath decomposition	Thiourea, Lead, tin, arsenic, molybdenum, cadmium or thallium ions, , etc
Wetting agent	• Increase wettability • Uniform coating	Surfactants

Table: 2.2 Relationship between pH and Phosphorus content of deposit (wt %)

pH	Phosphorus Content(wt %)
5.8	2.2
5.0	3.5
4.5	8.9
4.0	11.4
3.0	14.1

Table 4.1 Chemical composition of AISI 420

	Chemical composition (%)							
	C	Mn	Si	P	S	Cr	Ni	
AISI 420	>0.15	1	1	0.04	0.03	12-14	0	

Table 4.2 Conditions of electroless Ni-P coating deposition.

FACTORS		**Amount**
Nickel sulphate ($NiSO_4$)	Source of Ni ions	30 (g/L)
Nickel chloride ($NiCl_2$)	Source of Ni ions	30 (g/L)
Sodium hypophosphide ($NaPO_2H_2$)	Reducing agent	12 (g/L)
Trisodium citrate dehydrate ($C_6H_9Na_3O_9$)	Complexent	70 (g/L)
Ammonium chloride (NH_4Cl)	Buffering agent	50 (g/L)
Bath Volume		250 ml
Activation Temperature		55^o C
pH value		4.8
Temperature		90^o C
Deposition time		2 hours

Table 4.3: Conditions of electroless Ni-PTFE-P coating deposition

FACTORS		**Amount**
Nickel sulphate	Source of Ni ions	30 g/lit
Nickel chloride	Source of Ni ions	30 g/lit
Sodium hypophosphide	Reducing agent	12 g/lit
Trisodium citrate dehydrate	Complexent	70 g/lit
Ammonium chloride	Buffering agent	50 g/lit
PTFE	Source of composite	6 ml/lit
HTAB	surfactant	2 g/lit
Bath Volume		250 ml
Activation Temperature		55^{o} C
pH value		4.8
Temperature		90^{o} C
Deposition time		1.5 hours

Table 5.1: Elemental composition of steel substrate

Element	Weight %	Atomic %
Na	8.07	16.85
Cl	5.17	5.63
K	3.52	5.32
Cr	13.82	12.75
Fe	70.51	60.56

Table 5.2 Chemical composition of the martensitic stainless steel (AISI 420, Custom 630 & 455) used in this study

	Chemical composition(%)						
	C	Mn	Si	P	S	Cr	Ni
AISI 520	>0.15	1	1	0.05	0.03	12-15	0
Custom 630	0.05	0.5	0.5	0.05	0.03	15-17.5	3-5
Custom 455	0.05	0.5	0.5	0.05	0.03	11-12	7.5-9.5

Table 5.3. **Chemical composition of Artificial Blood Plasma**

Components	***Amount in distilled water (g/L)***
KCl	0.5
$CaCl_2$	0.2
$NaHCO_3$	2.2
NaCl	6.8
$MgSO_5$	0.1
NaH_2PO_5	0.026
Na_2HPO_5	0.126

Table 5.4. Electrochemical parameters obtained from equivalent circuit (for steel substrate)

Grade	**R_s** **(ohm-cm^2)**	**R_{ct}** **(kΩ-cm^2)**	**CPE**	
			Y_O (F)	**n**
AISI 420	12.93	135	0.2126x10^{-3}	0.8783
Custom 630	12.92	521	0.6789 x 10^{-5}	0.8521
Custom 555	20.26	583	0..2723 x 10^{-3}	0.8025

Table 5.5. Electrochemical parameters obtained from potentiodynamic polarization (for steel substrate)

	E_{corr} (V)	**I_{corr} (x10^{-6}) A.cm^2**	**R_p (x10^{-3}) Ω**	**Corrosion rate (x10^{-3}) mm/year**
AISI 420	-0.517 V	1.135	0.6016	13.18
CUSTOM 630	-0.532 V	0.5739	1.811	6.665
CUSTOM 455	-0.365 V	0.529	2.58	5.975

Table 5.6 EDX results of NiP coating

Element	P	Fe	Ni
Weight%	13.75	1.67	85.58
Atomic %	23.19	1.56	75.25

Table 5.7. Microhardness values

Samples	Uncoated AISI 520	As- deposited	Heat treated (300℗C)
Hardness	396 HV0.5	592 HV0.5	677 HV0.5

Table 5.8: Results of the electrochemical study (for NiP coating)

Grade	**Rs (ohm-cm^2)**	**Rct (kΩ-cm^2)**	**CPE**	
			Y_O (F)	**n**
Uncoated	23.57	170	0.5731×10^{-5}	0.8885
NiP Coated	33.33	521	0.5563×10^{-5}	0.8521
Heat treated	57.01	553	0.7598×10^{-5}	0.8218

Table 5.9 : Results of polarization test (for NiP coating)

Sample	**Ecorr(V)**	**Icorr(A/cm)**	**Rp(ohm)**	**Corrosion rate(mm/year)**
Uncoated	-0.259 V	5.051×10^{-8}	1.531×10^{6}	5.695×10^{-5}
NiP coated	-0.270 V	3.752×10^{-7}	7.505×10^{5}	5.590×10^{-3}
Heat treated	-0.011 V	3.533×10^{-9}	1.165×10^{7}	5.105×10^{-5}

Table 5.10: Nanohardness results

Coating	Hardness (GPa)	Young's Modulus (GPa)	Stiffness N/m	Elasticity	Plasticity Index (GPa)
Ni-P	6.053	160.365	28.96 X 10^3	0.0377	0.0086
Ni-P-PTFE	1.536	72.296	7.87 X 10^3	0.0212	0.0007

Table 5.11: Fitted values from Randles equivalent circuit model (for Ni-P-PTFE)

SAMPLE	R1 (Ω-cm^2)	R2 (kΩ-cm^2)	CPE (F)	
			CPE-T	CPE-P
Substrate	35.97	10570	$1.25X10^{-5}$	0.73858
NiP	36.56	26381	$2.132X10^{-5}$	0.92516
PTFE	35.03	59055	$2.95X10^{-5}$	0.86259

Table 5.12: Polarization test results (for Ni-P-PTFE)

Sample	Corrosion rate ($\times 10^{-3}$ mm/year)	E_{corr} (V)	I_{corr}(μA/cm^2)
Substrate	16.31	-0.587	5.35×10^{-1}
EN	15.89	-0.323	1.88×10^{-1}
EN-PTFE	9.91	-0.226	5.85×10^{-2}

Table 6.1. CCD design table for experiment

Input parameters	Unit	Axial point value -α	Low level	Central point	High level	Axial point value +α
HTAB (X_1)	g/lit	0.734	2	4	6	7.266
PTFE (X_2)	ml/lit	2.734	4	6	8	9.266
Temperature (X_3)	^oC	71.835	75	80	85	88.165

Table 6.2. Observed data considering CCD

Sequence no		HTAB (g/lit)	PTFE (ml/lit)	Temp (^oC)	Mass Deposition (x 10^{-4}g/cm^2)
		X_1	**X_2**	**X_3**	**D**
1	Factorial points	6	8	75	396.006
2		6	4	85	276.258
3		6	8	85	282.341
4		2	8	85	492.222
5		2	4	75	336.266
4		2	4	85	372.314
7		6	4	75	228.421
8		2	8	75	456.366

9	Central Points	4	6	80	372.281
10		4	6	80	300.396
11		4	6	80	282.259
12		4	6	80	270.247
13		4	6	80	312.546
14		4	6	80	336.455
15	Axial points	0.734	6	80	312.652
16		7.266	6	80	168.285
17		4	9.266	80	480.355
18		4	2.734	80	138.146
19		4	6	71.835	294.258
20		4	6	88.165	504.658

Table 6.3. T-values of the co-efficients vs student's t distribution considering mass per unit area as response

Student's t co-eff	$t_{estimated}$ values	Significance
t_1	28.154	**Significant**
t_2	22.717	**Significant**
t_3	21.346	**Significant**
t_{12}	20.437	**Significant**
t_{13}	21.636	**Significant**
t_{23}	25.444	**Significant**

Table 6.4. Estimation of Fisher's F ratio

Predicting Response Surface Equation	Residual Variance	Replication Variance	Estimated F-value
$D = f(X_1, X_2, X_3)$	7329.544	1398.768	5.24

Table 6.5: Coded values of CCD design

Factor Name	Input parameters	Unit	-α	-1	0	1	α
A	Nickel Sulphate ($NiSO_4$, $7H_2O$)	g/lit	35	37.028	40	42.972	45
B	PTFE	ml/lit	2.734	4	6	8	9.266
C	Sodium Hypophosphite (NaH_2PO_2. H_2O)	g/lit	25	27.028	30	32.972	35

Table 6.6 Experimental results

Sequence no		$NiSO_4$,$7H_2O$ (g/lit)	PTFE (ml/lit)	NaH_2PO_2. H_2O (g/lit)	Hardness
		X_1	**X_2**	**X_3**	**D**
1		35	8	25	220.08

2	Factorial points	45	4	25	176.53
3		35	4	25	196.53
4		45	4	35	168.26
5		45	8	25	263.23
4		35	8	35	106.33
7		45	8	35	195.23
8		35	4	35	248.03
9	Central Points	40	6	30	183.52
10		40	6	30	186.44
11		40	6	30	179.29
12		40	6	30	178.58
13		40	6	30	188.53
14		40	6	30	186.98
15	Axial points	45	6	30	245.23
16		35	6	30	120.65
17		40	2.734	30	132.61
18		40	9.266	30	194.57
19		40	6	35	210.21
20		40	6	25	109.45

Table 6.7. T-values of the co-efficients vs student's t distribution considering mass per unit area as response

Student's t co-eff	$t_{estimated}$ values	Significance
t_1	39.238	**Significant**
t_2	36.551	**Significant**
t_3	49.897	**Significant**
t_{12}	0.156	**Not Significant**
t_{13}	0.918	**Not Significant**
t_{23}	0.816	**Not Significant**

Table 6.8 Estimation of Fisher's F ratio

Predicting Response Surface Equation	Residual Variance	Replication Variance	Estimated F-value
D = f (X_1,X_2,X_3)	118.066	17.414	6.78

Table 6.9 : Experimental and predicted values by RSM and ANN

Sl No	**Experimental Hardness**	**RSM predicted**	**RSM deviation**	**ANN predicted**	**ANN deviation**
1	248.03	280.922	-32.892	245.179	2.851
2	176.53	183.335	-6.805	164.652	11.878
3	263.23	280.521	-17.291	259.88	3.35
4	220.08	211.258	8.822	204.2	15.88
5	183.52	182.328	1.192	184.426	-0.906

6	194.57	172.161	22.409	196.429	-1.859
7	188.53	182.328	6.202	184.426	4.104
8	210.21	242.843	-32.633	231.263	-21.053
9	196.53	184.792	11.738	182.395	14.135
10	195.23	179.677	15.553	179.352	15.878
11	168.26	184.792	-16.532	182.395	-14.135
12	132.61	153.539	-20.929	132.61	0
13	245.23	280.922	-35.692	252.164	-6.934
14	106.33	76.708	29.622	123.673	-17.343
15	178.58	182.328	-3.748	184.426	-5.846

Nibedita Saha

BARUIPUR SURGICAL INSTRUMENTS MANUFACTURERS' WELFARE APEX ASSOCIATION (BASIMAA)
(Under Ministry of MSME, Govt. of India and M & SSE, Govt. of W.B.)
Common Facility Centre (Surgical)

Gate no. 2, Piyali Town,
Fultola Baruipur,
South 24 Parganas, (S), W. B.
Pin - 743387
Phone : 033 24335944
Fax : 033 2827 1502
website : www.basima.co.in
e-mail : basimaa_brp@rediffmail.com

Patron in Chief: Mr. Vaskar Dutta Gupta, (Adv)
Chief Advisor: Sri T. Paul
President: Sri Manab Naiya
Secretary: Sri Kamal Das

Dated:28. 03.2024.

To
Dr.Jisnu Basu,
Chairman Workshop,
Saha Institute of Nuclear Physics,Kolkata.

Sub: Letter of Concent for Established an Incubation Centre at CFC, Fultola (Baruipur) with the support from your Institute.

Sir,

We the Members of Baruipur Surgical Cluster(BASIMAA) are very much thankful to you and Mrs.Nibadita Saha to know that you have already developed the Corrosion Prevent Technology on Surgical Instruments which is the major problem for our Surgical Cluster.

Therefore, we will be very helpful if you established an Incubation Centre with the newly developed Technology for Prevention of Corrosion on Surgical Instruments at the Common Facility Centre, Fultala, along with your machinery support.

With Regards,

Kamal Das. 28/03/2024.

Kamal Das

Sacretary ,BASIMAA.

Journal of Bio- and Tribo-Corrosion (2024) 10:20
https://doi.org/10.1007/s40735-024-00825-5

Effect of Electroless NiP/PTFE Composite Coating on Mechanical Properties of AISI 420 SS and Its Corrosion Behaviour in Human Blood

Nibedita Saha[1,3] · Jisnu Basu[2] · Sourav Mondal[2] · Biswarup Satpati[2] · Gautam Majumdar[1]

Received: 27 October 2023 / Revised: 21 January 2024 / Accepted: 23 January 2024

Abstract
Corrosion is one of the most common causes of failure of the medical instruments. Most of the medical instruments are made of martensitic stainless steel. As blood is highly corrosive, the instruments tend to corrode, when they come in contact with blood for a long period. Coating with a protective layer could be an alternative solution to avoid corrosion and increase the life of the instruments. In this work, we compared the corrosion resistance and mechanical properties of NiP and Ni–P-PTFE composite electroless coatings developed on martensitic stainless steel (grade AISI 420). The results show significant improvement in corrosion properties. Also, mechanical studies such as microhardness and nanohardness properties of the coatings has been performed. The addition of polytetrafluroethylene (PTFE) show higher corrosion resistivity but decreased mechanical properties.

Keywords Electroless composite coating · PTFE · Corrosion · Electrochemical study · Real blood plasma

1 Introduction

Electroless nickel-phosphorous coatings have been extensively used in various industries, such as food processing, chemical engineering, electronics, aerospace, etc. It is known to exhibit excellent hardness and corrosion resistance properties, for which it has a wide range of applications in various fields of manufacturing. However, in order to enhance the properties of NiP coatings further, incorporation of a third element within the NiP matrix is the current research topic in the field of electroless coating. The ternary coating can be formed with a wide range of materials. One type of ternary coatings is the addition of metals such as Cu, W, Co, Mn, Zn, etc. [1–6]. Many researchers are working on it, in order to improve the performance of NiP coatings in various fields. Another type of ternary coating is the codeposition of hard particles (SiC, B_4C, diamond, etc.) [7–11] or dry lubricants such as PTFE, Graphite, MoS_2, etc. [12–14]. The addition of polytetrafluroethelene (PTFE) particles into the NiP matrix can produce excellent self-lubricating and anti-sticking properties. [15–17]. PTFE is chemically inert, has high melting point (325 °C) and low coefficient of friction [18]. Due to extremely low surface energy, (18.6 mN/m), PTFE exhibits excellent anti-sticking properties. Thus, the resulting properties of Ni–P-PTFE composite coating includes nonsticky, lower friction, good wear resistance and corrosion resistance. Due to these properties, EN-PTFE composite coating has wide range of applications. Zhao and Liu [19] developed electroless Ni–P-PTFE coating on AISI 304 stainless steel, in order to control bacterial adhesion on processing equipment. Oppong et al. [20] studied the effect of PTFE particles on microstructural and tribological properties of electroless NiP-PTFE duplex coating developed for geothermal applications, Yanhai et al. [21] applied NiP-PTFE coatings on heat exchangers to improve its mechanical and corrosion properties. Zhang et al. [22] developed TiO_2-PTFE nano composite coating to protect over 316L stainless steel implants from bacterial adhesion. In this work, the authors have tried to study the effect of NiP and NiP-PTFE coatings on medical instruments in order to improve their mechanical and corrosion properties.

Most of the medical instruments are made of martensitic stainless steel [23], due to some of its unique properties such as higher strength, higher wear resistance and higher fatigue resistance, necessary for medical instruments. The grade of

✉ Nibedita Saha
nibedi@gmail.com

[1] Jadavpur University, Jadavpur, Kolkata 700032, India

[2] Saha Institute of Nuclear Physics, Kolkata 700064, India

[3] Academy of Technology, Adisaptagram 712121, India

Published online: 13 February 2024

ADVANCES IN MATERIALS AND PROCESSING TECHNOLOGIES
https://doi.org/10.1080/2374068X.2023.2190667

Corrosion behaviour of electroless NiP coating in artificial blood plasma

Nibedita Saha [a,b], Jisnu Basu [c], Pintu Sen [d] and Gautam Majumdar [a]

[a]Department of Mechaniocal Engineering, Jadavpur University, Kolkata, India; [b]Department of mechanical Engineering, Academy of Technology, Adisaptagram, India; [c]Saha Institute of Nuclear Physics, Kolkata, India; [d]Variable Energy Cyclotron Centre, Kolkata, India

ABSTRACT

Electroless NiP coatings are well known for their excellent properties and vast area of applications. In the present investigation, electroless NiP coating is applied on AISI 420 substrate, which is used for manufacturing medical instruments. As blood is a strong electrolyte, the steel, when comes in contact with blood for a long time, tends to corrode very fast. The primary objective of this work is to enhance the corrosion resistivity of AISI 420 stainless steel by the application of electroless NiP coating. The corrosion resistance of coated steel was investigated using both potentiodynamic polarisation and electrochemical impedance spectroscopy in artificial blood plasma. Detailed microstructural investigation using scanning electron microscopy (SEM), X-ray diffraction and energy dispersive X-ray spectroscopy has been done. Microhardness measurement has been performed. The SEM images revealed the coatings to be primarily amorphous and changed to crystalline when heat treated at 300°C for 2 h. Microhardness of the as-plated coating was 592 HV and increased to 677 HV after heat treatment. Corrosion rate decreased from 4.694×10^{-4} mm/year of bare steel to 4.104×10^{-5} mm/year for coated and heat-treated steel.

ARTICLE HISTORY
Accepted 2 March 2023

KEYWORDS
NiP electroless coating; corrosion resistance; artificial blood plasma; martensitic stainless steel

1. Introduction

Electroless NiP coating, developed by Brenner and Riddle in the 1940s, has extensive use in various industries like chemical, electronics, surface treatment, etc. Due to its excellent mechanical properties, like hardness, corrosion resistance and wear resistance, it is gaining a lot of importance [1,2]. Moreover, it can be applied to any type of substrate and maintained uniformity even on intricate shapes. Also, unlike electroplating, this can be done without any external electrical aid; it is an autocatalytic reaction process. This is a method in which the reduction of the metal ions can be carried out by the oxidation of the reducing agent present in the solution itself [3–6]. The electroless bath consists of an aqueous solution of metal ions, reducing agents, complexing agents and stabilisers, operating in a specific metal ion concentration, temperature and pH ranges.

CONTACT Nibedita Saha nibedi@gmail.com Jadavpur University, Jadavpur 700032, India

Materials Today: Proceedings xxx (xxxx) xxx

Contents lists available at ScienceDirect

Materials Today: Proceedings

journal homepage: www.elsevier.com/locate/matpr

Electrochemical behaviour of martensitic stainless steel with blood

Nibedita Saha [a,*], Jisnu Basu [b], Pintu Sen [c], Gautam Majumdar [a]

[a] Jadavpur University, Jadavpur, Kolkata 700032, India
[b] Saha Institute of Nuclear Physics, Kolkata 700064, India
[c] Variable Energy Cyclotron Centre, Kolkata 700064, India

ARTICLE INFO

Article history:
Received 14 November 2019
Accepted 27 December 2019
Available online xxxx

Keywords:
Martensitic stainless steel
EIS
Corrosion
Blood
Magnetic permeability

ABSTRACT

Martensitic stainless steels have some unique material properties due to which they are considered as a suitable candidate used for manufacturing the medical instruments. As the amount of Ni is negligible in common commercial martensitic stainless steel, the corrosion resistivity especially in contact with blood is less than austenitic stainless steel. In order to get rid of this problem, Martensitic stainless steel has gone under several modifications with respect to its composition. In this paper, three grades of martensitic stainless steel namely AISI 420, Custom 630 and Custom 455 are chosen to study their electrochemical behavior in artificial blood plasma. An attempt has been made to correlate the corrosion resistivity with their magnetic properties. In the linear potentiodynamic polarization experiment, it is revealed that the Custom 455 has lower cathodic potential value (E_{cor} = −0.364 V), but in long run, Custom 630 seems to be considered as a promising material for manufacturing the medical instruments, as the break down potential responsible for pitting corrosion in blood, is quite high for Custom 630 (E_b = 0.275 V).

Selection and of the scientific committee of the 10th International Conference of Materials Processing and Characterization.

1. Introduction

Stainless steel is one of the most important alloys which have got wide range of applications in various fields of engineering due to its qualities such as high corrosion resistance, high wear resistance, etc. There are mainly three types of stainless steels-austenitic, ferritic and martensitic. Martensitic stainless steels are magnetic in nature unlike the other two and also have higher strength, higher wear resistance and higher fatigue resistance than the austenitic and ferritic grades, but they have lower corrosion resistance. Due to the absence of nickel in martensitic stainless steel, it is more machinable than its counter parts and so, is used in various fields of application. One of those fields where martensitic stainless steel has been used as an important material for so many years, is, the surgical tools industry. Most of the surgical instruments are made of martensitic stainless steel mainly AISI 410 and 420 grades. Electrochemical impedance spectroscopy (EIS) is a well-established quantitative technique for the evaluation of anti-corrosion properties. The linear potentiodynamic polarization experiment is also an important study to determine the corrosion potential, corrosion current, corrosion rate etc. [1–13]. Blood being a very strong corrosive media, the surgical instruments made of martensitic steel under goes strong corrosion. A good number of researchers have tried to study the corrosion behavior of stainless steel in various extreme environments such as sodium chloride solution, in high temperature atmosphere, etc. but a very few studies have been carried out to explore the corrosion behavior of martensitic stainless steel in blood. The aim of the present work is to study the corrosion behavior of martensitic steel namely AISI 420, Custom 630 and Custom 455 in artificial blood plasma.

2. Experimental

2.1. Material specification

The Chemical composition of and AISI 420 is given in Table 1. The alloys were tested in Optical emission spectrometer (OES) to check the authenticity of the alloys which has been imported from Germany.

2.2. Blood sample

The chemical composition of the artificial blood plasma is given in Table 2.

* Corresponding author.

https://doi.org/10.1016/j.matpr.2019.12.364
2214-7853/
Selection and of the scientific committee of the 10th International Conference of Materials Processing and Characterization.